Analysis of machine foundation vibrations: state of the art

GEORGE GAZETAS

Rensselaer Polytechnic Institute, Troy, New York, USA

The paper reviews the state-of-the-art of analysing the dynamic response of foundations subjected to machine-type loadings. Following a brief outline of the historical developments in the field, the concepts associated with the definition, physical interpretation and use of the dynamic impedance functions of foundations are elucidated and the available analytical/numerical methods for their evaluation are discussed. Groups of crucial dimensionless problem parameters related to the soil profile and the foundation geometry are identified and their effects on the response are studied. Results are presented in the form of simple formulae and dimensionless graphs for both the static and dynamic parts of impedances, pertaining to surface and embedded foundations having circular, strip, rectangular or arbitrary plan shape and supported by three types of idealized soil profiles: the halfspace, the stratum-over-bedrock and the layer-over-halfspace. Consideration is given to the effects of inhomogeneity, anisotropy and non-linearity of soil. The various results are synthesized in a case study referring to the response of two rigid massive foundations, and practical recommendations are made on how to inexpensively predict the response of foundations supported by actual soil deposits.

INTRODUCTION

The basic goal in the design of a machine foundation is to limit its motion to amplitudes which will neither endanger the satisfactory operation of the machine nor will they disturb the people working in the immediate vicinity. Thus, a key ingredient to a successful machine foundation design is the careful engineering analysis of the foundation response to the dynamic loads from the anticipated operation of the machine. Furthermore, when excessive motions of an existing foundation obstruct the operation of the supported machinery, analysis is necessary in order to understand the causes of the problem and hence to guide appropriate remedial action.

The theory of analysing the forced vibrations of shallow and deep foundations has advanced remarkably in the last 15 years and has currently reached a mature state of development. A number of formulations and computer programs have been developed to determine in a rational way the dynamic response in each specific case. Numerous studies have been published exploring the nature of associated phenomena and shedding light on the role of several key parameters influencing the response. Solutions are also presently available in the form of dimensionless graphs and simple mathematical expressions from which one can readily estimate the response of surface, embedded and pile foundations of various shapes and rigidities, supported by deep or shallow layered soil deposits. Clearly, the current state-of-the-art of analysing machine foundation vibrations has progressed substantially beyond the state of the art of the late 1960s which had been reviewed by Whitman and Richart in 1967[1] and by McNeil in 1969.[2]

In addition to the selection and application of analysis procedures to predict the response, the design of a machine foundation involves (1) the establishment of performance criteria, (2) the determination of dynamic loads, and (3) the establishment of the soil profile and evaluation of critical soil properties. Great progress has also been made in current years in developing *in situ* and laboratory testing procedures to obtain representative values of dynamic soil parameters; a comprehensive review of the available experimental methods has been presented by Woods,[3] while Ozaydin *et al.*,[4] Woods[5] and Richart[6] have summarized the present knowledge on the factors influencing the dynamic soil parameters. These developments in determining material properties complement the advances in analysing foundation vibrations, and provide considerable justification for the use of sophisticated numerical formulations in the design of machine foundations.

On the other hand, little if any progress has been made in reliably estimating dynamic machine loads and improving (through calibration with field data) the available performance criteria. The state-of-the-art in these two areas has remained essentially unchanged during the last decade; reference is made to McNeil[2] and Richart, Woods and Hall[7] for comprehensive reviews of these subjects.

An additional and often overlooked step in machine foundation design is the post-construction observation of the foundation performance and its comparison with the predicted foundation behavior. Such comparisons are needed to calibrate new analysis procedures – an essential task in view of the simplifying assumptions on which even sophisticated formulations are based.

In the final analysis, confidence in the advantages provided by the use of advanced methods of analysis can only be gained if these are shown to have the capability to predict the field performance of actual machine foundations. Unfortunately, only a limited number of case histories has so far been published evaluating state-of-the-art methods of analysis through detailed field observations.

The objective of this paper is to review the present state-of-the-art of determining the dynamic response of foundations subjected to machine-type loadings. The outline of the paper follows the chronology of historical developments: from the dynamics of circular footings resting on the surface of an elastic halfspace to the behavior of cir-

* Presented at the International Conference on Soil Dynamics and Earthquake Engineering, held at the University of Southampton, England, 13-15 July 1982.

0261-7277/83/010002-41 $2.00

cular and non-circular foundations embedded in a layered soil deposit and, finally, to the response of piles. Particular emphasis is accorded to the effects of dimensionless groups of geometric and material parameters on the dynamic stiffness functions and on the response of massive foundations. Normalized graphs and simple formulas are presented for a variety of idealized soil profiles and foundation geometries. The use of such data to estimate to translational and rotational motions of actual foundations in practice is clearly demonstrated and the various results are synthesized by means of a case study. Practical recommendations are then made on how to approximately obtain dynamic stiffness and damping coefficients for actual foundations, accounting only for the most crucial parameters of the problem.

Since the limiting motion for satisfactory performance of a machine foundation usually involves displacement amplitudes of a few thousandths or even ten-thousandths of an inch, soil deformations are quasi-elastic, involving negligible nonlinearity and no permanent deformations. Thus, most of the solutions reported herein assume linear isotropic viscoelastic soil behavior, with a hysteretic soil damping to model energy losses at those small strain amplitudes. However, some consideration is also given to the effects of soil nonlinearity on the vibration of strip footings under strong horizontal and rocking excitation. Moreover, the importance of soil anisotropy and soil inhomogeneity are also considered.

OLDER METHODS OF ANALYSIS

In the past, machine foundations were frequently designed by rules-of-thumb without any analysis of the expected vibration amplitudes. For instance, one such design rule called for a massive concrete foundation of a total weight equal to at least three to five times the weight of the supported machine(s). Although such a proposition may at first glance seem logical, it is in fact an obsolete one since it ignores the effect on the motion of all the other variables of the problem (e.g. type of excitation, nature of supporting soil, and so on). For one thing, increasing the mass of a foundation decreases the resonant frequency of the system and, perhaps more importantly, reduces its effective damping.[7] Obviously, this is not what those applying the rule had in mind.

Following the pioneering experimental studies carried out by the German Degebo in the early 1930s, a number of empirical analysis procedures were developed and used extensively at least until the 1950s. These methods focused on determining only the 'natural frequency' of a foundation. To this end, the concepts of 'in-phase mass' and 'reduced natural frequency' were developed. The former assumes that a certain mass of soil immediately below the footing moves as a rigid body, in-phase with the foundation. The latter postulates that the 'natural frequency' is solely a function of the contact area, the soil bearing pressure and the type of soil.

Physical reality contradicts the concept of an 'in-phase mass'. No soil mass moves as a rigid body with the foundation. Instead, shear and dilational waves emanate from the footing-soil interface into the soil, causing oscillating deformations at the surface and carrying away some of the input energy. The factors that have an influence on these phenomena cannot be possibly accommodated through such an artificial concept. Indeed, the early attempts to obtain specific values of the 'in-phase mass' were frustrated by the sensitivity of this 'mass' to the foundation weight, mode of vibration, type of exciting force, contact area, and nature of the underlying soil. Apparently, there is absolutely no value in this concept and its use in practice may very well mislead the designer.

Tschebotarioff's 'reduced natural frequency' method, based on the results of a few case histories, went a step beyond the original 'in-phase mass' methods.[8] The 'reduced natural frequency' was defined as the 'natural frequency' multiplied by the square-root of the average vertical contact pressure and was given graphically as a function of the type of soil and of the contact area. Although this method was not without merit, it was often interpreted to mean that 'the single most important factor in machine-foundation design was the soil bearing pressure'.[2] Thus, in more than one occasion, the design was based on soil bearing capacity values taken from local building codes!

In addition to the aforementioned drawbacks, these old rules were only concerned with the resonant frequency, providing no information about vibration amplitudes that are primarily needed for design purposes. As a consequence, such rules are now obsolete and will not be further addressed in this paper. Reference is made to Richart *et al.*[7] for more details on the subject.

Dynamic Winkler model

This model was introduced as an extension of the well known 'Winkler' or 'elastic subgrade reaction' hypothesis, which is still rather successfully employed in some static soil-foundation interaction problems.[9] In order to simulate the stiffness characteristics of the actual system, the model replaces the supporting soil by a bed of independent elastic springs resting on a rigid base. Plate bearing tests, conducted in the field, form the basis for evaluating the spring constants (often called 'coefficients of subgrade reaction'). On the basis of field measurements in the USSR, Barkan[10] has presented tables and empirical formulae with which one can readily estimate design values of the coefficient for several types of soil, for each possible mode of vibration (translational or rotational). He has also shown that, in each case, the dynamic coefficient is approximately equal to the ratio of applied pressure increment to the resulting displacement during static repeated loading tests. In these tests static loads 'similar' to the combined dead and live load of the actual foundation are first imposed, followed by repeated slow loading, at frequencies of the order of 0.001 cps, i.e. much slower than those expected in reality.

It is evident that this model can at least give some reasonable information on the low-frequency (near-static) response of a foundation. But since no radiation damping is included, the amplitude of motion at frequencies near resonance cannot be realistically estimated. It has been argued that by neglecting damping one obtains conservative estimates of the response and very good estimates of natural frequencies. In fact, this is the procedure currently incorporated into the 1970 'Indian Standard Code of Practice for Design of Machine Foundations'.[11] There is little merit in this argument, however. For instance, the high damping values present in the translational modes of vibration (of the order of 50% of critical) do affect the 'resonant' frequencies, in addition to drastically reducing amplitudes. Moreover, avoiding 'resonance' (by a safety factor of 2) in such cases is an unfortunate design recommendation which may lead to an overly conservative solution. In other cases, especially when the rotational modes are of main concern, an unsafe design is quite possible since the actual foundation stiffness at high frequencies may very well be appreciably smaller than the static stiffness used in the analysis (see, for example, Fig. 5).

An improved version of the dynamic Winkler model (called 'Winkler–Voigt' model) places a set of independent viscous dampers in parallel with the independent elastic springs to provide the 'dynamic subgrade reaction'. According to Barken and Ilyichev,[12] this model forms the basis of the 1971 USSR machine-foundation code. Again, however, the model itself provides no information on its spring and dashpot coefficients. These are instead backfigured from dynamic plate-load tests conducted in the field. Both the observed amplitude and frequency at resonance are utilized to backfigure the two coefficients. Analyzing the results of numerous field tests, Barkan and his co-workers found a discrepancy between the spring constants backfigured from resonance plate tests and from static repeated loading tests (described previously). They, thus, resorted to the 'in-phase soil mass' concept to essentially match the model constants obtained from the two types of tests. This added soil mass was found to depend on the size and embedment of the foundation and on the nature and properties of the soil deposit, for a given mode of vibration.

It therefore appears that the 'Winkler–Voigt' model is a purely empirical one, requiring field static and dynamic plate-load tests for each particular situation. Such tests are not only very expensive and difficult to successfully conduct, but, moreover, they yield results which cannot be readily interpreted and extrapolated to prototype conditions. If I may slightly rephrase Gibson:[13]

> 'The model conspicuously lacks what all models
> should possess – predictive power.'

The only possible explanation for the present-day use of dynamic Winkler models in machine-foundation analysis is the accumulation in some countries of a wealth of pertinent field data. Such data, often available in the form of tables,[12] can be directly utilized in practice, thus avoiding the burden of performing plate-load tests. Again, one should be very careful in picking up values for the coefficients from published field data. For it is practically impossible to ensure a similarity in all the crucial physical and geometric response parameters of the new prototype and of the old model foundation schemes.

FUNDAMENTALS OF CURRENT METHODS OF VIBRATION ANALYSIS

Historical perspective

Modern methods of analysis of foundation oscillations attempt to rationally account for the dynamic interaction between the foundation and the supporting soil deposit. Cornerstone of the developed methods is the theory of wave propagation in an elastic or viscoelastic solid (continuum). This theory has seen a remarkable growth since 1904, when Lamb published his study on the vibration of an elastic semi-infinite solid (half-space) caused by a concentrated load ('dynamic Boussinesq' problem). Numerous applications, primarily in the fields of seismology and applied mechanics, have given a great impetus in the development of the 'elastodynamic' theory. Reissner in 1936[14] attempted what is considered to be the first engineering application; his publication on the response of a vertically loaded cylindrical disk on an elastic halfspace marked the beginning of modern soil dynamics. The solution was only an approximate one since a uniform distribution of contact stresses was assumed for mathematical simplification. Nonetheless, Reissner's theory offered a major contribution by revealing the existence of radiation damping – a phenomenon previously unsuspected but today clearly understood. Every time a foundation moves against the soil, stress waves originate at the contact surface and propagate outward in the form of body and surface waves. These waves carry away some of the energy transmitted by the foundation on to the soil, a phenomenon reminiscent of the absorption of energy by a viscous damper (hence the name).

For many massive foundations the assumption of a uniform contact stress distribution is an unrealistic one, for it yields a non-uniform pattern of displacements at the soil-footing interface. To closer approximate the rigid body motion of such foundations, a number of authors in the middle 1950s assumed contact stress distributions which produce uniform or linear displacements at the interface, under statically applied force or moment loadings, respectively. Thus, Sung[15] and Quinlan[16] presented results for vertically oscillating circular and rectangular foundations while Arnold *et al.*[17] and Bycroft[18] studied both horizontal and moment loading of a circular foundation. These solutions are only approximate: in reality the pressure distributions required to maintain uniform or linear displacements are not constant but vary with the frequency of vibration.

The first 'rigorous' solutions appeared about ten years later when the vibrating soil-foundation system was analysed as a mixed boundary-value problem, with prescribed patterns of displacements under the rigid footing and vanishing stresses over the remaining portion of the surface. Introducing some simplifying assumptions regarding the secondary contact stresses ('relaxed' boundary), Awojobi *et al.*[19] studied all possible modes of oscillation of rigid circular and strip footings on a halfspace, by recourse to integral transform techniques. On the other hand, Lysmer[20] obtained a solution for the vertical axisymmetric vibration by discretizing the contact surface into concentric rings of uniform but frequency-dependent vertical stresses consistent with the boundary conditions. A conceptually similar approach was followed by Elorduy *et al.*[21] for vertically loaded rectangular foundations.

Perhaps equally important with the aforementioned theoretical developments of this period was the discovery by Hsieh[22] and by Lysmer[20] that the dynamic behavior of a vertically loaded massive foundation can be represented by a single-degree-of-freedom 'mass-spring-dashpot' oscillator with frequency-dependent stiffness and damping coefficients. Lysmer[20] went a step farther by suggesting the use of the following frequency-independent coefficients to approximate the response in the low and medium frequency range:

$$K_v = \frac{4GR}{1-\nu}; \quad C_v = \frac{3.4R^2}{1-\nu}\sqrt{G\rho} \tag{1}$$

in which: K_v = spring constant (stiffness), C_v = dashpot constant (damping), R = radius of the circular rigid loading area, G and ν = shear modulus and Poisson's ratio of the homogeneous halfspace (soil), and ρ = mass density of soil. Note that the expression for K_v in equation (1) is identical with the expression for the static stiffness of a vertically loaded rigid circular disk on a halfspace.

The success of Lysmer's approximation (often called 'Lysmer's Analog') in reproducing with very good accuracy the actual response of the system had a profound effect on the further development and engineering applications of the 'halfspace' theories. Richart and Whitman[23] extended Lysmer's Analog by demonstrating that all modes of vibration can be studied by means of lumped-parameter mass-spring-dashpot systems having properly selected frequency-independent parameters. The axisymmetric (vertical and torsional) oscillations of a cylindrical foundation can be represented by a 1-degree-of-freedom (1-dof) system described by:

$$m\ddot{x} + C\dot{x} + Kx = P(t) \tag{2}$$

in which x, $\dot{x}$ and $\ddot{x}$ = the displacement, velocity and acceleration, respectively, of the vertically oscillating mass; $P(t)$ = the external dynamic force arising from the operation of the machine(s). The lumped parameters are the equivalent mass, m, the effective damping, C, and the effective stiffness K. (For torsional oscillations m should be replaced by I_z, the effective mass polar moment of inertia and x should be interpreted as the angle of rotation around the vertical axis of symmetry.) On the other hand, the two antisymmetric modes of oscillation (horizontal translation and rocking) of a cylindrical foundation are coupled and can be represented by a 2-dof system characterized by the effective mass and mass moment of inertia, the two effective values of damping (for swaying and rocking), and the two effective values of the stiffness (for swaying and rocking).

Different values of the inertia, stiffness and damping parameters are needed for each one of these four modes of excitation. Whitman and Richart[23] suggested the choice of stiffnesses appropriate for low frequencies, and of average damping values over the range of frequencies at which resonance usually occurs. In order to obtain a good agreement between the resonant frequencies of the lumped-parameter and the actual system, they recommended that a fictitious mass (or mass moment of inertia) be added to the actual foundation mass (or mass moment of inertia). The need for such a recommendation stemmed not from the existence of any identifiable soil mass moving in-phase with the foundation, but rather from the fact that in reality the stiffnesses decrease with increasing frequency (see Figs. 5 and 7), instead of remaining constant and equal to the static stiffnesses, as the model assumes. In other words, instead of decreasing K, the lumped-parameter model increases m to keep the resonant frequency, ω_r, unchanged. Recall that ω_r is proportional to the square-root of (K/m).

Whitman and Richart[23] and later Richart, Woods and Hall[7] and Whitman[24] presented expressions for these parameters for all four vibration modes. Table 1 displays these expressions, which have enjoyed a significant popularity over the last decade.

Primarily because of its simplicity, the lumped-parameter approximation had a great impact on the application of the 'half-space' theory. It demonstrated that this rational theory can be cast into a tractable, simple engineering form, which can be used by the profession with hardly any greater difficulty than the older empirical procedures.

Motivated to a large extent by the need to understand the phenomena associated with seismic soil-structure interaction, the analysis of the dynamic response of foundations has been a subject of considerable interest throughout the 1970s. A significant amount of related research has led to the development of new formulations and computer programs, while numerous publications have studied the importance of critical foundation, soil and loading parameters and have presented graphs, tables and simple expressions, suitable for direct use in practical applications. It is worth mentioning some of the most important contributions to the current state of the art.

*Table 1. Equivalent lumped parameters for analysis of circular foundations on elastic halfspace**

Mode	Vertical	Horizontal	Rocking	Torsion
Stiffness:	$\frac{4GR}{1-\nu}$	$\frac{8GR}{2-\nu}$	$\frac{8GR^3}{3(1-\nu)}$	$\frac{16GR^3}{3}$
Mass ratio $\bar{m}$:	$\frac{m(1-\nu)}{4\rho R^3}$	$\frac{m(2-\nu)}{8\rho R^3}$	$\frac{3I_x(1-\nu)}{8\rho R^5}$	$\frac{I_z}{\rho R^5}$
Damping ratio:	$\frac{0.425}{\bar{m}^{1/2}}$	$\frac{0.29}{\bar{m}^{1/2}}$	$\frac{0.15}{(1+\bar{m})\bar{m}^{1/2}}$	$\frac{0.50}{1+2\bar{m}}$
Fictitious added mass:	$\frac{0.27m}{\bar{m}}$	$\frac{0.095m}{\bar{m}}$	$\frac{0.24I_x}{\bar{m}}$	$\frac{0.24I_z}{\bar{m}}$

I_x, I_z = mass moments of inertia around a horizontal, vertical axis, respectively; damping ratio = C/C_{cr} where $C_{cr} = 2(Km)^{1/2}$ or $C_{cr} = 2(KI)^{1/2}$ for translational or rotational modes of vibration, with $I = I_x$ or I_z for rocking or torsion, respectively.

Newly developed (mid-1960s) mathematical techniques to solve mixed boundary-value elastodynamic problems were utilized by Luco *et al.*[25] and Karasudhi *et al.*[26] to obtain 'exact' numerical solutions for all modes of vibration of strip footings on a halfspace, and by Luco *et al.*[27] and Veletsos *et al.*[28,29] to extend the available halfspace solutions for circular foundations to the high frequency range and, also, to a viscoelastic material with linear hysteretic damping. The development of dynamic finite-element formulations with energy absorbing ('viscous' and 'consistent') lateral boundaries prompted the study of the response of surface and embedded foundations supported by a layered soil stratum.[30–34] Only plane-strain and axisymmetric geometries could be handled with these finite element formulations, however, and the presence at a relatively shallow depth of a non-compliant rock-like material underlying the stratum was an unavoidable requirement regardless of whether such rock did actually exist.

On the other hand, Luco[35] and Gazetas[36] presented analytical solutions for circular, strip and rectangular foundations on the surface of a layered halfspace or a layered stratum (i.e. with or without a rigid rock as the last layer, respectively). Utilizing these formulations they offered results[37–39] which bridged the gap between the two previously studied extreme profiles – the halfspace and the stratum-on-rigid-base. At about the same time, Novak[40] obtained approximate analytical solutions for circular foundations embedded in a halfspace, by deriving closed-form expressions for the dynamic stiffness and damping coefficients along the vertical sides of the foundation. Later on this method was easily adapted to study the dynamic response of piles.[41–43]

In more recent years research efforts have been primarily directed to determining solutions: (a) for rigid foundations of rectangular and arbitrary shapes;[44–48] (b) for foundations of finite flexural rigidity;[49–51] (c) for foundations on inhomogeneous and on anisotropic soils;[52–55] and (d) for foundations on nonlinear (Ramberg-Osgood) soils.[56] Furthermore, a very substantial amount of research work has been devoted to the dynamic behavior of single (floating and end-bearing) piles embedded in homogeneous, inhomogeneous or layered soil deposits, and the first attempts have already been made to obtain solutions for dynamic loaded pile groups. For comprehensive lists of related references, see Dobry *et al.*,[57] Kagawa *et al.*,[58] and Novak.[59]

Impedance and compliance functions: definition and physical interpretation

An important step in current methods of dynamic analysis of rigid massive machine foundations is the determination (using analytical or numerical methods) of the dynamic impedance functions, $\mathbf{K}(\omega)$,* of an 'associated' rigid but massless foundation, as a function of the excitation frequency, ω. As shown in Fig. 1 the 'associated' foundation-soil system is identical (in both material properties and geometry) with the actual system, except that the foundation mass is taken equal to zero. It will be explained in the following section how, once the harmonic response of such a massless foundation has been determined, the steady-state response of the massive foundation, or of any structure supported on it, may be evaluated using standard procedures. In addition, the transient response to non-harmonic machine forces can also be evaluated by recourse to Fourier analysis and synthesis techniques.

For each particular harmonic excitation with frequency ω, the dynamic impedance is defined as the ratio between the steady-state force (or moment) and the resulting displacement (or rotation) at the base of the massless foundation. For example, the vertical impedance of a foundation whose plan has a center of symmetry is defined by:*

$$\mathbf{K}_v = \frac{\mathbf{R}_v(t)}{v(t)} \tag{3}$$

in which $\mathbf{R}_v(t) = R_v \exp(i\omega t)$ is the harmonic vertical force applied at the base of the disk, and $v(t) = v \exp(i\omega t)$ is the uniform harmonic settlement of the soil-foundation interface. It is evident that $\mathbf{R}_v$ is the total soil reaction against the foundation; it is made up of the normal stresses against the basemat plus, in case of embedded foundations, the shear stresses along the vertical side walls, as illustrated in Fig. 1.

Similarly one may define the torsional impedance, $\mathbf{K}_t$, from the torsional moment and rotation; the horizontal impedances, $\mathbf{K}_h$, from the horizontal forces and displacements along the principal axes of the base; and the rocking impedances, $\mathbf{K}_r$, from the moments and rotations around the same horizontal principal axes. However, since horizontal forces along the principal axes produce rotations in addition to horizontal displacements, cross-horizontal-rotational impedances $\mathbf{K}_{rh}$ may also be defined; they are usually negligibly small in case of surface and very shallow foundations, but their effect may become appreciable for greater depths of embedment.

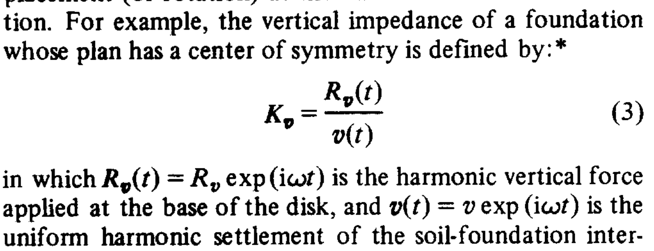

Figure 1. Machine foundation and the associated rigid massless foundation

* Bold letters are used in the text for impedances, compliances and some stiffness and damping coefficients (equation (17)); in the figures, calligraphic characters are used for these quantities.

Referring to equation (3), it is interesting to note that dynamic force and displacement are generally out of phase. In fact, any dynamic displacement can be resolved into two components: one in phase and one 90° out of phase with the imposed harmonic load. It is convenient then to introduce complex notation to represent forces and displacements. As a consequence, impedances may also be written in the form:*

$$\mathbf{K}_a(\omega) = K_{a1}(\omega) + iK_{a2}(\omega) \tag{4}$$
$$a = v, h, r, hr, t; \quad i = \sqrt{-1}$$

The real and imaginary components are both functions of the vibrational frequency ω. The real component reflects the stiffness and inertia of the supporting soil; its dependence on frequency is attributed solely to the influence which frequency has on inertia, since soil properties are essentially frequency independent. The imaginary component reflects the radiation and material damping of the system. The former, being the result of energy dissipation by waves propagating away from the foundation, is frequency dependent; the latter, arising chiefly from the hysteretic cyclic behavior of soil, is practically frequency independent.

A very instructive analogy between the dynamic response of a simple 1-dof oscillator and of a three-dimensional massless foundation-soil system has been drawn by Roesset.[60] Assuming a harmonic excitation $P(t) = P_0 \exp(i\omega t)$, the steady-state response $x(t) = x_0 \exp(i\omega t)$ of the 1-dof oscillator may be obtained by substitution into equation (2);

$$(K - m\omega^2) + iC\omega = \frac{P(t)}{x(t)} \tag{5}$$

Contrasting equations (5) and (3) prompts the definition of a dynamic impedance function for the 1-dof mass-spring-dashpot system:

$$\mathbf{K} = (K - m\omega^2) + iC\omega \tag{6}$$

and, by comparison with equation (4):

$$K_1 = K - m\omega^2 \tag{7}$$

$$K_2 = C\omega \tag{8}$$

In other words, the dynamic impedance of our familiar 1-dof oscillator is indeed a complex number with a frequency dependent real part representing the stiffness and inertia characteristics of the system, and a frequency dependent imaginary part expressing the energy loss in the system. Therefore, it is quite natural to express the dynamic impedance of soil-footing systems in a complex form, as done in equation (4).

Having, thus, established the analogy between 1-dof and massless footing-soil systems, let equation (6) for the 1-dof be rewritten as:

$$\mathbf{K} = K \cdot \left\{ \left(1 - \frac{\omega^2}{\omega_n^2}\right) + i2\beta \frac{\omega}{\omega_n} \right\} \tag{9a}$$

or

$$\mathbf{K} = K \cdot \{k + i\omega c_s\} \tag{9b}$$

in which the critical viscous damping ratio is:

$$\beta = \frac{C}{C_{cr}} = \frac{C}{2K/\omega_n} \tag{10}$$

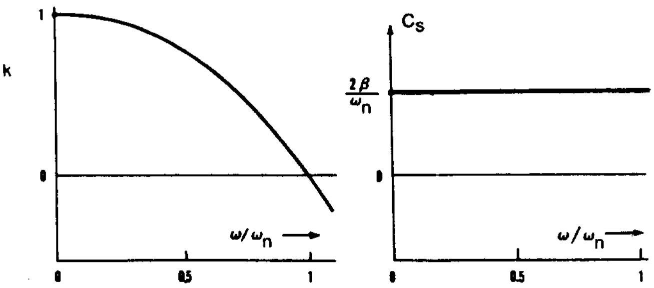

Figure 2. Dynamic stiffness and damping coefficients of a 1-dof simple oscillator

the natural frequency $\omega_n = (K/m)^{1/2}$, $k = (1-\omega^2/\omega_n^2)$ and $c_s = C/K$. Equation (9b) implies that the dynamic impedance of a 1-dof simple oscillator may be expressed as a product of the spring constant K, which happens to be the static stiffness of the system, times a complex number $k + i\omega c_s$, which encompasses the dynamic characteristics of the system (inertia and viscous damping) and is hereafter called '*dynamic part*' of the impedance. At zero frequency the dynamic part becomes a real number, equal to 1, and the impedance coincides with the static stiffness K of the simple system. k and c_s are named respectively stiffness and damping coefficients and their variation with frequency for the 1-dof's is plotted in Fig. 2. Notice that k decreases as a second degree parabola with increasing ω, whereas c_s remains constant.

It should not surprise the reader that the actual variation with ω of the stiffness and damping coefficients, k_v and c_{sv}, of a vertically vibrating circular disk on an elastic halfspace is indeed very similar to the variation of the k and c_s of the 1-dof system! (To see this similarity just compare Fig. 2 to Fig. 5(a).) However, in general, k and c_s of a foundation-soil system may vary in a rather complicated manner with ω, depending primarily on the mode of vibration, the geometry, rigidity and embedment of the foundation, and, finally, the profile and properties of the supporting soil deposit. Figures 5, 8, 9, 10 and 20 may be previewed to confirm this statement. Nonetheless, in all cases, the dynamic impedance functions can be expressed as products of a static and a dynamic part, as described by equation (9b). Alternatively, a dimensionless frequency factor is often introduced:

$$a_0 = \frac{\omega B}{V_S} \tag{11}$$

in which: B = a critical foundation dimension like, e.g., the radius of a circular foundation or half the width of a strip or a rectangular foundation; and V_S = a characteristic shear wave velocity of the soil. Combining equations (9b) and (11) allows the impedance to be case in the form:

$$\mathcal{K} = K(k + ia_0 c) \tag{12}$$

with

$$c = c_s \frac{V_S}{B} \tag{13}$$

Since both a_0 and c are dimensionless quantities, equation (12) is strongly preferred to equation (9b) in presenting the results of dynamic analyses.

Let it now be assumed that a 'hysteretic damper' is added in-parallel with the spring and the 'viscous damper' to support the mass of the simple oscillator. This damper is described through a hysteretic damping ratio, ξ. During each cycle of motion it dissipates an amount of energy proportional to the maximum strain energy, W, of the system:

$$\Delta W_h = 4\pi\xi W \tag{14}$$

in which $W = (\tfrac{1}{2})Kx_0^2$. On the other hand, during a cycle of motion the viscous damper has consumed an amount of energy equal to:

$$\Delta W_v = \pi C\omega x_0^2$$
$$= 4\pi\beta \frac{\omega}{\omega_n} W \tag{15}$$

so that the total dissipated energy, $\Delta W = \Delta W_h + \Delta W_v$, as a function of W is:

$$\frac{\Delta W}{W} = 4\pi\left(\beta\frac{\omega}{\omega_n} + \xi\right) \tag{16}$$

This expression suggests that the simple addition rule, $\xi + \beta\omega/\omega_n$, may be used to obtain the 'effective' damping ratio of a system possessing both viscous, β, and hysteretic, ξ, damping. A vibrating foundation-on-soil is one such system, with its radiation damping being of a viscous nature while the material damping is of the hysteretic type.

The presence of material damping in the soil affects both the stiffness and damping coefficients, k and c. In an attempt to isolate the effects of hysteretic material damping, an alternative expression to equation (12) is often used for the dynamic impedance:

$$\mathcal{K} = K(k + ia_0 c)\cdot(1 + 2i\xi) \tag{17}$$

Recalling the so-called 'correspondence principle,[61] one may anticipate that the new coefficients, k and c, are independent of material damping. If this were true, it would then be sufficient to obtain solutions for a purely elastic soil and then extrapolate the results to soils with any hysteretic damping ratio by multiplying the undamped impedances by $1+2i\xi$. Indeed, for very deep soil deposits which can be modeled as a halfspace the above 'principle' is reasonably accurate and has been repeatedly utilized to obtain solutions for damped soils.[29,62,63] However, in the case of a shallow stratum on rigid rock both k and c are fairly sensitive to the assumed material damping ratio (see Fig. 9, for example); this discredits to a large extent the 'correspondence principle', as Kausel[33] had first noticed.

None the less, it is convenient to express the impedance functions in the form of equation (17), and this practice is frequently followed in the sequel. Alternatively, however, equation (12) is also used in some cases.

Dynamic compliance functions

Also given the names dynamic 'displacement' functions and dynamic 'flexibility' functions, they are essentially the ratios between dynamic displacements (or rotations) and the dynamic reactive forces (or moments) at the base of a foundation. They were first introduced by Reissner.[14] Following the previous discussion, it is convenient to express each compliance using complex notation:

$$F_a = F_{a1}(\omega) + iF_{a2}(\omega) \tag{18}$$
$$a = v, h, r, hr, t$$

The real and imaginary parts represent the displacement components which are in-phase and 90°-out-of-phase with the reactive force, respectively, and they both are functions of frequency, as discussed in detail previously. For a foundation which in plan has a center of symmetry, the vertical and torsional compliances are simply the inverse of the vertical and torsional impedances:

$$F_b = \frac{1}{K_b} \; ; \quad b = v, t \tag{19a}$$

However, due to the coupling between rocking and swaying motions, the corresponding compliances should be obtained by inverting the matrix of impedances:

$$\begin{bmatrix} K_h & K_{hr} \\ K_{hr} & K_r \end{bmatrix}^{-1}$$

The following alternative form to equation (18) is also frequently used in presenting compliance functions:

$$F_a = \frac{1}{K_a} \left[f_{a1}(\omega) + \mathrm{i} f_{a2}(\omega) \right] \tag{20}$$

where K_a is the corresponding static stiffness.

Computational procedures for determining impedance functions

Several alternative computational procedures are presently available to obtain dynamic impedance functions for each specific machine-foundation problem. The choice among these methods depends to a large extent on the required accuracy, which in turn is primarily dictated by the size and importance of the particular project. Furthermore, the method to be selected must reflect the key characteristics of the foundation and the supporting soil. Specifically, one may broadly classify soil-foundation systems according to the following material and geometry characteristics:

1. The shape of the foundation (circular, strip, rectangular, arbitrary).
2. The type of soil profile (deep uniform deposit, deep layered deposit, shallow layered stratum on rock).
3. The amount of embedment (surface foundation, embedded foundation, deep foundation).
4. The flexural rigidity of the foundation (rigid foundation, flexible foundation).

Two computationally different approaches have been followed over the years to obtain the dynamic impedances of foundations with various characteristics: a 'continuum' approach, which led to the development of analytical and semi-analytical formulations, and a 'discrete' approach, which resulted in the development of finite-difference and, primarily, finite-element models. In the past (mid-1970s), considerable controversy was held about the relative merits and deficiencies of each approach and some extreme and unjustified positions were advocated. Today, it is quite clear that both procedures, if correctly understood and implemented, are very useful tools in analysing the behavior of dynamically loaded foundations. Moreover, they yield very similar results if they are appropriately used to solve the same problem. Hadjian *et al.*[64] and Jakub *et al.*[65] have presented excellent discussions and comparative studies on this subject. The following paragraphs intend to rather briefly introduce the most important analytical, semi-analytical and numerical procedures which are currently available to the machine-foundation analyst. The list is by no means exhaustive, and the emphasis is on discussing the strong and weak points of each method.

'Continuum' methods. Starting point of all the developed formulations is the analytical solution of the pertinent wave equations governing the imposed deformations in each uniform soil layer or halfspace. However, the boundary conditions at the soil-footing interface are handled differently by the various methods. In that respect, one may very broadly classify the available continuum formulations into analytical and semi-analytical solutions.

The known *analytical* solutions simplify the mechanical behavior of the soil-footing contact surface by assuming a 'relaxed' boundary. That is, no frictional shear tractions can develop during vertical and rocking vibrations, while for horizontal vibrations the normal tractions at the interface are assumed to be zero. This assumption has been necessary to avoid the more complex mixed boundary conditions resulting from the consideration either of a perfect attachment between foundation and soil ('rough' foundation) or of a contact obeying Coulomb's friction law (an even more realistic idealization).

By recourse to integral transform techniques (involving Hankel or Fourier transforms for axisymmetric or plane-strain geometries, respectively) the relaxed boundary conditions yield sets of dual integral equations for each mode of vibration. Each set is then reduced to a Fredholm integral equation which is finally solved numerically.

Such analytical solutions have so far been published for surface circular and strip foundations of infinite flexular rigidity supported by an elastic or viscoelastic halfspace;[26–29] for circular foundations on a layered elastic or viscoelastic soil deposit;[35,66] for circular foundations of finite flexural rigidity supported on a halfspace;[49] for circular foundations on a cross-anisotropic halfspace;[67] and even for vertically loaded rigid rectangular foundations on a halfspace.[45]

The *semi-analytical* type solutions are based on the determination of the displacements at any point within the footing-soil interface, caused by a unit normal or shear time-harmonic force applied at another point of the same interface. Then, by properly discretizing the contact surface, the matrix of dynamic influence or Green's functions is assembled and the problem is solved after imposing the rigid-body motion boundary conditions. Several different techniques (in essence different integration procedures) have been formulated to carry out these steps of the analysis. For example, Elorduy *et al.*[21] and Whittaker *et al.*[50] utilized Lamb's solution for a point loaded halfspace; Luco *et al.*[27] obtained pairs of Cauchy type integral equations which they numerically solved after reducing to coupled Fredholm equations; Gazetas[36] and Gazetas *et al.*[38] utilized a fast Fourier transform algorithm; Wong[68] and Wong *et al.*[44] used the solution for a uniformly loaded rectangle; and so on.

For the purpose of this discussion, one may list as a semi-analytical solution the formulation of Dominguez and Roesset,[47] who applied the so-called 'boundary integral equation' or, more simply, 'boundary element' method to obtain dynamic impedance functions of rectangular foundations at the surface of, or embedded in a halfspace. To this end, they utilized the closed-form solution to the 'dynamic Kelvin' problem of a concentrated load in an infinite medium,[69] and discretized either only the contact surface, in the case of surface footings with 'relaxed' boundaries, or both the contact and the surrounding soil surfaces, in the cases of embedded footings and of surface footings 'adhesively' attached to the soil.

So far rigorous semi-analytical solutions have been published for rigid strip foundations on the surface of a layered halfspace or stratum-on-rock;[36, 38, 39, 70] for rigid rectangular foundations on a halfspace;[21, 36, 44, 46–48, 56, 65, 68, 71] for rectangular foundations of finite flexural rigidity;[50, 51] for rigid rectangular foundations embedded in a halfspace;[47] and, finally, for rigid foundations of arbitrary shape.[44]

Note that *approximate semi-analytical* procedures have already been developed to obtain the impedances of cylindrical embedded foundations and circular piles.[40–43, 57, 72] These procedures assume that only horizontally propagating waves generate at the vertical foundation-soil interface, and they neglect the coupling between forces and displacements at various points. Instead, they only compute the displacement at the point of application of the load. Thus, in effect, the soil is modeled as a Winkler medium, the spring and dashpot characteristics of which are estimated from realistic, albeit simplified, wave propagation analyses.

Finally, several similar *approximate analytical* formulations have been developed, again for deeply embedded cylindrical foundations and end-bearing piles in soil strata.[73–78] These procedures attempt to analytically solve the governing wave equations for the stratum, by neglecting the secondary component of displacement (i.e. the vertical component for lateral vibrations or the radial one for vertical vibrations). The boundary conditions at the soil-pile interface are analytically enforced by expanding the contact pressure distribution to an infinite series in terms of the natural modes of vibration of the soil layer.

'Discrete' models. Dynamic finite difference and finite element models have been developed for problems of complicated geometry which are not easily amenable to analysis with continuum type, analytical or semi-analytical formulations. Today, finite difference formulations such as those proposed by Ang *et al.*,[79] Agabein *et al.*,[80] Krizek *et al.*,[81] and Tseng *et al.*,[82] find very little if any application in solving foundation vibration problems, and, therefore, will not be further addressed in this paper. On the other hand, several finite element formulations and computer programs are presently widely available and frequently used in analysing foundation oscillations.

The use of finite elements in dynamic foundation problems is different from other applications of finite elements in statics and dynamics in that soil strata of infinite extent in the horizontal and even in the vertical direction must be represented by a model of a finite size. Such a finite model creates a fictitious 'box' effect, trapping the energy of the system and distorting its dynamic characteristics. To avoid this problem, wave absorbing lateral boundaries are introduced to account for the radiation of energy into the outer region not included in the model. Two main types of such boundaries are available. The approximate 'viscous' boundary proposed by Lysmer *et al.*[83] and extended by Valliappan *et al.*[84] must be placed at some distance from the foundation. The alternative 'consistent' boundary developed by Waas[31] and extended by Kausel[33] is very effective in accurately reproducing the physical behavior of the system, and it also results in considerable economy by being placed directly at the edge of the foundation. This 'consistent' boundary provides a dynamic stiffness matrix for the medium surrounding the plane or cylindrical vertical cavity which is assumed to occupy the central region under the strip or circular foundation. This matrix corresponds exactly to the boundary stiffness matrix that would be obtained from a continuum type formulation.

Unfortunately, 'consistent' boundaries have been developed only for plane-strain and axisymmetric (cylindrical) geometries. No such boundary is available for truly three-dimensional (3D) geometries, in cartesian coordinates. Thus, to solve 3D problems a finite-element model must resort to 'viscous' or elementary boundaries placed far away from the loaded area. In this way the fictitiously reflected waves are dissipated through hysteresis and friction (material damping) in the soil before they return to the foundation region. However, the cost of such analyses is prohibitive and truly 3D solutions are very rarely used in practice. An attempt has been made to modify a 2D computer program by adding viscous dashpots to the lateral faces of its plane-strain elements, in order to simulate the radiation damping of 3D situations.[85] Notwithstanding the popularity enjoyed by this pseudo-3D model, its only difference from the 2D model is that it introduces an artificial increase in damping, which cannot possibly reproduce all aspects of the true 3D behavior. In fact, in some cases the actual 3D radiation damping in rocking is over-estimated rather than under-estimated by a 2D model;[86] thus by adding viscous dashpots the situation may worsen instead of improving.[56, 65]

Consequently, today, two types of finite-element models are practically available: plane-strain 2D models appropriate for strip footings or elongated rectangular structures;[34, 84, 87] and 3D axisymmetric-geometry models appropriate for cylindrical foundations and nearly square structures.[31, 33, 88]

It is noted that embedded foundations and layered soil strata can be routinely handled with all the finite-element formulations. On the other hand, the presence of a fixed bottom boundary is required by most of the available codes. This is hardly a drawback if a stiff, rock-like stratum does exist at a relatively shallow depth. Otherwise, when the supporting soil deposit is very deep, the cost of a realistic finite-element analysis may become substantial.

Conclusion. With the available analytical, semi-analytical and finite-element computer programs the foundation vibration analyst may obtain solutions for foundations of various shapes, surface or embedded, supported by deep or shallow soil deposits. In selecting the most appropriate code for each specific situation, attention should first focus on the depth of embedment and the nature of the underlying soil. When dealing with very shallow footings on deep deposits which can be well reproduced by a small number of layers with different properties, continuum type analytical or semi-analytical formulations are clearly more advantageous; the choice of the most appropriate among them will be mainly dictated by the shape of the footing (strip, circular, rectangular, arbitrary) and the desired degree of accuracy. On the other hand, for embedded foundations in a shallow stratum or whenever a large number of layers with sharply different properties exists below the footing, finite element models are particularly appropriate.

Furthermore, attention should be accorded to the operational frequencies of the machine and the inertia characteristics of the foundation. At very high frequencies of vibration, f, discrete models may become very costly; because, in order to transmit high frequencies, a large number of sufficiently small-sized elements must be used. For instance, it is usually recommended that the maximum dimension of an element should not exceed $\lambda/8$, where $\lambda = V/f$ is the wavelength in a particular soil layer having shear wave velocity V. Therefore, with high frequencies, analytical models may become advantageous. Notice, though, that the computer costs of semi-analytical formulations may also be adversely affected by a large increase in the operational frequency, since they, too, discretize the contact area or the whole uppermost surface.

Regarding the inertia characteristics of the foundation, the author and Roesset[39] have demonstrated that for heavy foundations (i.e. with high mass ratios) small errors in modeling the different soil layers are unimportant and one can safely base the design on available halfspace solutions or on the results of analytical type computer programs. On the other hand, relatively light foundations are quite sensitive to the existence of competent rock at a shallow depth and of different soil layers beneath the footing, thus requiring a good soil exploration followed by finite-element analyses. These conclusions are further illustrated and generalized in a later section of this paper.

In addition to the existing computer programs numerous solutions have been published in the literature in the form of dimensionless graphs, tables and simple formulae for impedance and compliance functions of foundations with several different geometries, depths of embedment and stiffness characteristics, supported by various idealized soil profiles (halfspace, stratum, etc.). These solutions can give very satisfactory results in many practical cases and are especially valuable in conducting preliminary analyses and parameter sensitivity studies. One of the goals of this state-of-the-art paper is to present and discuss the most significant of these available solutions. Before doing this, however, it is expedient to illustrate how the impedance functions may be utilized to obtain the dynamic response of rigid massive foundations.

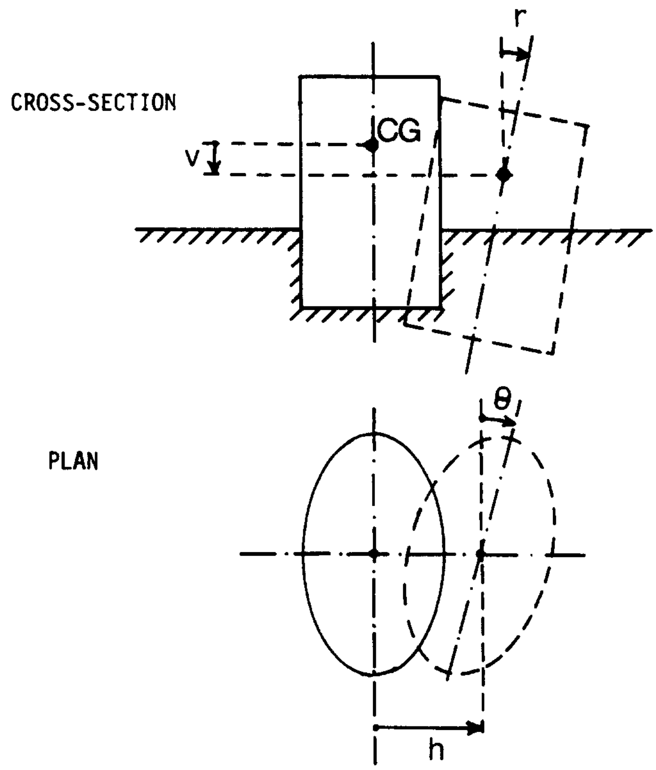

Figure 3. Definition of deformation variables

Use of impedance functions: response of massive machine foundations

The first step in analysing the response of a massive machine foundation is to evaluate the pertinent dynamic impedances at the anticipated frequency, or range of frequencies, of the machine. This is done either by utilizing existing discrete or continuum type formulations, or by resorting to published solutions available in the soil dynamics literature. The use of dynamic impedance to obtain the response is illustrated herein.

Figure 3 portrays a massive, rigid foundation having equal depth of embedment along all the sides and possessing two orthogonal vertical planes of symmetry, the intersection of which defines a vertical axis of symmetry. The foundation plan, having two axes of symmetry, may be of any axi-symmetric or orthogonal shape, including the infinitely long strip (2D geometry). For such foundations, vertical and torsional oscillations are uncoupled, while horizontal forces and moments along and around the principal axes produce displacements and rotations only along and around the same axes. Thus, with the notation of Fig. 3, the equations of motion in vertical translation $v(t)$, torsional rotation $\theta(t)$, and coupled horizontal translation $h(t)$ and rocking $r(t)$, all referred to the center of gravity of the machine-foundation system, are respectively:

$$m \cdot \ddot{v}(t) + R_v(t) = Q_v(t) \tag{21}$$

$$I_z \cdot \ddot{\theta}(t) + T_z(t) = M_z(t) \tag{22}$$

$$m \cdot \ddot{h}(t) + R_h(t) = Q_h(t) \tag{23}$$

$$I_{0x} \cdot \ddot{r}(t) + T_r(t) - R_h(t) \cdot z_c = M_r(t) \tag{24}$$

in which: m = total foundation mass; I_{0x} = mass moment of inertia about a principal horizontal axis passing through the center of gravity; I_z = mass moment of inertia around the vertical axis of symmetry; R_v, T_z, R_h and T_r = vertical, torsional, horizontal and rocking reactions of the soil acting at the center of the foundation base (remember Fig. 1b); Q_v, M_z, Q_h and M_r = vertical, torsional, horizontal and rocking exciting forces and moments, acting at the center of gravity and resulting from the operation of the machine.

As already mentioned, only the steady-state response due to a harmonic excitation is of interest here. Not only because most machines usually produce unbalanced forces which indeed vary harmonically with time (rotary or reciprocating engines), but also because non-harmonic forces (such as those, for example produced by punch presses and forging hammers) can be decomposed into a large number of sinusoids through Fourier analysis. Therefore, the excitations may be written as:

$$Q_a = Q_a \exp[\mathrm{i}(\omega t + \phi_a)] \quad a = v, h \tag{25}$$

$$M_a = M_a \exp[\mathrm{i}(\omega t + \phi_a)] \quad a = z, r \tag{26}$$

in which the amplitudes Q_a and M_a are either constants or (more frequently) proportional to the square of the operational frequency $\omega = 2\pi f$; ϕ_a are the phase angles of the four excitations, v, h, r and z.

With the excitation forces described by equations (25)–(26), the steady-state motions may be cast in the form:

$$v(t) = v \cdot \exp(\mathrm{i}\omega t); \quad v = v_1 + \mathrm{i}v_2 \tag{27}$$

$$\theta(t) = \theta \cdot \exp(\mathrm{i}\omega t); \quad \theta = \theta_1 + \mathrm{i}\theta_2 \tag{28}$$

$$h(t) = h \cdot \exp(\mathrm{i}\omega t); \quad h = h_1 + \mathrm{i}h_2 \tag{29}$$

$$r(t) = r \cdot \exp(\mathrm{i}\omega t); \quad r = r_1 + \mathrm{i}r_2 \tag{30}$$

in which: v, θ, h and r are complex, frequency-dependent displacement and rotation amplitudes at the center of gravity. Note that equations (27)–(30) do *not* by any means imply that the four components of motion are all in phase, nor that the phase-angles between the corresponding excitations and motions are equal to ϕ_a (equations (25)–(30)). Instead, the true phase angles ψ_a are 'hidden' in the complex form of each displacement component. For instance, the vertical motion will exhibit:

$$\psi_a = \arctan(v_2/v_1) \tag{31}$$

in which v_1 and v_2 are the real and imaginary parts of v (equation (27)), while its amplitude is of a magnitude:

$$|v| = (v_1^2 + v_2^2)^{1/2} \tag{32}$$

Also, since Q_a and M_a in equations (25)–(26) are real quantities, the phase lags between excitations and motions will be simply equal to $\phi_a - \psi_a$.

Using similar arguments with regard to the soil reactions, one may, without loss of generality, set:

$$R_a = R_a \cdot \exp(i\omega t) \quad a = v, h \tag{33}$$

$$T_a = T_a \cdot \exp(i\omega t) \quad a = z, r \tag{34}$$

whereby the complex amplitudes R_a and T_a are related to the complex displacement and rotation amplitudes through the corresponding dynamic impedances K_a, $a = v, h, r, hr, t$ (see equations (3)–(4)). Recalling that the latter are referred to the center of the foundation base, one can promptly write:

$$R_v = K_v \cdot v \tag{35}$$

$$T_z = K_t \cdot \theta \tag{36}$$

$$R_h = K_h \cdot (h - z_c r) + K_{hr} \cdot r \tag{37}$$

$$T_r = K_r \cdot r + K_{hr} \cdot (h - z_c r) \tag{38}$$

Substituting equations (25)–(30) and (33)–(38) into the governing equations of motion (21)–(24) and solving the resulting system of four algebraic equations yields the following complex-valued displacement and rotation amplitudes at the center of gravity:

$$v = \frac{Q_v \cdot \exp(i\phi_v)}{K_v(\omega) - m\omega^2} \tag{39}$$

$$\theta = \frac{M_z \cdot \exp(i\phi_z)}{K_t(\omega) - I_z\omega^2} \tag{40}$$

$$h = \{K_r^* \cdot Q_h \exp(i\phi_h) - K_{hr}^* \cdot M_r \exp(i\phi_r)\} \cdot N \tag{41}$$

$$r = \{K_h^* \cdot M_r \exp(i\phi_r) - K_{hr}^* Q_h \exp(i\phi_h)\} \cdot N \tag{42}$$

in which the following substitutions have been performed:

$$K_h^* = K_h(\omega) - m\omega^2 \tag{43}$$

$$K_{hr}^* = K_{hr}(\omega) - K_h(\omega)\, z_c \tag{44}$$

$$K_r^* = K_r(\omega) - I_{0x}\omega^2 + K_h(\omega)\, z_c^2 - 2K_{hr}(\omega)\, z_c \tag{45}$$

and, finally,

$$N = (K_h^* K_r^* - K_{hr}^{*2})^{-1} \tag{46}$$

Notice that, for a particular frequency ω, determination of the motions from equations (39)–(42) is a straightforward operation once the dynamic impedances are known. Of course, the computations are somewhat tedious if performed by hand, since complex numbers are involved; but even with small microcomputers the calculations can be done routinely, at a minimal cost.

Therefore, the author proposes that this procedure (equations (39)–(42), in connection with an appropriate evaluation of impedances at the frequency(ies) of interest, should be used in machine foundation analysis in place of the currently popular 'equivalent lumped frequency-independent-parameter' approach.

PRESENTATION OF RESULTS FOR SURFACE AND EMBEDDED FOUNDATIONS

The subsequent four sections of the paper present a comprehensive compilation of characteristic numerical results

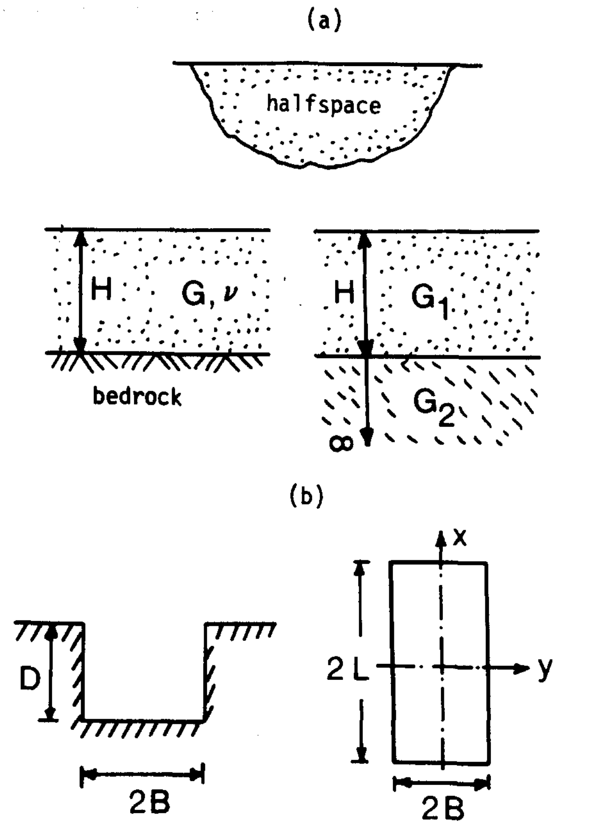

Figure 4. (a) The three soil profiles studied; (b) definition of geometric parameters

for the dynamic impedances (or compliances) of massless foundations, pertaining to all possible (translational and rotational) modes of vibration. These results can be directly used in equations (40)–(43) to make satisfactory and inexpensive predictions of the dynamic behavior of machine foundations in many practical cases, without the need to resort to costly computer programs for evaluating the impedances; this should be of especially great value in preliminary design calculations.

A second, equally important objective of the presentation is to assess the significance of various phenomena and to illustrate the role of key dimensionless geometric and material parameters on the response. It is thus hoped that the reader can gain a valuable insight into the mechanics of foundation vibrations.

Results are presented for three categories of idealized soil profiles (Fig. 4): the halfspace, the uniform stratum on rigid base and the layer on top of a halfspace. These models represent a wide spectrum of actually encountered soil profiles and are simple enough for their geometry to be described in terms of a single quantity, namely, the thickness H of the uppermost layer. (For the halfspace $H \to \infty$.) For most problems considered, the following groups of dimensionless parameters which appreciably influence the dynamic impedances have been identified:

(a) the ratio H/B of the top layer thickness, H, over a critical foundation-plan dimension, B; the latter may be interpreted as the radius, R, of a circular foundation or half the width of a rectangular or a strip foundation
(b) the embedment ratio D/B, where D is the depth from the surface to the horizontal soil-footing interface

(c) the shape of the foundation plan: circular, strip, rectangular, circular ring; in the last two cases the plan geometry may be defined in terms of the length-to-width or 'aspect' ratio, L/B, or the internal-to-external radii ratio, R_i/R, respectively
(d) the frequency factor $a_0 = \omega B/V_s$, where V_s is a characteristic shear wave velocity of the soil deposit
(e) the ratio G_1/G_2 of the shear moduli corresponding to the upper soil layer and the underlying halfspace, respectively; this ratio may attain values ranging from 0, in case of a uniform stratum on rigid base, to 1, in case of a uniform halfspace
(f) the Poisson's ratio(s) ν of the soil layer(s)
(g) the hysteretic critical damping ratio(s) ξ of the soil layer(s)
(h) the factors n and $\tilde{m}$ which express the 'degree' of anisotropy and the 'rate' of inhomogeneity, respectively; $n = E_H/E_V$, where E_H and E_V are the horizontal and vertical Young's moduli of a cross-anisotropic soil; while $\tilde{m}$, for a certain type of inhomogeneity, describes the change of shear modulus from the surface to a depth equal to B
(i) the relative flexural rigidity factor $RF = (E_f/E_s)(1-\nu_f^2)\cdot(t/B)^3$ where E_f, ν_f and t are, respectively, the Young's modulus, Poisson's ratio and thickness of the foundation raft; RF ranges from ∞, for a perfectly rigid foundation, to 0, for an ideally flexible mat.

RIGID SURFACE FOUNDATIONS ON HOMOGENEOUS HALFSPACE

Rigid circular foundation

When dealing with a deep and relatively uniform soil deposit, it makes engineering sense to model it as a homogeneous halfspace. This idealization, primarily because of its simplicity, has been widely employed to determine stresses and deformations in soils, and its use in soil dynamics has led to results in qualitative agreement with observations. From a practical point of view, perhaps the greatest value of the model has been in explaining important features associated with foundation vibrations.

The dynamic impedance functions for a rigid circular foundation on the surface of a homogeneous halfspace have been tabulated by Veletsos *et al.*[28] and Luco *et al.*;[27, 28, 62] Fig. 5 presents their results in the form of equation (17), with zero hysteretic damping ratio. (Obviously, in this case, $\boldsymbol{k} = k$ and $\boldsymbol{c} = c$.) The values of k and c corresponding to non-zero values of internal damping are, for all practical purposes, very similar to those plotted in Fig. 5, in accord with the correspondence principle. Reference is made to Veletsos *et al.*,[29] Luco[66] and Lysmer[63] for a more detailed discussion on this subject. Notice that only the diagonal elements of the impedance matrix are shown in the figure, as the cross swaying-rocking impedance is essentially zero.

It is evident from Fig. 5 that the normalized impedances K_a/GR and K_b/GR^3, where a refers to the translational modes v and h and b to the rotational modes r and t, depend only on the Poisson's ratio ν of the halfspace and the frequency factor a_0. The following trends are worthy of note in Fig. 5.

1. The vertical and rocking stiffness, K, and dynamic stiffness coefficients, $\boldsymbol{k}$, are the most sensitive to variations in Poisson's ratio. On the other hand, the horizontal impedance function has a small dependence on ν, while the torsional response is totally independent of ν at all frequencies. It thus appears that the importance of Poisson's ratio increases when the relative contribution of generated dilational (P) waves increases. Indeed, in the vertical and rocking modes P waves are significant; in the horizontal mode P waves are of secondary importance; and in the torsional mode only SH waves are generated and P waves play no role in the response.

2. The coefficients $\boldsymbol{k}_h$, $\boldsymbol{c}_h$ and $\boldsymbol{c}_v$ are essentially independent of frequency and can be considered constant without any appreciable error. On the other hand, $\boldsymbol{k}_v$, $\boldsymbol{k}_r$, $\boldsymbol{c}_r$ and $\boldsymbol{c}_t$ exhibit a strong sensitivity to variations in the frequency parameter, while $\boldsymbol{k}_t$ shows an intermediate behavior. Of particular interest is the rapid decrease of the vertical and rocking stiffness coefficients $\boldsymbol{k}_v$ and $\boldsymbol{k}_r$ with increasing a_0, for values of Poisson's ratio close to 0.5* (typical for saturated clays). In fact, $\boldsymbol{k}_v$ and $\boldsymbol{k}_r$ become negative for values of a_0 greater than 2.5 and 5, respectively. Some years ago it appeared that use of 'added masses' could adequately account for the decrease with a_0 of the stiffness coefficients, in the range of low frequencies. Such 'masses' would in effect produce dynamic stiffness coefficients of the form $k - m\omega^2$ – a reasonable approximation indeed for low frequencies, which formed the basis of the 'lumped-parameter' model, described in a preceding section of the paper. Unfortunately, as is evident from Fig. 5, this approximation may lead to substantial errors for larger frequencies. Moreover, the concept of 'added mass' has all too often been confused with the physically incorrect notion of an 'in-phase soil mass', which at much earlier times had found considerable use in the design practice.

3. While the damping coefficients of the translational modes, $\boldsymbol{c}_v$ and $\boldsymbol{c}_h$, attain large and nearly constant values throughout the frequency range $0 < a_0 \leqslant 8$, the coefficients $\boldsymbol{c}_r$ and $\boldsymbol{c}_t$ of the two rotational modes are very sensitive to variations in frequency in the low range of a_0, tending to zero as a_0 approaches zero. At larger frequencies (a_0 greater than about 3) $\boldsymbol{c}_r$ and $\boldsymbol{c}_t$ are essentially frequency-independent, but their values both equal to about 0.30, are significantly smaller than the corresponding values of $\boldsymbol{c}_v \simeq 0.95$ and $\boldsymbol{c}_h \simeq 0.60$. These differences imply that a smaller radiation of wave energy takes place during rocking and torsional than during vertical and horizontal oscillations. It seems that the dynamic stress and strain fields induced in the soil by the two types of rotational loadings are of limited extent, with the generated waves decaying very rapidly away from the loading area due to 'constructive interference'. These phenomena will become more evident in connection with the behavior of footings on layered or inhomogeneous soil deposits.

In any case, the practical implication of the existence of only a small amount of radiation damping in the rocking and torsional modes of oscillation is that a realistic estimate of the response may be obtained by incorporating the effects of material (hysteretic) damping in the soil. On the contrary, material damping is insignificant for horizontal and, especially, vertical oscillations and, with little loss in accuracy, it may be neglected in the presence of the much higher radiation damping.

---

* It is noted that although for saturated soft clays under static undrained loading one should use $\nu = 0.50$, with dynamic loading $\nu = 0.50$ leads to infinite dilatational wave velocity, which is not observed in the laboratory; instead the Biot–Ishihara theory for poroelastic media yields a maximum value of ν slightly less than 0.50.

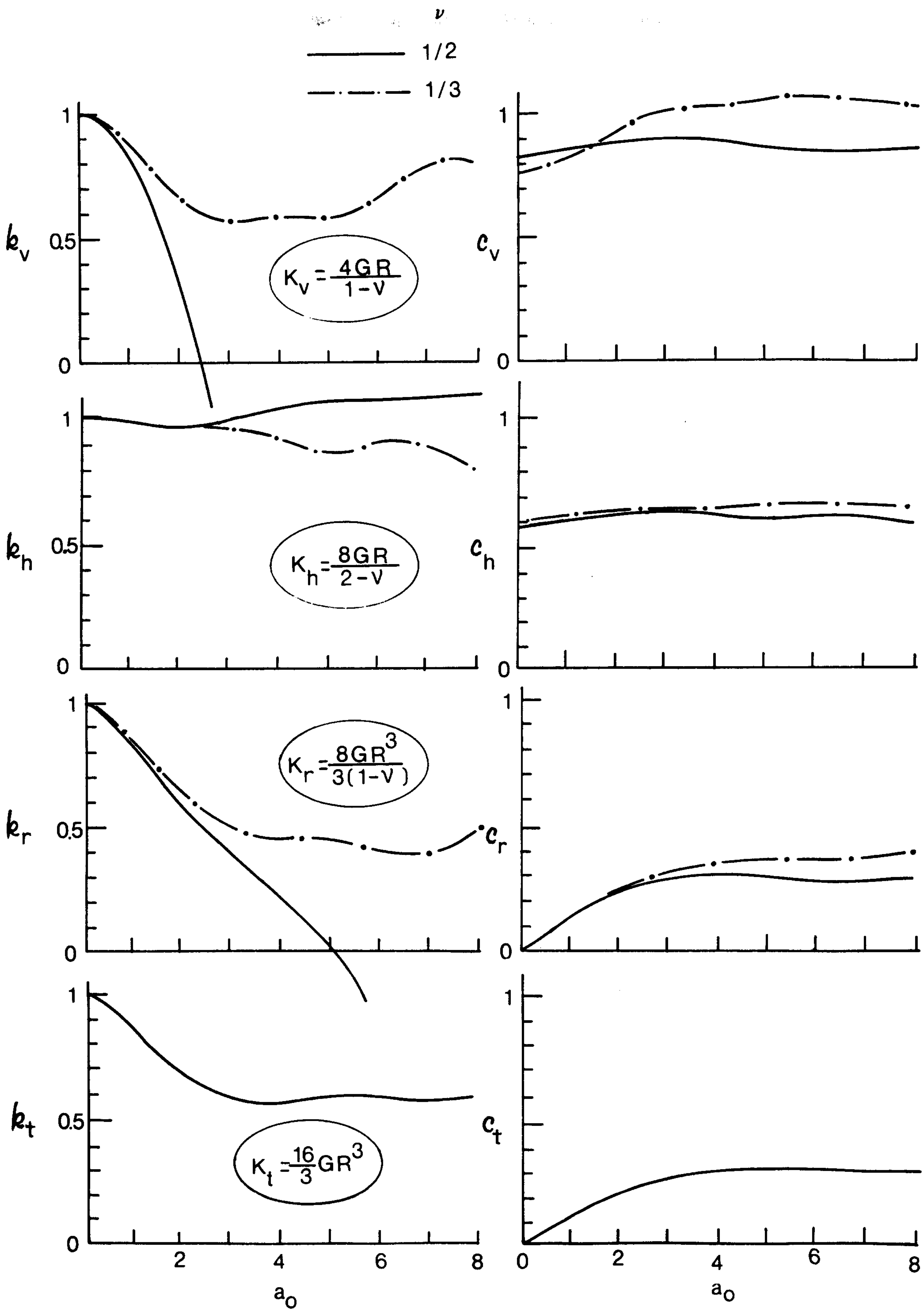

Figure 5. Impedance functions of rigid circular footings on homogeneous halfspace[27, 28, 62]

Clearly, soil deposits having a constant G and extending to practically infinite depths, as the homogeneous halfspace model assumes, do not abound in nature. In addition, circular foundations are rather rarely constructed. Nonetheless, the results of Fig. 5 for a circular foundation on a halfspace are of great value in understanding the phenomena associated with foundation vibrations. From a practical point of view, however, the shape and trends of these impedance functions are more important than their exact values.

Rigid strip foundation

When dealing with long and narrow foundations, the length of which is larger than their width by a factor of 5 or greater, it is a common practice to idealize their shape as an infinitely long strip. If, moreover, the dynamic loading is reasonably uniform along the longitudinal direction, plane-strain conditions prevail throughout and 2D analyses are sufficient to obtain the response.

Figure 6 displays the dynamic impedance of a rigid strip foundation on the surface of a homogeneous halfspace. These results were obtained by the semi-analytical procedure of Gazetas[36] and Gazetas and Roesset[38] and are in agreement with the results of Karasudhi *et al.*[26] It is noted that in this case the impedance functions are presented in the form described by equation (4), and not in one of the most usual forms of equations (12) or (17). The necessity for this change stemmed from the fact that the static vertical and horizontal stiffnesses of an infinite strip on a halfspace are zero, in agreement with the classical theory of elasticity. This is at variance with the behavior of circular foundations, whose (nonzero) static stiffnesses can be

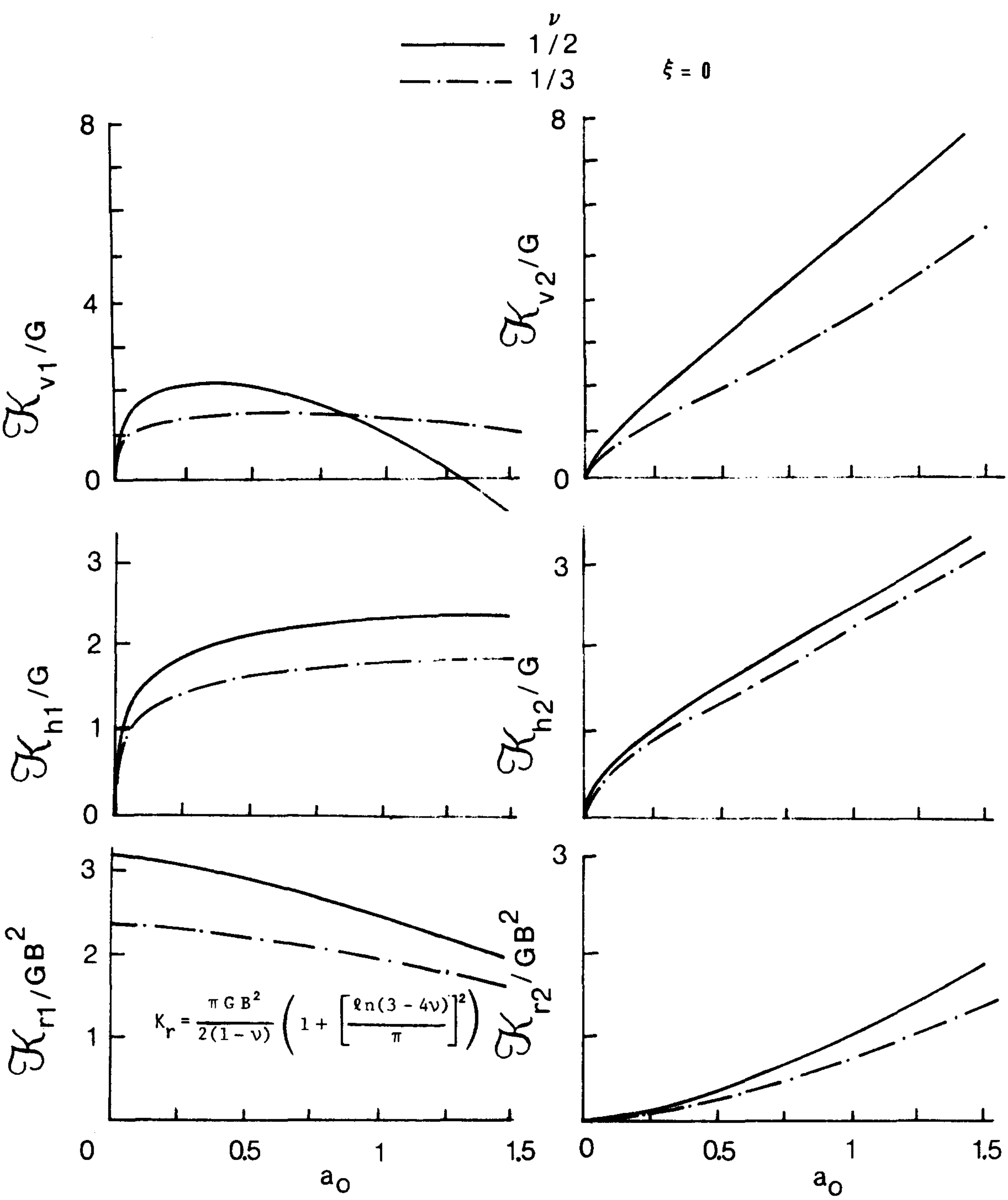

Figure 6. Impedance functions of rigid strip footings on homogeneous halfspace

found from the expressions included in Fig. 5. The infinite displacement of a strip-loaded halfspace arise from the large depths of the corresponding 'zones of influence'. In other words, the static stresses induced by the strip surface loads decay slowly with depth and, thus, cause appreciable straining of even remote soil elements; accumulation of these strains yields infinite displacements.

On the other hand, the stress and strain fields induced by moment loading are confined to the near surface soil only, thereby producing small surface displacements and non-zero static stiffnesses. For a rigid strip foundation, an expression for the static rocking stiffness is included in Fig. 6.

A few other trends are worthy of note in Fig. 6. First, one should notice that there are only three possible modes of vibration of a strip (vertical, horizontal and rocking) as compared to the four modes of a circular footing. Apparently, torsional oscillations involve out-of-plane motions and hence are impossible with strip footings.

In general, the dependence of the dynamic impedances on the Poisson's ratio of soil is very similar for strip and circular foundations. Thus, the discussion of the preceding section on the sensitivity of circular impedance functions to ν, is also applicable to the present case.

Regarding the variation of impedances with frequency, on the other hand, there are some differences between circular and strip footings, although clearly the general trends are similar. Thus, in the very low frequency range, the real parts K_{v1} and K_{h1} of the two translational modes increase with increasing a_0 and they attain peak values of a_0 ranging from about 0.25 to about 1.0, depending primarily on the Poisson's ratio and the type of oscillation. This implies that 'constructive interference' of various P and S waves originating at the soil-foundation interface reduces the depth of the 'zone of influence'; this results into finite displacements and non-zero dynamic stiffnesses.

Beyond their peak values, K_{v1} and K_{h1} behave much like their circular counterparts. Notice, however, that at Poisson's ratios close to 0.50 the vertical strip stiffness becomes negative at a_0 values greater than 1.3, as compared with the corresponding value of 2.5 which was observed for circular footings in Fig. 5.

The imaginary parts K_{v2} and K_{h2} of the vertical and horizontal modes increase almost linearly with a_0, thus indicating qualitatively similar radiation damping characteristics of strip and circular foundations. (Notice that the damping coefficients c in the latter case are proportional to the slopes of the imaginary component of impedance-versus-a_0 curves; hence a constant c implies a linearly varying K_2.)

Finally, the rocking stiffness and damping terms of both strip and circular foundations exhibit essentially identical trends. Evidently, rocking induced static or dynamic stresses influence only the near-surface soil under both plane-strain and axisymmetric loading conditions.

Rigid rectangular foundation

Results are now available for the complete dynamic impedance matrix of rigid rectangular foundations with varying aspect ratios L/B, over the low and medium frequency range.[47] For the vertical, horizontal and rocking modes, in particular, results are available even for moderately high values of a_0.[44, 46, 48]

Again, in presenting the variation with frequency and aspect ratio of impedances it is convenient to express them in the form of equation (17), with $a_0 = \omega B/V$, where $2B$ is the width of the smallest side of the foundation. Results for the static stiffnesses are presented first.

It has been known for some time that the static stiffness of a typical rectangular foundation can be approximated with reasonable accuracy by the corresponding stiffness of '*equivalent*' circular foundations. For the translational modes in the three principal directions (x, y and z) the radius R_0 of the 'equivalent' circular foundation is obtained by equating the areas of the contact surfaces; hence:

$$R_0 = \left(\frac{2B \cdot 2L}{\pi}\right)^{1/2} \tag{47}$$

For the rotational modes around the three principal axes, the 'equivalent' circular foundations have the same area moments of inertia around x, y and z, respectively, with those of the actual foundation. Thus, the equivalent radii are:

$$R_{0x} = (16L \cdot B^3/3\pi)^{1/4} \tag{48}$$

for rocking around the x-axis;

$$R_{0y} = (16B \cdot L^3/3\pi)^{1/4} \tag{49}$$

for rocking around the y-axis; and

$$R_{0z} = \left[\frac{16B \cdot L \cdot (B^2+L^2)}{6\pi}\right]^{1/4} \tag{50}$$

for torsion around the z-axis.

The results of recent parametric studies have confirmed the similar static behavior of rectangular and equivalent circular foundations. Table 2 is a synthesis of the results of several such investigations. It presents theoretically 'exact' formulae for all the translational and rotational static stiffnesses of rigid rectangular foundations having a wide range of aspect ratios. These formulae are cast in the form:

$$K = K_0(R_0) \cdot J(L/b) \tag{51}$$

in which: K = the actual static stiffness; $K_0(R_0)$ = the corresponding stiffness of the equivalent circular foundation, obtained from Fig. 5; R_0 = the radius of the 'equivalent' circle; and $J(L/B)$ = a 'correction' factor, function of the aspect ratio, L/B. If $J(L/B)$ were equal to 1 for all aspect ratios, the static equivalence between the two types of footings would have been perfect. Conversely, the larger the difference is between $J(L/B)$ and 1, the less accurate it would be the approximate a rectangular with a circular footing.

It may first be noted that only small discrepancies exist in the values of the 'correction' functions computed from the results of several authors. These discrepancies are due to either the assumed soil-footing interface behavior ('smooth' versus 'adhesive' contact), or the employed different numerical solution schemes. In practice, however, in view of the small magnitude of these differences, one may safely use for $J(L/B)$ the average of the values presented in Table 2, for each particular aspect ratio.

The following conclusions are evident from this Table.

1. Even for aspect ratios, L/B, as high as 8, the 'equivalent' circular foundations yield stiffnesses which are within 30% of the corresponding stiffness of the actual rectangular foundation. This is by no means a large error, in view, for example, of the uncertainty in estimating the soil modulus in practice.

2. For aspect ratios, L/B, less than 4 the 'equivalent' stiffnesses are in very good agreement with the actual

Table 2. Static stiffnesses for rectangular rigid foundation

1. Vertical stiffness

$$K_z \equiv K_v = \frac{4GR_0}{1-\nu} \cdot J_v(L/B)$$

$\frac{L}{B}$	Gorbunov-Posadov (1961)	Barkan (1962)	Savidis (1977)	Dominguez *et al.* (1978) 'Adhesive'	Dominguez *et al.* (1978) 'Smooth'
	'Correction' factor J_v				
1	1.023	0.953	0.944	1.052	1.081
2	1.025	0.975	0.973	1.063	1.130
4	1.108	1.077	1.072	1.107	1.196
6	1.197	1.152	–	–	–
8	1.266	1.196	1.200	–	–
10	1.313	1.250	–	–	–
20	1.572	–	–	–	–

2. Horizontal stiffnesses

$$K_x = \frac{8GR_0}{2-\nu} \cdot J_x(L/B) \quad K_y = \frac{8GR_0}{2-\nu} \cdot J_y(L/B)$$

$\frac{L}{B}$	'Correction' factor J_x: Barkan (1962)	'Correction' factor J_x: Dominguez *et al.* (1978)	'Correction' factor J_y: Barkan (1962)	'Correction' factor J_y: Dominguez *et al.* (1978)
1	0.993	1.035	0.993	1.035
2	0.983	1.044	1.008	1.105
4	1.000	1.085	–	1.221
6	1.055	–	–	–
8	1.132	–	–	–
10	1.191	–	–	–

3. Rocking stiffnesses

$$K_{r_x} = \frac{8GR_{0x}^3}{3(1-\nu)} \cdot J_{rx}(L/B) \quad K_{r_y} = \frac{8GR_{0y}^3}{3(1-\nu)} \cdot J_{ry}(L/B)$$

$\frac{L}{B}$	'Correction' factor J_{rx}: Gorbunov-Posadov *et al.* (1961)	'Correction' factor J_{rx}: Dominguez *et al.* (1978)	'Correction' factor J_{ry}: Gorbunov-Posadov *et al.* (1961)	'Correction' factor J_{ry}: Dominguez *et al.* (1978)
1	0.991	0.965	0.991	0.965
2	1.034	1.039	1.035	1.031
4	1.0488	1.117	1.072	1.140
8	1.178	–	1.226	–
10	1.281	–	1.319	–

4. Torsional stiffness

$$K_{r_z} \equiv K_t = \frac{16}{3} GR_{0z}^3 \cdot J_t(L/B)$$

$\frac{L}{B}$	'Correction' factor J_t: Dominguez *et al.* (1978)	'Correction' factor J_t: Roesset *et al.* (1977)
1	0.950	1.0332
2	1.000	–
3	1.016	–
4	1.166	–

ones. Typically, the error is within 10% and, hence, it is insignificant for all practical purposes.

3. The greatest differences are observed between actual and 'equivalent' stiffnesses for torsion (K_t) and for horizontal displacement in the y direction (K_y). For $L/B = 4$, the error in K_t is about 17% and in K_y about 22%. It is worthy of note that whereas for a circular foundation $K_{x0} = K_{y0} = 8GR_0/(2-\nu)$, where R_0 is given by equation (47), a rectangular foundation with the larger side $2L$ normal to the y-axis (Fig. 4) is characterized by:

$$K_y \simeq K_x + \tfrac{1}{2}GB\left(\frac{L}{B} - 1\right) \tag{52}$$

for typical values of Poisson's ratio.

Variation with a_0. Figure 7 portrays the dependence of the dynamic stiffness and damping coefficients, k and c, on the frequency factor a_0 and the aspect ratio L/B. These results were obtained with the Boundary Element Method by Dominguez and Roesset,[47] for a single value of Poisson's ratio, $\nu = \frac{1}{3}$. Only the coefficients of the six diagonal components of the impedance matrix are shown, they correspond to the translational modes of vibration (x, y and z) along each of the three principal axes, and to the rotational modes (r_x, r_y and r_z) around each of the same three principal axes. The two cross-swaying-rocking (coupling) impedances, corresponding to the xr_y and yr_x modes, are negligibly small for surface foundations, and are thus omitted from this presentation. Also shown in Fig. 7 as circles are the predictions of the 'equivalent' circular foundations, computed from Fig. 5 in conjunction with equations (47)–(50). One may notice the following trends in Fig. 7.

1. The terms k_x and c_x of the impedance against motion normal to the smaller side $2B$ are insensitive to variations in a_0. Moreover, k_x is essentially independent of the aspect ratio, L/B, while c_x increases almost in proportion to the square-root of L/B. Recall that c_x must be multiplied by $a_0 = \omega B/V_s$ to obtain the imaginary component of the dynamic part of the impedance (equations (12) or (17)), in which $2B$ is the width of the smallest side of the footing. On the other hand, the frequency factor a_{00} of the 'equivalent' footing equals $\omega R_0/V_s$, with:

$$R_0 = \frac{2}{\sqrt{\pi}} B\left(\frac{L}{B}\right)^{1/2} \tag{47a}$$

i.e. a_{00} is proportional to the square-root of L/B. Hence, plotted in Fig. 7, both stiffness and damping coefficients of the 'equivalent' footing are in excellent agreement with the corresponding coefficients of the actual rectangular footing, for all aspect ratios studied ($L/B = 1-4$), at least in the frequency range, $0 < a_0 \leqslant 1.5$.

2. The variation of the vertical stiffness and damping coefficients, k_v and c_v, has a similar shape with the variation of k_x and c_x. In this case, however, the two coefficients are more sensitive to variations in a_0 and L/B and the damping term c_v is always larger than c_x. Moreover, the agreement between actual and 'equivalent' coefficients is reasonably good, for all practical purposes.

3. The coefficients k_y and c_y, for a motion parallel to the smaller side $2B$, show a greater sensitivity to both a_0 and L/B. Furthermore, the discrepancies between 'equivalent' and actual values for these coefficients are appreciable, increasing with the aspect ratio. In fact, footings with a large L/B ratio (e.g. $\geqslant 4$) tend to behave more like strip rather than circular footings, as a comparison between Figs. 5, 6 and 7 indicates.

4. The stiffness coefficient k_{r_x} for rocking around the longest axis, x, exhibits no sensitivity to the aspect ratio,

L/B; moreover, its variation as a function of a_0 is nearly identical with the variation of the corresponding stiffness coefficient of both the 'equivalent' circular footing and a strip footing with the same width B (Fig. 6). The damping coefficient c_{r_x} attains negligible values in the low frequency range and increases approximately in proportion to the fourth-root of L/B at high frequencies. Recalling that the frequency factor of the 'equivalent' circular footing is proportional to:

$$R_{0x} = \frac{2}{(3\pi)^{1/4}} B \left(\frac{L}{B}\right)^{1/4} \tag{48a}$$

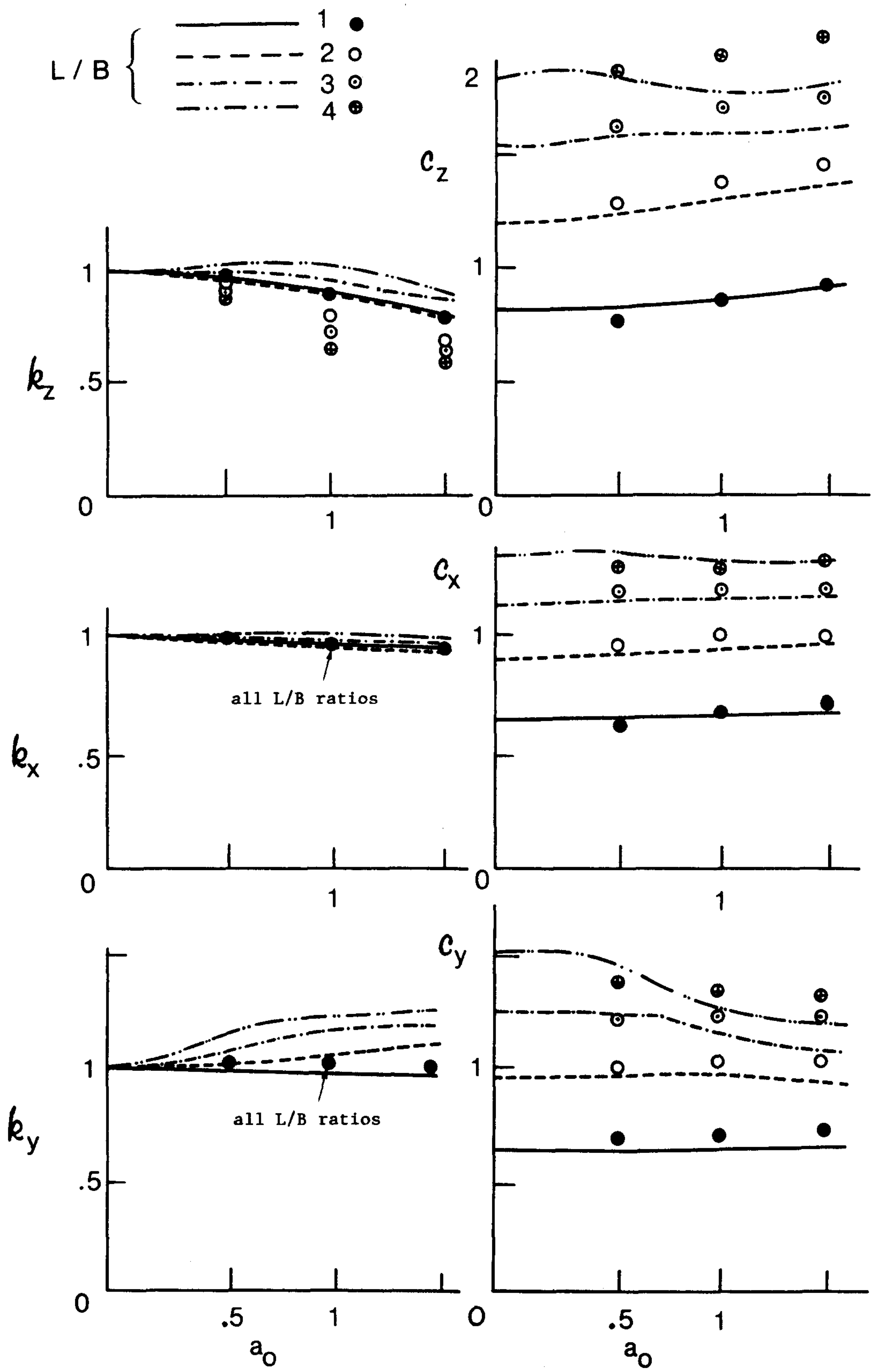

Figure 7. Dynamic coefficients of rigid rectangular footings on homogeneous halfspace;[47] (circles obtained by this author for 'equivalent' circular footings)

Figure 7 – continued

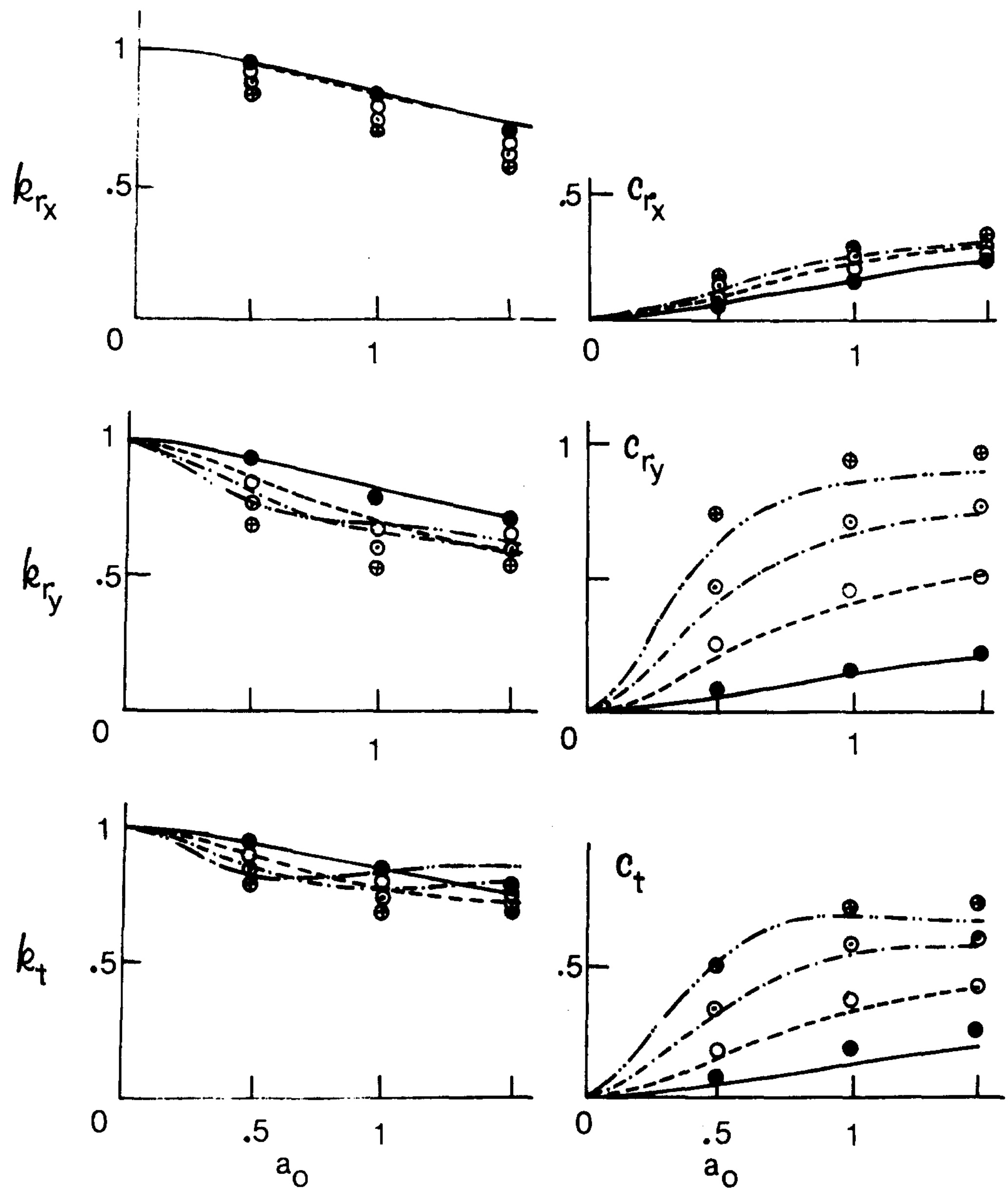

whereas the term c_{r_x} is multiplied simply by $a_0 = \omega B/V_s$ in equations (12) or (17), one can directly unveil the very close proximity between the actual and 'equivalent' damping coefficients.

5. The stiffness coefficients k_{r_y} and k_t for rocking around the shortest axis and torsion, respectively, show a somewhat similar dependence on L/B and exhibit some fluctuations with a_0 as L/B increases. The two coefficients are predicted only with small accuracy by the 'equivalent' circular footings. On the other hand, the two damping coefficients c_{r_y} and c_t grow rapidly with both frequency and aspect ratio. In this regard, it is interesting to notice that, for instance, the frequency factor for the r_y mode is proportional to:

$$R_{0y} = \frac{2}{(3\pi)^{1/4}} B\left(\frac{L}{B}\right)^{3/4} \qquad (49a)$$

which reveals a much stronger increase of c_{r_y} with L/B, as compared with the corresponding increase of c_{r_x} (a power of $\frac{3}{4}$ for c_{r_y} versus $\frac{1}{4}$ for c_{r_x}). Again, the values of the two coefficients may be reasonably well predicted by the 'equivalent' circular foundation.

In conclusion, with the help of the formulae of Table 2 and the graphs of Fig. 7, the dynamic behavior of rectangular foundations with essentially any aspect ratio can be obtained. Furthermore, the 'equivalent' circular footings described through equations (47)-(50), yield reasonably good estimates of the response for values of L/B less than about 4 and frequency factors at least up to 1.5. For larger values of L/B, the static stiffnesses of Table 2 can be utilized in conjunction with the dynamic coefficients of an equal-width strip foundation (Fig. 6). More parametric studies are, however, necessary to obtain results in the high frequency range ($1.5 < a_0 \leqslant 8$).

RIGID SURFACE FOUNDATIONS ON A HOMOGENEOUS SOIL STRATUM

Natural soil deposits very rarely have uniform properties within large depths from the loaded surface. More typical is the presence of a stiffer material or even bedrock at a relatively shallow depth. The response of a foundation on a soil stratum underlain by such a stiffer medium can be substantially different from the response of an identical foundation resting on a uniform halfspace. It is, thus, imperative to study the dynamics of massless foundations on such soil deposits. Specifically two types of idealized soil profiles are considered in this section:

(a) a homogeneous soil stratum over a rigid base, and
(b) a homogeneous soil stratum over a homogeneous halfspace.

Results for non-homogeneous soil strata, with moduli continuously increasing or decreasing with depth, will be presented in a subsequent section of the paper.

In addition to the four dimensionless parameters which control the behavior of rigid footings on a halfspace, namely, a_0, ν, ξ and L/B, the ratio H/B (or H/R) is of crucial importance in the response of footings on a homogeneous stratum. Its effect is, thus, studied throughout this section. Furthermore, the moduli ratio G_1/G_2 is of interest whenever the soil stratum is underlain by a non-rigid base (halfspace).

Circular foundation on stratum over a rigid base

Results for the dynamic impedance functions of a rigid circular disk at the surface of a stratum-on-rigid-base are presented in Table 3 and in Figs. 8 and 9. Specifically, Table 3 offers simple and quite accurate formulae for the determination of the static stiffnesses; Fig. 8 studies the effect of the H/B ratio on the dynamic stiffness and damping coefficients, k and c, for a single value of hysteretic damping ratio, $\xi = 0.05$; and Fig. 9 shows the sensitivity of k and c to variations in ξ, for a single value of the ratio, $H/B = 2$. These results have been derived by Kausel[33] and Kausel *et al.*[89, 90] and have been discussed by Roesset.[60, 91] Several significant conclusions may be drawn from this data.

Static stiffnesses. It is evident from the formulae of Table 3 that the existence of rigid bedrock at a relatively shallow depth may drastically increase the static stiffnesses of a rigid surface foundation. The four expressions reduce to the corresponding halfspace stiffnesses when H/R tends to infinity, but their values increase with decreasing H/R.

Vertical stiffnesses are particularly sensitive to variations in the depth to bedrock (notice the 1.28 factor). Horizontal stiffnesses are also appreciably affected by H/R (factor of 0.5) while the rotational stiffnesses (rocking and torsion) are the least affected. In fact, for $H/R > 1.5$ the response to torsional loads is practically independent of the layer thickness.

An indication of the causes of this different behavior of a circular footing to the four different types of loading can be obtained by observing the depths of the 'zone of influence' (known as 'pressure bulb' ever since Terzaghi) in each case. Thus, from Gerrand and Harrison,[92] in a homogeneous halfspace, the vertical normal stress, σ_z, along the centerline of a vertically loaded rigid circular disk becomes less than 10% of the average applied pressure at depths greater than $z_v \cong 4R$; the horizontal shear stress, τ_{zr}, becomes less than 10% of the average applied shear traction at depth greater than $z_h \cong 2R$. From Gazetas,[93] the horizontal shear stresses $\tau_z\theta$ and $\tau_r\theta$ due to linearly distributed torsional surface stresses become less than 10% of the maximum applied shear traction at $z > z_t \simeq 0.75R$. Finally, moment loading with a linear distribution of normal tractions varying from 0 to p yields $z_r \simeq 1.25R$, below which σ_z is less than $0.10p$.

Variation with a_0, H/R and ξ. The variation of the dynamic stiffness and damping coefficients with frequency reveals an equally strong dependence on H/B. On a stratum, both k and c are not as smooth functions as on a halfspace, but exhibit undulations (peaks and valleys) associated with the natural frequencies (in shear and dilation) of the soil layer. In other words, the observed fluctuations are the outcome of resonance phenomena: waves emanating from the oscillating foundation reflect at the soil-bedrock interface and return back to their source at the surface. As a result, the amplitude of foundation motion may significantly increase at specific frequencies of vibration, which, as shown subsequently, are close to the natural frequencies of the deposit. Thus, the stiffness coefficients exhibit valleys which are very steep when the hysteretic damping in the soil is small (in fact, in certain cases, k would be exactly zero if the soil were ideally elastic); on the other hand, with large amounts of hysteretic damping ($\xi = 0.10-0.20$) the valleys become less pronounced (Fig. 9). They also become less pronounced as the relative thickness of the layer, H/R, increases (Fig. 8).

Another important phenomenon is revealed through the variation with a_0 of the damping coefficients. At low frequencies, below the first resonant frequency, radiation damping is zero. This is due to the fact that no surface waves can be physically created in a soil stratum at such frequencies and, since the bedrock prevents waves from propagating downward, geometrical spreading of wave energy is negligible. The small values of the damping in this range (Fig. 9) just reflect the energy loss through hysteretic damping; for a purely elastic soil c would be zero.

*Table 3. Static stiffnesses of rigid circular foundation on a stratum-over-rigid-base**

Type of loading	Static stiffness	Range of validity†	Soil profile
Vertical:	$K_v = \dfrac{4GR}{1-\nu}\left(1 + 1.28\dfrac{R}{H}\right)$	$H/R > 2$	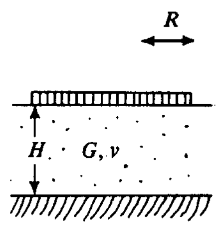
Horizontal:	$K_h = \dfrac{8GR}{2-\nu}\left(1 + \dfrac{1}{2}\dfrac{R}{H}\right)$	$H/R > 1$	
Rocking:	$K_r = \dfrac{8GR^3}{3(1-\nu)}\left(1 + \dfrac{1}{6}\dfrac{R}{H}\right)$	$4 > H/R > 1$	
Torsion:	$K_t = \dfrac{16}{3}GR^3$	$H/R > 1.25$	

* Adapted from Kausel[33] and Kausel *et al.*[90]
† For $H/R < 2$ or 1 these expressions would still provide reasonable estimates of the actual static stiffnesses

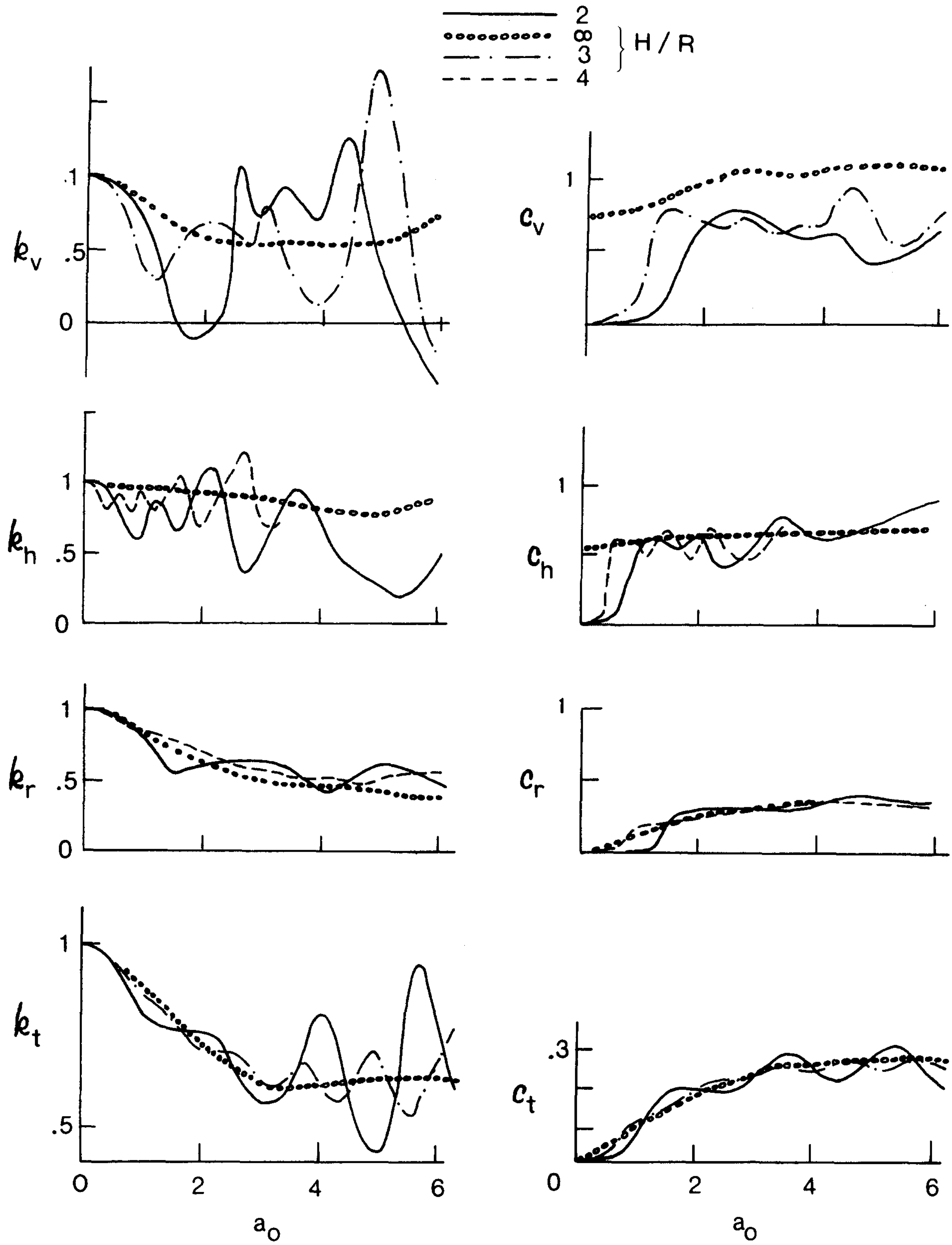

Figure 8. Dynamic coefficients of rigid circular footing on stratum-over-bedrock; effect of H/R ratio ($\nu = 1/3$, $\xi = 0.05$)[33, 88, 90]

The phenomena described in the two preceding paragraphs are observed to a larger or lesser degree in all four modes of vibration. However, there exist marked differences among the dynamic coefficients of vertical, swaying, rocking and torsional oscillations. Specifically:

1. For rocking and torsion, k and c are relatively smooth functions of a_0, rapidly approaching the corresponding half-space curves as the layer thickness increases beyond $3R$. Thus, H/R exerts only a small influence on the variation of these two coefficients. On the other hand, for vertical and horizontal translation, k and c display some very pronounced fluctuations with a_0. Both the location and the shape of the resonant valleys are quite sensitive to variations in H/R, and only for H/R values larger than 8 do

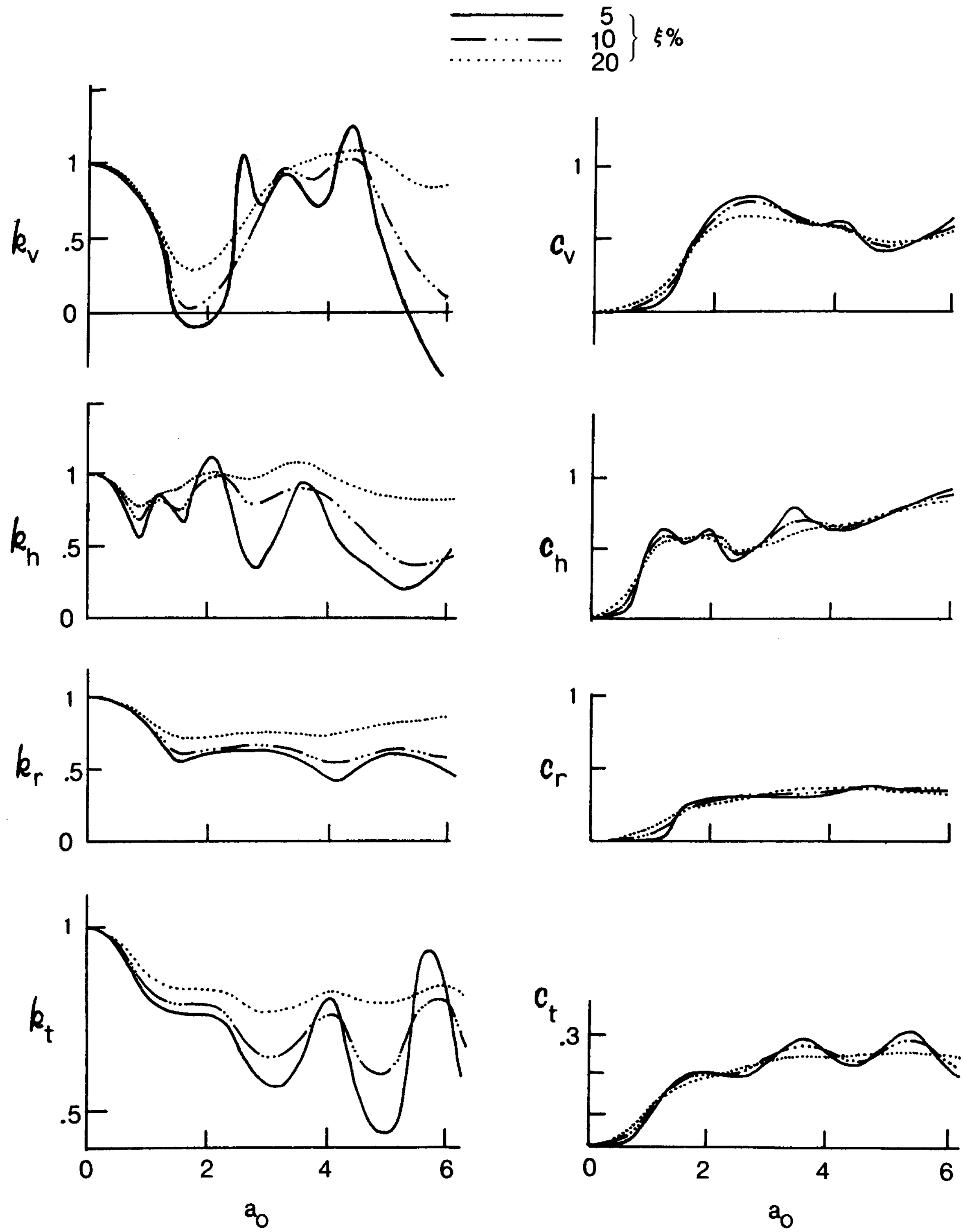

Figure 9. Dynamic coefficients of rigid circular footing on stratum-over-bedrock; effect of ξ ($\nu = 1/3$, $H/R = 2$)[33,90]

$k(a_0)$ and $c(a_0)$ approach the corresponding halfspace curves, if $\xi = 0.05$. These results are consistent with the conclusions derived previously regarding the depth of the 'pressure bulb' or 'influence zone' of a statically loaded foundation. Under dynamic loads, 'constructive interference' of downward propagating waves leads to a *shallow dynamic 'pressure bulb' in both rocking and torsion*.

2. The resonant frequencies of horizontal (swaying) oscillations are in remarkable agreement with the natural frequencies of the stratum. As an example, the fundamental frequency of the stratum in vertical shear waves, $f_{s,1}$, equals $V_s/4H$ and, thus:

$$a_{0s,1} = \frac{\pi}{2}\frac{R}{H} \tag{53}$$

which is equal to $\pi/4$, for $H/R = 2$. As seen in Fig. 9, this value of a_0 essentially coincides with the first resonant frequency in swaying. It is not difficult to explain how the simple one-dimensional wave propagation theory can so successfully predict the first resonant frequency of a three-dimensional problem: at values of a_0 below resonance essentially *only shear waves exist in the stratum*, propagating vertically between foundation and bedrock. Therefore, when this first resonance occurs we have a nonedimensional 'standing' wave and, in addition, little damping and thus high response. Of course, as it may be inferred from Figs. 8-9, the situation becomes a little more involved at higher resonant frequencies. Thus, the second 'resonance' occurs at about the fundamental natural frequency of the stratum in dilational waves, and the third 'resonance' at about the second natural frequency in shear waves. In both cases, however, some non-vertical waves also participate in the motion, as evidenced by the existence of non-zero radiation damping. Due to multiple wave reflections, P, S and Rayleigh waves are also generated and, hence, the one-dimensional theory predicts with smaller accuracy the pertinent swaying resonant frequencies of the soil-foundation system.

On the other hand, vertical and rocking foundation oscillations *induce mainly P but also S waves in the stratum*. The relative importance of each type of wave depends to some extent on the Poisson's ratio of the soil. Recall that the ratio between the two wave velocities and between the corresponding natural frequencies of the stratum is given by:

$$\frac{V_p}{V_s} = \frac{f_{p,n}}{f_{s,n}} = \left[\frac{2(1-\nu)}{1-2\nu}\right]^{1/2} \qquad n = 1, 2, 3, \ldots \tag{54}$$

which, for $\nu = \frac{1}{3}$ yields a ratio of 2. Figures 8-9 clearly show that the first resonant frequencies for both vertical and rocking oscillations are reasonably close to the fundamental frequency of the stratum in vertical P-waves ($a_{0p,1} = \pi/2$ for $H/R = 2$). Higher resonances, however, can hardly be predicted by the simple one-dimensional wave propagation theory since, apparently, they involve a mixture of P-, S- and Rayleigh (R) waves.

Referring to Fig. 9, it is observed that k and c are quite sensitive to variations in material damping, especially at frequencies near resonance. This is contrary to the so-called 'correspondence principle' which assumes that the impedances derived for an undamped but otherwise identical medium by a simple multiplication with the factor $1+2i\xi$. Remember, however, that this 'principle' works reasonably well for a homogeneous halfspace.

The effect of Poisson's ratio is not studied in detail herein and reference is made to Kausel *et al.*[89] for a rigorous assessment of its importance in swaying and rocking. Note, nonetheless, that the variation of the dynamic coefficients with frequency may be sensitive to this parameter, because of its influence on V_p and $f_{p,n}$ as previously explained (equation (54)). Thus, vertical and rocking coefficients are highly sensitive to ν, especially with shallow layers; but swaying and torsional coefficients are practically independent of ν.

Strip foundation on stratum over a rigid base

Table 4 and Figs. 10 and 11 present the results for vertical, horizontal and rocking oscillations of a massless rigid strip footing which rests on the surface of a homogeneous soil layer overlying bedrock. These results were obtained with the formulation of Gazetas and Roesset[38, 39] and are in excellent agreement with the results of Chang-Liang.[87] Additional numerical studies can be found in Jakub *et al.*[56, 65] and Gazetas.[54]

Static behavior. Simple expressions of sufficient accuracy for practical purposes have been derived for the three static stiffnesses and these are listed in Table 4. Evidently, the presence of (infinitely rigid) bedrock at shallow relative depths has a dramatic effect on the static behavior of strip foundations. Vertical and horizontal stiffnesses, being no longer zero as in the case of a halfspace, are strongly increasing functions of B/H. Rocking stiffness also increases with B/H. Two noteworthy conclusions may be drawn by contrasting the expressions of Table 4 to those of Table 3:

1. The effect of Poisson's ratio on the static stiffnesses is the same for both strip and circular rigid foundations. The effect is greatest for vertical and rocking loading [factor $(1-\nu)$] and smallest for horizontal loading [factor $(2-\nu)$].
2. Layer depth is substantially more important for strip than for circular foundations, especially with the two translational modes (factors of 3.5 and 2 in the vertical and rocking expressions for a strip, as compared with 1.28 and 0.5 in the corresponding expressions for a circle). This is a natural consequence of the much deeper 'pressure bulb' in a continuum subjected to plane-strain rather than axisymmetric surface loading, as it has already been illustrated in preceding sections.
3. Vertical stiffness is far more sensitive to variations in B/H (factor of 3.5) than horizontal and rocking stiffnesses are (factors of 2 and 0.20, respectively). The explanation lies again in the much greater 'depth of influence' of the vertical loads. On the other hand, moment loading induces stresses which decay very rapidly with depth; because on any horizontal plane, *small* normal stresses at large distances from the centerline contribute much to equilibrating the applied moment. Thus, rocking stiffnesses exhibit about the same small sensitivity to layer depth for

Table 4. Static stiffnesses of rigid strip foundation on a stratum-over-rigid-base

Type of loading	Static stiffness (per unit length)	Range of validity*	Soil profile
Vertical:	$K_v = \frac{1.23G}{1-\nu}\left(1 + 3.5\frac{B}{H}\right)$	$1 < H/B \leqslant 10$	
Horizontal:	$K_h = \frac{2.1G}{2-\nu}\left(1 + 2\frac{B}{H}\right)$	$1 < H/B \leqslant 8$	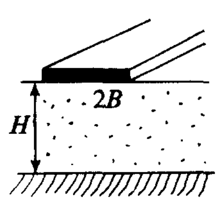
Rocking:	$K_r = \frac{\pi G B^2}{2(1-\nu)}\left(1 + \frac{1}{5}\frac{B}{H}\right)$	$1 < H/B \leqslant 3$	

* Outside this range the proposed expressions would still provide reasonable estimates of the actual static stiffnesses

both strip and circular footings (factors of 1/5 and 1/6, respectively).

Dynamic behavior. Figures 10 and 11 portray the variation with frequency of the dimensionless compliance functions GF_a, where $a = v$ or h, and GB^2F_r. Specifically, Fig. 10 intends to show the effect of H/B, and Fig. 11 the effect of ν. The results of Fig. 10 were obtained for $\nu = 0.49$ and $\xi = 0.05$, with four different values of H/B, i.e. 1, 3, 8 and ∞; the last value corresponds to the homogeneous halfspace and is included for a comparison. Figure 11 shows the effect of ν on vertical and rocking compliances only, for a layer with $H/B = 2$ and a homogeneous halfspace; the effect of ν on swaying, being of secondary importance, is not studied herein.

The same general trends observed in the dynamic behavior of circular foundations can now be seen in the response of strip footings, although some differences are also obvious.

One first notices in Figs. 10–11 that due to the presence of bedrock both the in-phase (real) and the 90°-out-of-phase (imaginary) components of displacement (compliance) are not smooth and monotonically decreasing functions of frequency, as on a halfspace. Instead, they exhibit peaks and valleys at frequencies related to the natural frequencies of the stratum. Note that, in general, the peaks of a compliance function correspond to valleys in the impedance function.

The major differences between strip and circular foundations stem from the much greater sensitivity of the vertical and swaying oscillation of a strip to variations in H/B. Even for $H/B = 8$, relatively high amplitude peaks are observed in the two compliance functions of the strip, for the case $\xi = 0.05$; their difference from the halfspace

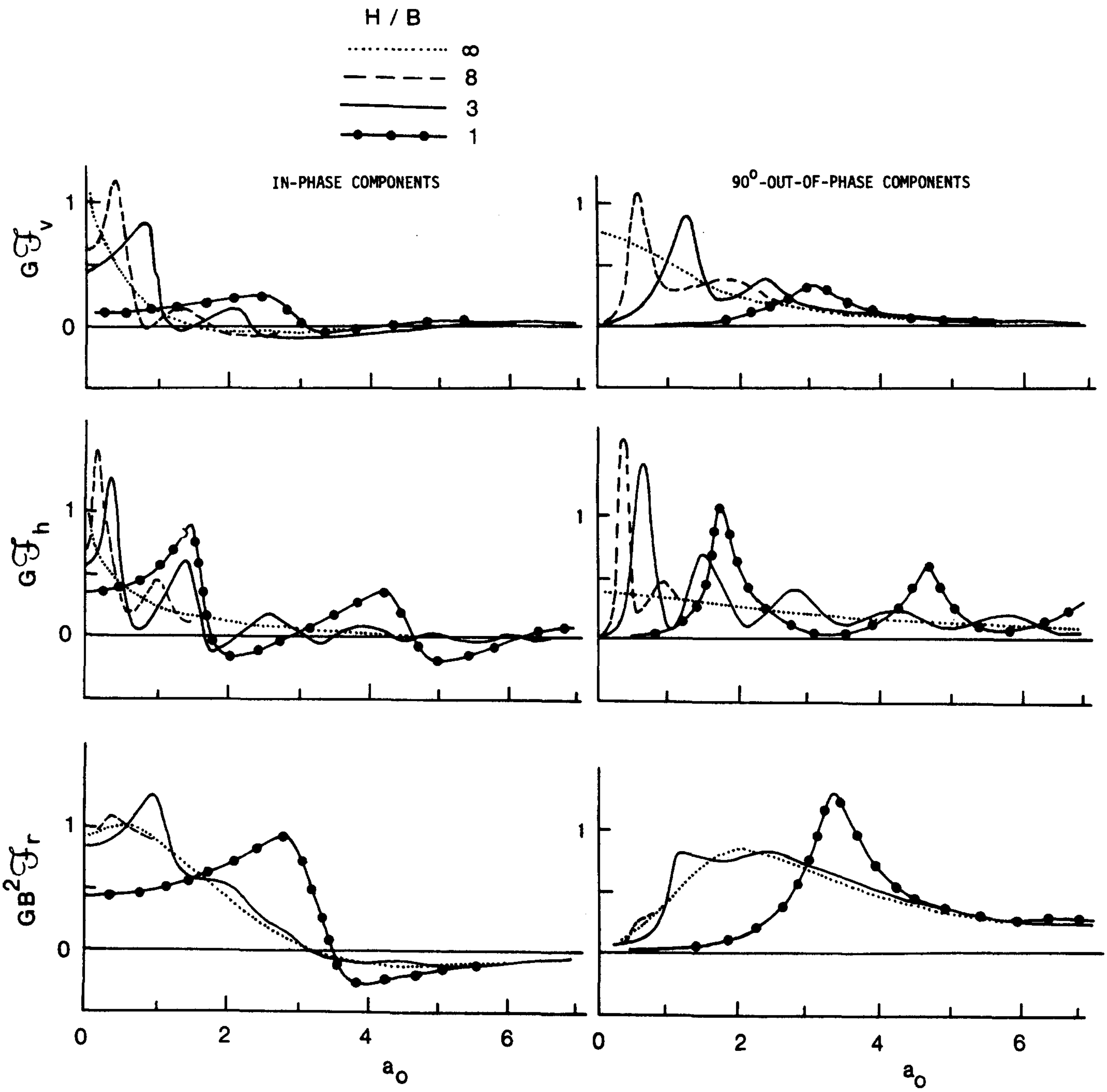

Figure 10. Compliance functions of rigid strip footing on stratum-over-bedrock; effect of H/B ratio ($\nu = 0.49$, $\xi = 0.05$)

compliances is substantial. On the other hand, rocking vibrations of a strip exhibit very similar trends with rocking of a circular plate; beyond $H/R = 3$ the presence of bedrock is hardly noticeable.

In the case of vertical loading, the resonant peaks are not as sharp as those of the horizontal displacements. In fact, on very shallow deposits ($H/B = 1$) only a single flat resonance takes place, which is characteristic of a highly damped system. A possible explanation of such a behavior has been suggested by Gazetas and Roesset[39]: at frequencies below the first resonance some 'leakage' of energy occurs in the form of laterally propagating *P*-, *S*- and *R*-waves. Evidence in favor in this explanation comes from the fact that the first resonant frequency, a_{0r}, lies in between the fundamental natural frequencies of the stratum in vertical *S*-waves, $a_{0s,1}$, and in vertical *P*-waves, $a_{0p,1}$. For example, Fig. 11 shows that, for $H/B = 2$ and $\nu = 0.40$, $a_{0r} \simeq 1.30$ compared to $a_{0s,1} = 0.785$ and $a_{0p,1} = 1.90$. Recall that for the circular foundation a_{0r} was much closer to $a_{0p,1}$.

No extensive numerical results for rigid rectangular foundations supported by a soil stratum have been found in the literature.

Foundation on stratum over a halfspace

The homogeneous halfspace and the stratum-over-rigid-base are two idealizations of extreme soil profiles. A more general soil model, the stratum-over-halfspace, is studied in this subsection. Besides the H/R or H/B ratio, the moduli ratio G_1/G_2 is needed to describe such a soil model. When G_1/G_2 tends to 0, the stratum-on-rigid base is recovered; when it becomes equal to 1, the model reduces to a homogeneous halfspace. Thus, the results presented in this section help in bridging the gap between 'halfspace' and 'stratum' solutions to which we have restricted our attention until now (Figs. 5-11).

Numerical solutions for a uniform layer over a halfspace have been published by Hadjian and Luco[37] who studied the dynamic of circular foundations, and by Gazetas and Roesset[38, 39] who studied the response of strip footings.

Based on the results provided by Hadjian and Luco,[37] the author has derived simple but reasonably accurate formulae for the static stiffnesses of a rigid circular disk, in terms of H/R and G_1/G_2. Table 5 displays these formulae, which are valid for the usual case in which $G_1 \leqslant G_2$, i.e. a halfspace stiffer than the layer. At the lower limit, $G_1/G_2 \rightarrow 0$, these expressions reduce to those of Table 3 for a layer-on-rigid-base; at the upper limit, $G_1/G_2 = 1$, the halfspace expressions of Fig. 5 are recovered. At intermediate values, as the rigidity of the supporting halfspace decreases, the static stiffnesses of the foundation decrease, apparently due to increasing magnitude of strains in the halfspace. The results are intuitively obvious and need no further explanation.

For circular footings, no results are presented here on dynamic stiffness and damping coefficients, but reference is made to the original publication by Hadjian and Luco.[37]

The variation of the dynamic compliances of a strip footing with a_0 and G_1/G_2 is portrayed in Fig. 12 for a layer with $H = 2B$, $\nu = 0.40$ and $\xi = 0.05$. Shallower as well as deeper layers have been examined by Gazetas and Roesset.[38, 39]

An inspection of Fig. 12 indicates that the effects of layering increase with increasing contrast between G_1 and G_2; these effects are extreme for a layer on rigid bedrock ($G_1/G_2 = 0$) and, naturally, disappear in the case of a homogeneous halfspace ($G_1/G_2 = 1$). There are two main effects of increasing the softness of the halfspace. First, even for small positive values of G_1/G_2, i.e. as long as we do not deal with an infinitely rigid bedrock, the static translational displacement tends to infinity, although at a

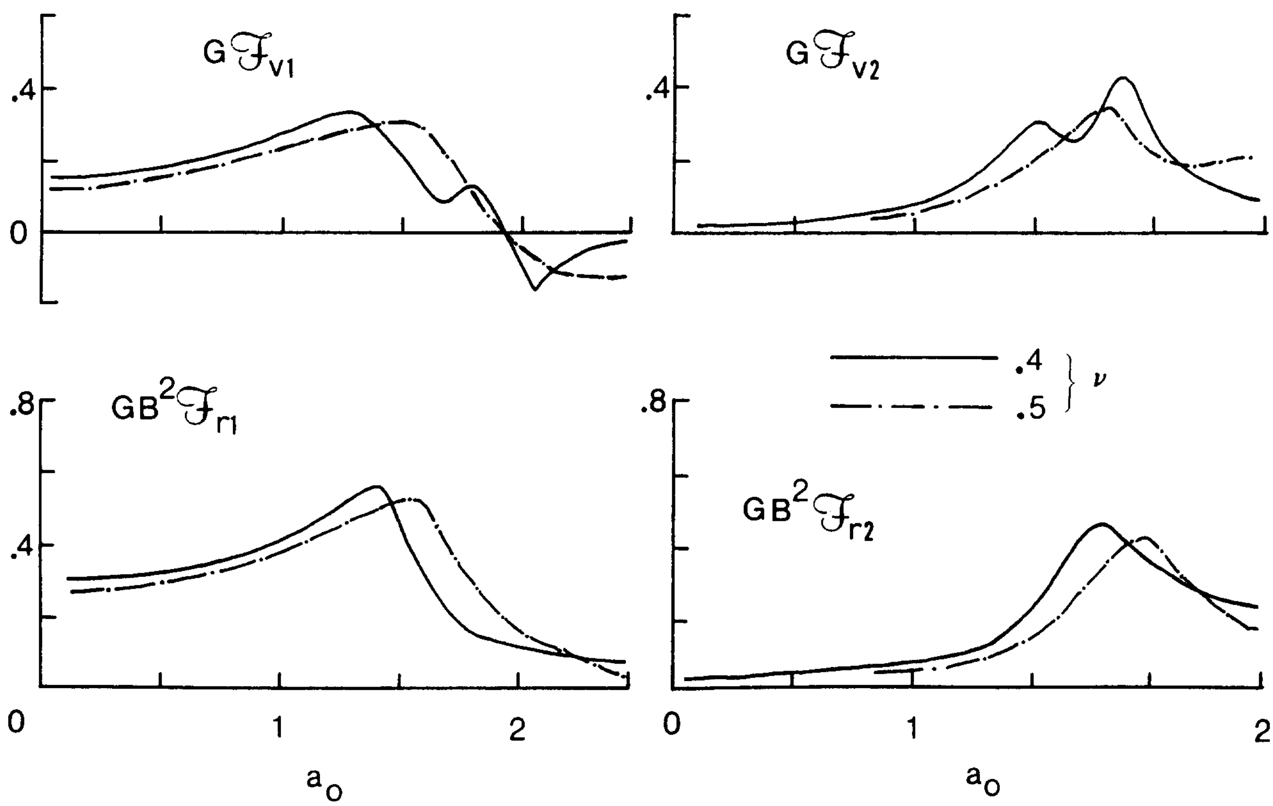

Figure 11. Compliance functions of rigid strip footing on stratum-over-bedrock; effect of ν ($H/B = 2$, $\xi = 0.05$)

*Table 5. Static stiffnesses of circular foundations on a stratum-over-halfspace**

Type of loading	Static stiffness*	Range of validity	Profile
Vertical:	$\dfrac{4G_1R}{1-\nu_1}\cdot\dfrac{1+1.28\dfrac{R}{H}}{1+1.28\dfrac{R}{H}\dfrac{G_1}{G_2}}$	$1<\dfrac{H}{R}<5$	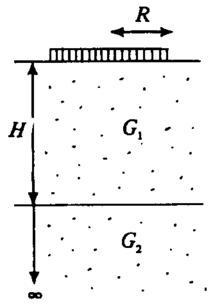
Horizontal:	$\dfrac{8G_1R}{2-\nu_1}\cdot\dfrac{1+\dfrac{1}{2}\dfrac{R}{H}}{1+\dfrac{1}{2}\dfrac{R}{H}\dfrac{G_1}{G_2}}$	$1<\dfrac{H}{R}<4$	
Rocking:	$\dfrac{8G_1R^3}{3(1-\nu_1)}\cdot\dfrac{1+\dfrac{1}{6}\dfrac{R}{H}}{1+\dfrac{1}{6}\dfrac{R}{H}\dfrac{G_1}{G_2}}$	$0.75<\dfrac{H}{R}<2$	$0<\dfrac{G_1}{G_2}<1$

* Derived by the author on the basis of results provided by Hadjian and Luco[37]

much slower rate compared to the halfspace displacements. Thus, in the very low frequency range the in-phase (real) components of the displacements (compliances) are larger than in the case of rigid bedrock.

On the other hand, at any specific frequency, the radiation damping of the system increases due to partial transmission of body-waves in the halfspace and the existence of surface waves at all frequencies. Consequently, the resulting variation of displacements with a_0 is smoother than in the rigid rock case.

The effects of decreasing stiffness and increasing radiation damping are of major importance at frequencies equal to or lower than the first resonant frequencies of the system. With G_1/G_2 ascending from 0 (rigid bedrock) towards 1 (homogeneous halfspace), the aforementioned resonant peaks become shorter and flatter and the corresponding resonant frequencies shift to lower values.

Higher resonant peaks also decrease substantially and may in some cases be completely suppressed. An example: the third resonant peak in swaying (which, we recall, occurs at the second natural frequency of the stratum in S-waves) disappears as soon as G_1/G_2 exceeds 0.10.

Finally, it is hardly surprising that the vertical dynamic compliances are most sensitive to variations in G_1/G_2, while rocking compliances are least sensitive. The concept of a 'dynamic pressure bulb' proves again very convenient in explaining these differences. The depth of the 'bulb' attains relatively large values in case of vertical vibrations, somewhat smaller values for swaying and very small values for rocking.

SOME RESULTS FOR RIGID SURFACE FOUNDATIONS OF 'ARBITRARY' SHAPE

Only a few numerical results are available for foundations having 'arbitrary' geometries, i.e. plan shapes other than strip, circular or rectangular. One reason for the lack of interest is that foundations of such 'arbitrary' shape are not constructed very frequently. Moreover, substantial computational effort must be expended to obtain dynamic solutions for such foundation geometries. The following presentation is divided into two parts: one dealing with vertically loaded footings of various 'solid' shapes and one with the complete response of annular footings.

Vertically loaded foundations of various 'solid' shapes

Analytical expressions for the static stiffnesses of rigid foundations supported to an elastic halfspace and having several different shapes (but without internal holes) can be derived from the results of Borodachev[94] (see also Selvadurai[9]). It is convenient to cast these expressions into our familiar form:

$$K_v = \frac{4GR_0}{1-\nu}\cdot J_v \tag{55}$$

in which: $R_0=\sqrt{A/\pi}$ is the radius of the 'equivalent' circular foundation, A being the area of the soil-footing contact surface; J_v is a shape-depended correction factor, numerical values of which have been tabulated in Table 6 for numerous plan shapes.

Table 6 in conjunction with Table 2 (part 1) can be used for determining the vertical static stiffnesses of a variety of foundations with very good accuracy. Moreover, the following trends are worthy of note:

1. The circular disk yields the smallest stiffness of all footings with a given contact area.

2. Of all rigid footings with an n-sided polygon-shaped plan of a given area, the regular n-sided polygon yields the smallest stiffness.

3. The correction factor depends primarily on the 'aspect' ratio of the foundation, being surprisingly insensitive to the details of each particular shape. By 'aspect' ratio we somewhat loosely mean the ratio between largest and smallest critical foundation dimensions. Thus, for example, a rhombus, a rectangle and an ellipse having the same aspect ratio, equal to 4, yield very similar correction factors of about 1.12.

In conclusion it seems that, by means of equation (55) and Tables 2 and 6, very good estimates can be routinely made of the vertical static stiffnesses of arbitrary-shaped rigid foundations on homogeneous halfspace.

No information is available regarding the variation with frequency of the dynamic stiffness coefficient k_v. However, inspection of Figs. 5 and 7 reveals that the 'equivalent' circular footing can successfully predict the actual k_v of rectangular footings with aspect ratios up to 4, at least in the low and medium frequency range ($a_0 \leq 1.5$). Hence, and in view of the observed insensitivity of the static stiff-

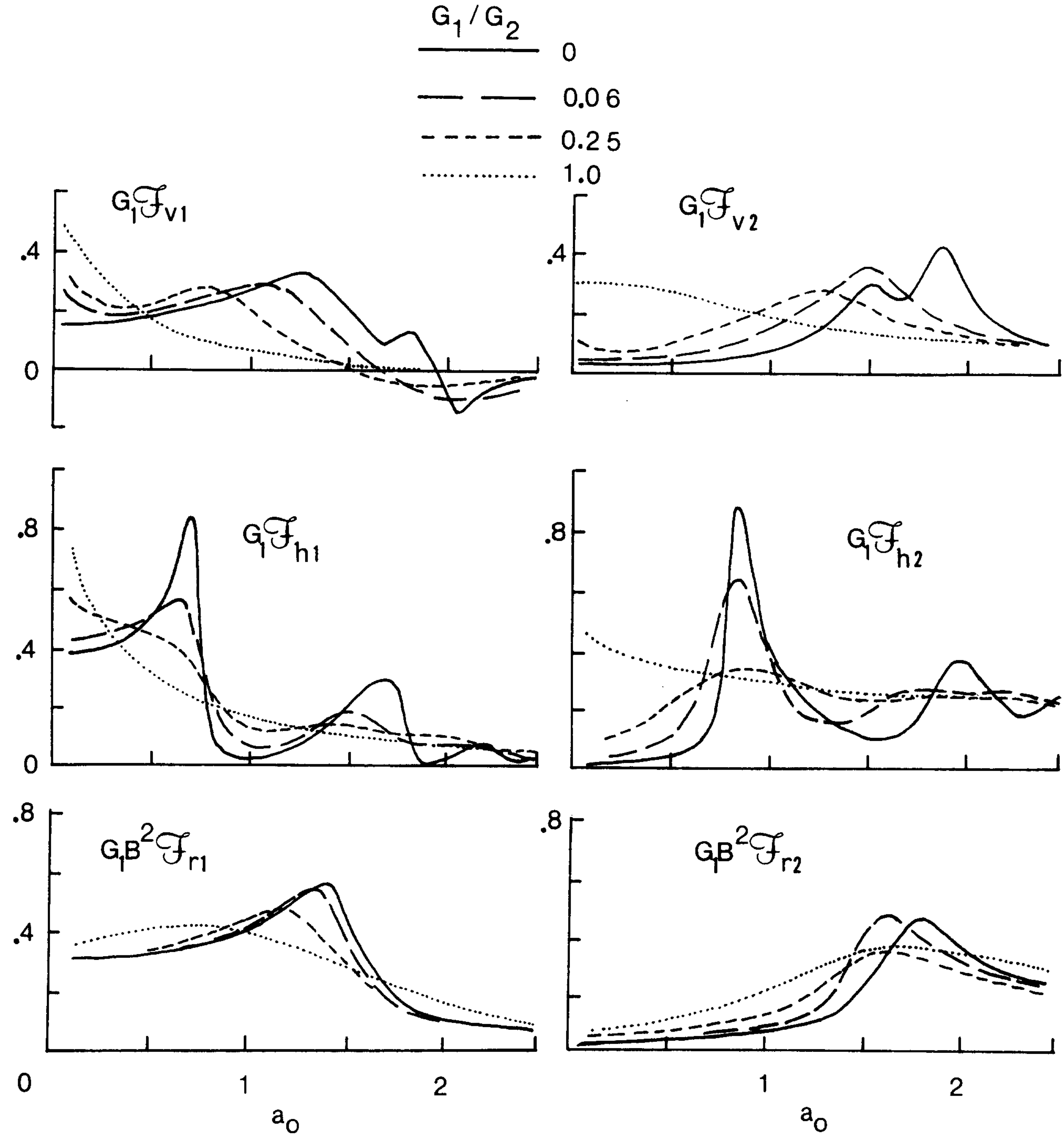

Figure 12. Effect of G_1/G_2 ratio on compliance functions of rigid strip footings on soil layer-over-halfspace ($H/R = 2$, $\nu = 0.40$, $\xi = 0.05$)

ness to the details of the foundation shape, it is proposed that the variation of k_v with a_0 for an 'arbitrary'-shaped foundation be estimated from Fig. 5 using the 'equivalent' radius, $R_0 = \sqrt{A/\pi}$.

On the other hand, the damping coefficient c_v is practically independent of frequency, as it is evident from Figs. 5 and 7. For an arbitrary-shaped foundation, moreover, Dobry *et al.*[95] have recently derived expressions for the (radiation) damping coefficients in vertical and swaying vibrations, based on simple but realistic physical approximations. For the vertical damping coefficient of a surface foundation their expression reduces to:

$$c_v = \frac{0.85}{J_v} \tag{56}$$

in which J_v = the shape correction factor to be read from Table 6 or Table 2. Consequently, the vertical dynamic impedance of an arbitrary-shaped rigid foundation on a homogeneous halfspace can be directly and reliably estimated using the provided information.

For the other translational and rotational modes of vibration of arbitrary-shaped rigid foundations, much less information is presently available. The 'equivalent-circle' approximation appears to be a simple and reasonable choice.

Rigid annular foundation on soil stratum

It appears that the conclusions of the preceding subsection cannot be extended to foundations containing internal holes, like annular and crossed-beam foundations.

*Table 6. Values of shape-depended correction factor for vertical static stiffnesses**

Shape of foundation plan	J_v
Circle	1.00
Regular hexagon	1.01
Semicircle	1.05
Equilateral triangle	1.07
Triangle with angles, 45°, 45°, 90°	1.10
Triangle with angles, 30°, 60°, 90°	1.12
Ellipse with $a/b = 2$†	1.03
Ellipse with $a/b = 3$	1.07
Ellipse with $a/b = 4$	1.13
Ellipse with $a/b = 6$	1.21
Rhombus with an angle of 60°	1.07
Rhombus with an angle of 45°	1.14
Rhombus with an angle of 30°	1.27
Rectangle with $L/B = 2$	1.03
Rectangle with $L/B = 4$	1.13
Rectangle with $L/B = 8$	1.23

* Based on Borodachev[94,9]
† a, b are the major, minor axes of the ellipse

For example, the vertical static stiffness of such foundations does not increase in proportion to the square-root of the contact area, A, as equation (55) implies. In other words, the 'equivalent-circle' approximation is no longer valid.

Results for the static displacements of a rigid circular ring on a halfspace have been published: by Egorov[96] and Dhawan[97] for vertical loading; by Dhawan[98] for moment loading; and by Dhawan[99] for torsional loading. Wong and Luco[44] studied the dynamic vertical response of a rigid square foundation with a square internal hole. Recently, Tassoulas[88] presented a comprehensive parametric investigation of the dynamic behavior of rigid circular-ring foundations on a homogeneous stratum-over-rigid-base. All modes of vibration were considered and the effect of the dimensionless parameters R_i/R, H/R and $a_0 = \omega R/V_s$ was graphically illustrated. The following discussion is based primarily on the results of Tassoulas,[88] although some results from Dhawan,[97-99] are also included for comparison.

Figure 13 plots the variation of all static stiffnesses of a circular ring versus R_i/R, where R_i is the internal radius. As expected, all stiffnesses invariably decrease as the size of the hole increases, while the radius R remains constant. In the limit, when R_i becomes equal to R, the stiffnesses vanish (concentrated ring load). However, the sensitivity of stiffnesses to increases in the R_i/R ratio is surprisingly small. Particularly insensitive are the rocking and torsional stiffnesses. For values of R_i/R up to 0.50, they are practically equal to the corresponding stiffnesses of the circular foundation with radius R; for $R_i/R = 0.95$, K_t and K_r are respectively equal to 86% and 83%, of the circular stiffnesses in torsion and rocking (while the contact area has been reduced to only 10% of the original circle). The explanation is rather obvious: the large shear or normal stresses which develop near the outside edge of the footing, i.e. at large distances from the center, contribute substantially to equilibrating the applied torsion or rocking moments. In other words, the central foundation 'core' is 'underutilized' and, hence, its 'removal' is of little consequence. Notice also that the variation of K_t and K_r with R_i/R is independent of H/R – a result consistent with the shallow 'pressure bulb' of moment loading discussed in preceding sections (e.g. Table 3).

The horizontal stiffness is only slightly more sensitive to R_i/R. In contrast, the vertical stiffness is relatively sensitive not only to R_i/R but to H/R as well. An example: increasing R_i from 0 to $0.95R$ reduces K_v to 70% of its original value for $H/R = 2$; for a halfspace the corresponding value is 77%. But, again, for values of R_i/R up to 0.5, K_v remains practically equal to its original value, $4GR(1+1.28R/H)/(1-\nu)$.

Figure 14 depicts the variation with a_0 of the dynamic stiffness and damping coefficients, k and c. Four values of R_i/R are considered, 0, 0.5, 0.8 and 0.90, with the first value corresponding to a solid circular foundation. It is clear that: (1) there is little change in k and c with R_i/R; (2) the effect of R_i/R is largest for vertical vibrations; and (3) the differences in the four sets of curves occur in the high frequency range ($a_0 \geq 1.5$).

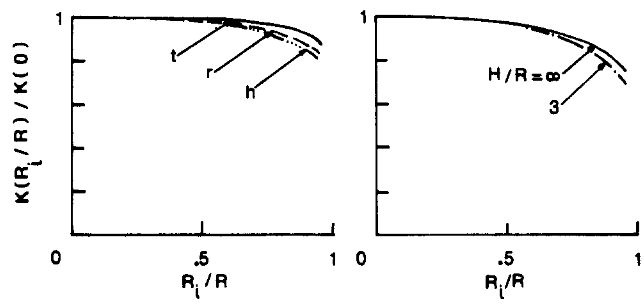

Figure 13. Static stiffnesses of a rigid annular foundation (R_i = internal radius)[88,97]

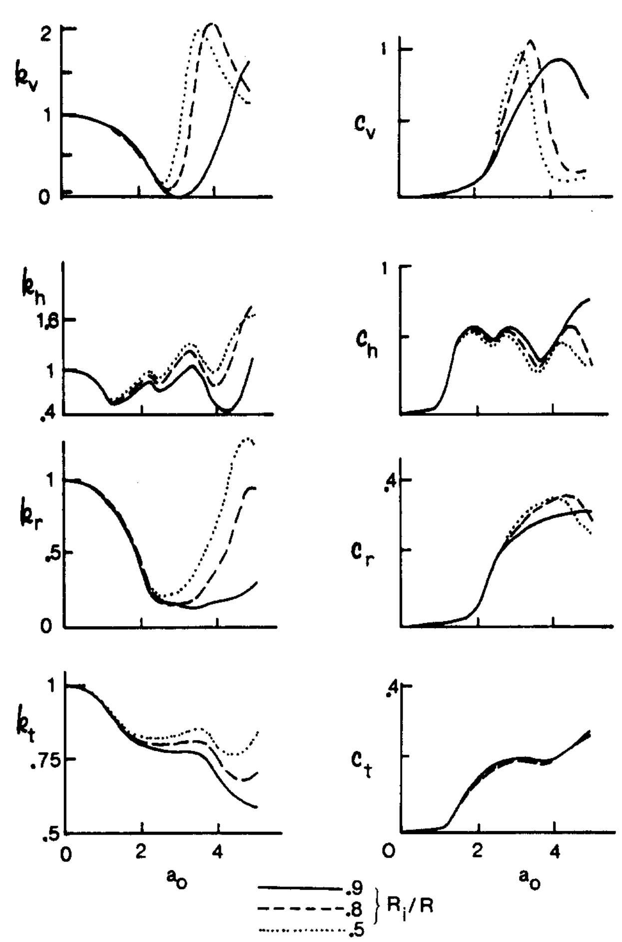

Figure 14. Dynamic coefficients of a rigid annular foundation[88]

THE INFLUENCE OF INHOMOGENEITY, ANISOTROPY AND NONLINEARITY OF SOIL

The results presented so far have been based on the simplifying assumption that the soil can be modeled as a homogeneous, isotropic and linearly visco-elastic stratum or halfspace. However, real soil strata frequently increase in rigidity with depth as a reflection of the increase in overburden pressure, while in some other cases weathered crusts, in which rigidity decreases with depth, overlay deposits of softer clay. Furthermore, laboratory tests show that soils deform differently in the vertical and horizontal directions – a manifestation of anisotropic fabric acquired during natural formation and subsequent loading. Finally, when subjected to large enough stresses, soils respond as nonlinear and inelastic materials.

This section of the paper presents characteristic results and important conclusions from a number of recent studies aimed at assessing the influence of soil inhomogeneity, anisotropy and nonlinearity on the behavior of dynamically loaded surface foundations.

Effect of soil inhomogeneity

Existing dynamic finite-element formulations can easily, albeit approximately, simulate a continuous variation of soil properties, by dividing the deposit into a number of homogeneous layers of increasing or decreasing stiffness. Yet, such formulations have not been adequately exploited to parametrically study the dynamic behavior of foundations. Thus, most of the available solutions have been derived using analytical and semi-analytical methods.

Numerous studies have been published for the vertical static problem. Prominent among them is the work of Gibson and his co-workers;[13,100,101] who studied the response to arbitrary surface loads of a halfspace or stratum whose moduli increase linearly with depth, i.e. in the form $G = G_0 + \tilde{m}(z/R)$, where G_0 and $\tilde{m}$ are the moduli at the surface and at a one-radius (or one-semiwidth) depth. These studies revealed that for an incompressible medium, i.e. with Poisson's ratio of 0.50, the stress distribution is hardly influenced by the degree of inhomogeneity; in the particular case of zero surface modulus ($G_0 = 0$) this distribution is identical with the distribution in a homogeneous halfspace, regardless of foundation geometry. The surface settlement, on the other hand, being quite sensitive to the assumed soil profile, becomes directly proportional to the applied normal pressure when $G_0 = 0$, independent of the size and shape of the loaded area and of the thickness, H, of the soil layer on a rigid but frictionless (smooth) base. Thus, such a soil behaves like a Winkler medium rather than a homogeneous halfspace, its spring constant being simply equal to $2\tilde{m}/R$. Expressions for the vertical static stiffnesses of surface foundations of several shapes supported by such a soil deposit (frequently referred to as 'Gibson soil') are shown in Table 7.

This behavior remains only qualitatively true when drained soil behavior is taking place (i.e. $\nu < 0.50$). Thus, with increasing degree of inhomogeneity (e.g. increasing $\tilde{m}$) normal and shear stresses affect the soil at greater vertical and lesser horizontal distances, in agreement with intuition that expects stiffer material to attract larger stresses. On the other hand, surface displacements, being moderately sensitive to ν, do tend to become proportional to the applied local pressures as m increases. It is, thus, generally concluded that an inhomogeneous deposit leads to more uniform distribution of stresses under rigid foundations than the simple elastic theory (homogeneous halfspace) predicts.

This general behavior of vertically loaded surface foundations on an inhomogeneous soil deposit has been recently shown to be applicable to torsionally loaded circular footings.[93]

The static and dynamic vertical, horizontal and rocking behavior of a rigid strip foundation supported by a halfspace or a stratum whose wave velocities increase linearly with depth, has been studied by the author.[53] Some results of that study are presented here for a halfspace consisting of soil with a constant mass density, a constant Poisson's ratio, $\nu = 0.25$, and a constant hysteretic damping, $\xi = 0.05$, and an S-wave velocity varying with depth according to:

$$V_s = V_0\left(1 + \lambda\,\frac{z}{B}\right) \tag{57}$$

in which: V_0 = surface velocity; $2B$ = foundation width; and λ = the dimensionless rate of inhomogeneity.

*Table 7. Static stiffnesses of rigid foundations on inhomogeneous and cross-anisotropic soils**

Type of loading	Static stiffness	Range of validity	Soil profile
Vertical, on foundation of any shape	$2\frac{\tilde{m}}{B}A$ A = contact area	Undrained loading conditions	Cross-anisotropic 'Gibson' halfspace obeying equation (60), with a modulus $G_{VH} = \tilde{m}\,(z/B)$
	$\frac{\tilde{m}}{B}A\left(1+\frac{E_V/G_{VH}}{4-n}\right)$ A = contact area		General cross-anisotropic 'Gibson' halfspace (i.e. not obeying equation (60)) with a modulus $G_{VH} = \tilde{m}\,(z/B)$
Vertical, on rigid strip	$\dfrac{45E_V}{\left(1+3.5\frac{H}{B}\right)[4-n]^{(1/6)(H/B)}}$	$1 \leqslant \frac{H}{B} \leqslant 4$ $0.5 \leqslant n \leqslant 2.5$	Shallow cross-anisotropic undrained layer; soil properties are uniform throughout the layer and they satisfy equation (60)
Horizontal, on rigid strip	$\frac{8}{5}E_V\dfrac{1+\frac{5}{3}\frac{B}{H}}{4.10-n(H/B)^{0.10}}$	$1 \leqslant \frac{H}{B} \leqslant 6$ $0.5 \leqslant n \leqslant 2.5$	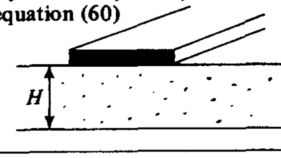

* Based on results by Gibson[13] and Gazetas[54]

Figure 15 portrays the dependence of λ of the normalized vertical, horizontal and rocking stiffnesses. As one might expect, the vertical stiffness exhibits the largest sensitivity to λ and the rocking stiffness the smallest – another manifestation of the difference in the 'pressure bulbs' of the three types of loading.

The effect of soil inhomogeneity on the three dynamic compliance functions is shown in Fig. 16. Two values of the parameter λ are considered: 0 and 1.5. The former value corresponds to a homogeneous halfspace, the wave velocity of which, V_{eff}, was selected to be the same with the wave velocity of the inhomogeneous halfspace at a depth equal to the foundation halfwidth, B; i.e.:

$$V_{eff} = V_0(1+\lambda) \tag{58}$$

The choice of such a homogeneous halfspace for the comparison has been motivated by the frequent use in practice of solutions developed for homogeneous soils, with an *effective* modulus equal to the actual modulus at a depth equal to B or R, to approximate the actual response.

It is evident from the comparison of Fig. 16 that, in the low frequency range examined, the inhomogeneous medium yields vertical and horizontal displacements (both in-phase and 90°-out-of-phase components) which are, indeed, of about the same average level with those of the 'equivalent' homogeneous halfspace. However, the rocking motions on the inhomogeneous deposit are seriously underpredicted by the chosen homogeneous halfspace model; to yield comparable rotation levels the two media must have the same moduli at a depth of about $B/2$, or somewhat less.

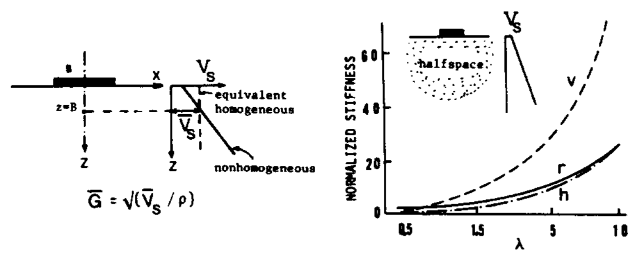

Figure 15. Static stiffnesses of a rigid strip foundation on an inhomogeneous halfspace ($\nu = 0.25$)[53]

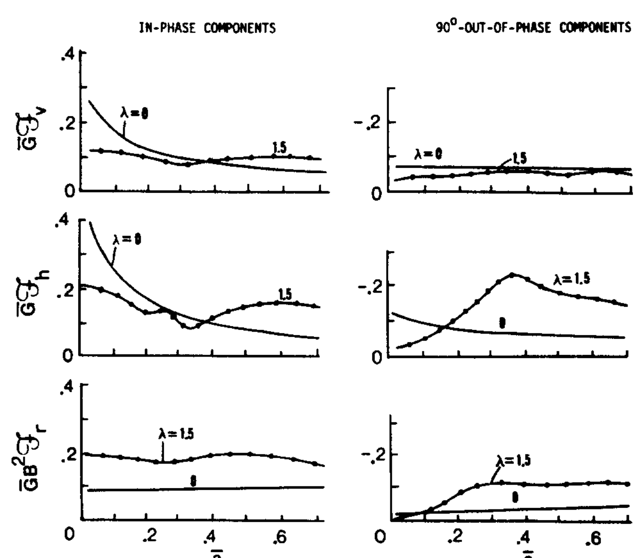

Figure 16. Compliance functions of a rigid strip foundation on an inhomogeneous halfspace ($\nu = 0.25$, $\xi = 0.05$)[53]

Furthermore, a substantial difference between the '$\lambda = 1.5$' and '$\lambda = 0$' compliance functions may be noted. Namely, the former are not smoothly varying functions of a_0, as are the latter, but exhibit peaks and valleys which are apparently the result of resonance phenomena. In the very low frequency range the imaginary components of the '$\lambda = 1.5$' compliances attain quite small values, increasing almost linearly with a_0.

These phenomena are reminiscent of the dynamic behavior of foundations supported by a stratum-over-a-rigid-base (Figs. 10-11). In this case, total reflection of the downward propagating waves is possible due to the increasing soil velocity with depth. A discontinuity in velocity is not necessary for such a reflection, since the wave rays in inhomogeneous media with linear velocity profiles are not straight lines but circular arcs. As a result, however, the resonant peaks on inhomogeneous soils are very flat and the radiation damping is never zero. In contrast, the presence of stiff rock-like material at some depth beneath the surface leads to very sharp and pronounced displacement peaks, occurring at well separated frequencies (see Fig. 8-11).

Deposits with a weathered crust. The dynamics of a rigid strip foundation on an idealized soil deposit consisting of a homogeneous stratum or halfspace overlain by a top stiffer layer in which the shear modulus decreases as a second-degree parabola (Fig. 17) has been recently studied by the author.[55] Also recently, Rowe and Booker,[102] presented comprehensive parametric results pertaining to vertical static uniform loading, both plane-strain and axisymmetric, on several realistic inhomogeneous deposits, including a homogeneous layer with a weathered crust.

Figure 17[55] illustrates the effect of the reduced crust thickness D_{cr}/B on the three normalized dynamic impedance functions of a rigid strip. The soil profiles are characterized by a shear modulus ratio, G_{cr}/G, equal to 4, and realistic values of the Poisson's ratios, ν_{cr} and ν, equal to 0.25 and 0.45, respectively. Note that the ratios G_{cr}/B and D_{cr}/B may be considered as indexes of the *degree and depth of weathering*.

It is evident that the presence of the crust has a pronounced effect on all impedances. Especially sensitive to changes in D_{cr}/B are the horizontal impedances, whereas the vertical and rocking ones are somewhat less affected. Variations in the assumed moduli ratio (not depicted in Fig. 17) have been shown to have a similar effect.

Furthermore, the weathering effects exhibit a strong dependence on frequency. For example, at low frequency factors vertical impedances are relatively indifferent to variations (within realistic limits) in either stiffness or depth of the crust. This is understandable in view of the fact that vertical surface strip loading affects the soil at great depths, of the order of $8B$, as discussed previously; thus, a stiff crust with $D_{cr} \leqslant B$ can only be of secondary importance. This picture, however, changes at higher frequency factors, i.e. lower wavelength-thickness ratios, as may be seen in Fig. 17. Greater participation of surface (Rayleigh) waves in the motion and stronger reflection of the body waves emanating from the foundation by the soft layer interface, may be part of the explanation.

It may also be noticed that rocking impedances show about the same sensitivity to weathering throughout the

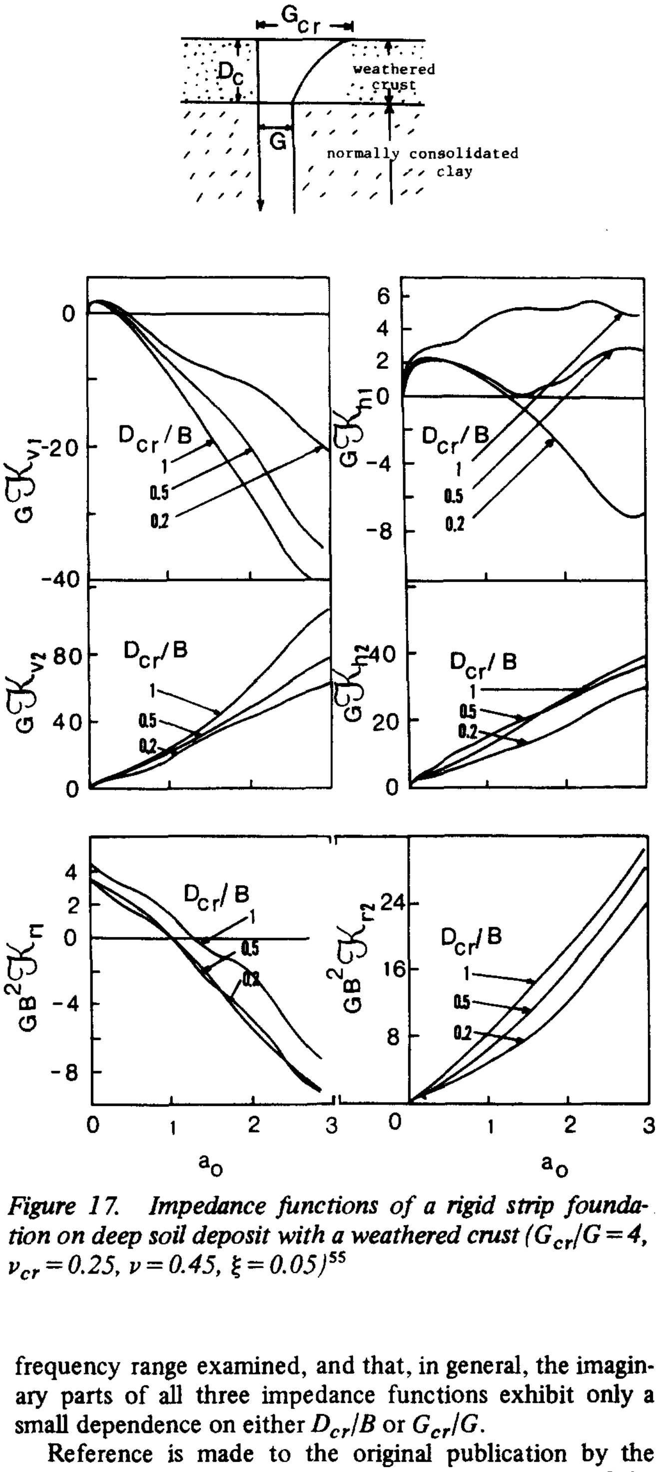

Figure 17. Impedance functions of a rigid strip foundation on deep soil deposit with a weathered crust ($G_{cr}/G = 4$, $\nu_{cr} = 0.25$, $\nu = 0.45$, $\xi = 0.05$)[55]

frequency range examined, and that, in general, the imaginary parts of all three impedance functions exhibit only a small dependence on either D_{cr}/B or G_{cr}/G.

Reference is made to the original publication by the author for a more complete parametric assessment of the dynamic effects of 'weathering' on strip foundations. The author sees a definite need to extend these studies to dynamically loaded circular foundations.

Effect of soil anisotropy

Numerous experimental studies have shown that most natural soils and rocks possess anisotropic deformational characteristics.[13, 103–106] This anisotropy stems from the fact that soil fabric is intimately related to the mechanical processes occurring during formation, which involves anisotropic stress systems. Thus, for example, natural clay deposits formed by sedimentation and, subsequently, one-dimensional consolidation over long periods of time acquire a fabric that is characterized by particles or particle clusters oriented in a horizontal arrangement. This preferred orientation makes the clay a cross-anisotropic material with a vertical axis of symmetry. Similarly, fabric anisotropy in sands arises from the influence of gravity forces and particle shape on the deposition process, while in rocks the anisotropy may result from the anisotropy of forming minerals and micro- or macro-fabric features.

While an isotropic elastic material is characterized by only two independent elastic constants (e.g. shear modulus and Poisson's ratio), five parameters are needed to describe the stress-strain relationships of an elastic cross-anisotropic material: a Young's modulus E_V in the vertical direction; a Young's modulus E_H in the horizontal direction ($E_H = nE_V$); a Poisson's ratio ν_{VH} for the effect of vertical on horizontal strain; a Poisson's ratio ν_{HH} for the effect of horizontal on complementary horizontal strain; and a shear modulus $G_{VH} = G_{HV}$ for distortion in any vertical plane, i.e. any plane parallel to the vertical axis of material symmetry. Note that isotropic materials are just a particular class (subset) of cross-anisotropic materials characterized by $n = 1$ (i.e. $E_H = E_V \equiv E$, $\nu_{VH} = \nu_{HH} \equiv \nu$ and $G_{VH} \equiv G = E/2(1+\nu)$).

The condition of incompressibility, appropriate for undrained loading conditions, requires that:

$$\nu_{VH} = 0.50, \quad \nu_{HH} = 1 - \frac{n}{2} \tag{59}$$

and, thus, reduces the number of independent material constants to three. Moreover, utilizing the results of several experimental investigations, the author has recently shown[54] that, in many clays, the shear modulus G_{VH} is closely related to the other four material constants. Under undrained conditions, for example, with a reasonable accuracy:

$$G_{VH} = \frac{E_V}{4-n} \tag{60}$$

Thus, the number of independent material constants reduces to two, under undrained conditions, and to four, under drained conditions.

Results for statically loaded rigid foundations on cross-anisotropic soils have been presented by Gerrard and Harrison,[92, 107] Gibson[13] and Gazetas.[54] Solutions for dynamically loaded foundations on cross-anisotropic homogeneous soil deposits whose elastic constants satisfy equation (60) (or its 'drained' counterpart, not given here) have been presented by Kirkner[67] for circular foundations on halfspace and by the author[54, 108, 109] for strip foundations on homogeneous stratum or on halfspace. Table 7 and Fig. 18 offer some characteristic results from the mentioned publications.

Specifically, Table 7 displays simple but fairly accurate formulae for the vertical static stiffness of arbitrary-shape foundations on a cross-anisotropic, incompressible and inhomogeneous halfspace ('Gibson' soil), and for the vertical and horizontal static stiffnesses on a homogeneous and incompressible cross-anisotropic shallow soil stratum-on-rigid base. Notice that on an anisotropic 'Gibson' halfspace obeying equation (60), the degree of anisotropy has no influence on the vertical stiffness. In all other cases, however, the stiffnesses increase substantially with $n = E_H/E_V$. In fact, for $n \to 4$ all stiffnesses tend to infinity, since the strain energy of such a material is zero for all possible applied stress systems.[13, 107]

Regarding the sensitivity of the dynamic response to variations in the degree of anisotropy, n, under undrained conditions, the main conclusions of the aforementioned studies are summarized as follows.

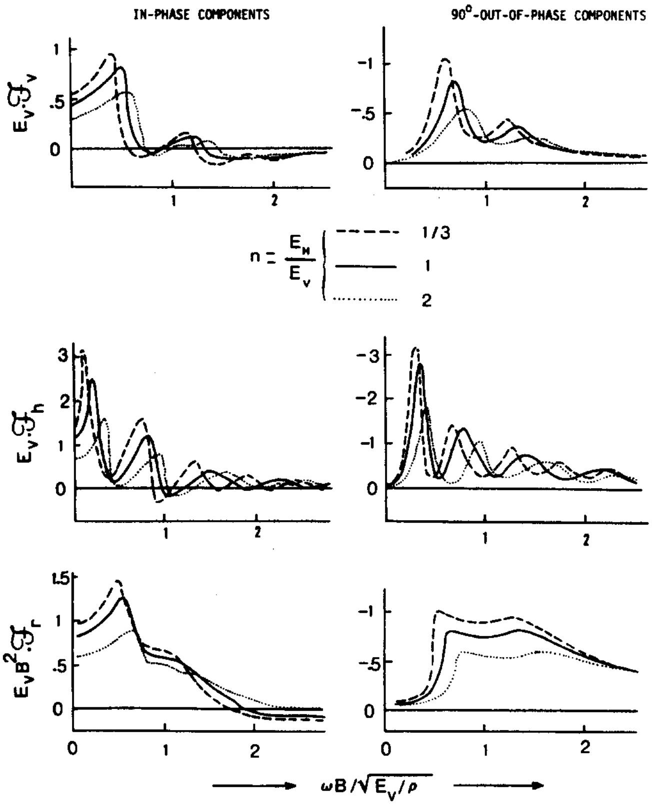

Figure 18. Effect of soil anisotropy on compliance functions of a rigid strip foundation on stratum-over-bedrock (undrained conditions, $H/B = 3$, $\xi = 0.05$)[54]

For the two compressional modes of vibration, i.e. vertical and rocking, the influence of anisotropy is appreciable but seems to decrease as the thickness of the stratum-on-bedrock decreases, with the shear modulus G_{VH} remaining constant. The effect of anisotropy on the shearing mode of vibration, i.e. swaying, is similar with the effect of anisotropy on G_{VH} and independent of the layer thickness; in other words, two soils with identical G_{VH} and H but with different Young's moduli and n, will yield very similar undrained dynamic displacements.

Figure 18 portrays the dependence on n of the three compliance functions of frequency, for a layer with $H = 3B$ and constant E_V. It is concluded that, in the low and medium frequency range, by increasing n the dynamic displacements decrease and the resonant frequencies shift to the right, roughly in proportion to $(4-n)^{-1/2}$. Obviously, the corresponding decrease in the static stiffness may be held responsible for this effect. At certain higher frequencies, however, rocking and vertical displacements increase, instead of decreasing, with n. Nonetheless, the practical significance of such a reversal will probably be small, in view of the small displacement amplitudes at such frequencies.

In conclusion, anisotropy exerts its main effect through the static stiffnesses of the soil-foundation system.

Effect of soil nonlinearity

In current soil-structure interaction practice the nonlinear plastic soil behavior is usually approximated through a series of iterative linear analyses, using soil properties (moduli and damping ratios) that are consistent with the level of shearing strains resulting from the previous analysis.[34,110] These analyses may utilize a wealth of available experimental soil data relating the decrease in (secant) shear modulus and the increase in (effective) damping ratio with increasing amplitude of shear strain.

Soil nonlinearities are not usually of a significant magnitude in machine foundation problems, for the reasons mentioned in the introduction. (In contrast, the response of soil-foundation systems to strong earthquakes is very sensitive to deviations from linear-elastic soil behavior.) Nonetheless, even with small amplitudes of vibration, it is almost certain that some soil elements will undergo plastic deformations. For instance, under the edges of rocking shallow foundations, large concentration of stresses and low confining pressures will invariably lead to yielding of soil.*

An interesting parametric investigation of the effects of soil nonlinearities on the dynamic impedance functions of a rigid strip foundation has been conducted by Jakub and Roesset.[56] In their studies the soil was modeled as a homogeneous or inhomogeneous stratum-over-rigid-base with reduced thicknesses $H/B = 1$, 2 and 4. A Ramberg-Osgood model was used to simulate the nonlinear constitutive relation of soil and iterative linear analyses were performed. One of the two parameters of the Ramberg-Osgood model, r, was kept constant equal to 2, while the second one, α, was varied so as to cover a wide range of typical soil stress-strain relations. For such a model the variation of secant modulus and effective damping ratio with stress amplitude is given by:

$$\frac{G}{G_0} = \frac{1}{1 + \alpha(\tau/G_0\gamma_y)} \tag{61}$$

and

$$\xi = \frac{2}{3\pi}\frac{G}{G_0}\frac{\tau}{G_0\gamma_y} \tag{62}$$

in which: G_0 = the initial shear modulus for low levels of strain; γ_y = a characteristic shear strain, typically ranging from 0.0001% to 0.01%, and τ = the amplitude of the induced shear stress.

From these studies Jakub and Roesset[56,65] concluded that a reasonable approximation to the swaying and rocking impedances of a rigid strip may be obtained from the available linear visco-elastic solutions (e.g. Table 4 and Figs. 10–11), provided that 'effective' values of G and ξ are estimated from equations (61)–(62) with:

$$\tau = \tau_c \tag{63}$$

where τ_c is the statically induced shear stress at a depth equal to $0.50B$, immediately below the foundation edge.

While more studies would be necessary to improve the reliability of this simple rule, its use in machine foundation analyses can be safely recommended, in view of the small local nonlinearities that usually develop.

RIGID EMBEDDED FOUNDATIONS

The response of embedded foundations to static and dynamic loads has received considerable attention. As a result, several finite-element as well as approximate continuum-type formulations have been developed, while parametric studies have explored the relative significance of the depth and 'type' of embedment. Reference is made to the work of Lysmer *et al.*,[83] Novak *et al.*,[111] Beredugo

* Evidence of such yielding has been presented by Richart *et al.*[7] (Figs. 10 and 26), while recent experimental work at the University of Michigan revealed a similar phenomenon under torsionally excited footings.[128]

et al.,[72] Waas *et al.*,[31] Kausel *et al.*,[89] Chang-Liang,[87] Johnson *et al.*,[112] Luco,[66] Dominguez *et al.*,[47] Harada *et al.*[76] and Tassoulas,[88] among several others.

Results have been presented for circular, strip and rectangular foundations and a variety of idealized soil profiles, including the halfspace, stratum-over-bedrock and stratum-over-halfspace. In each case, the new key dimensionless problem parameter, in addition to the parameters controlling the response of surface foundations, is the relative embedment, D/B or D/R. Moreover, the assumed interface behavior at the contact between vertical sidewalls and backfill is of crucial importance. Most of the aforementioned studies assume that walls and soil remain in full contact during vibrations, as if they were welded at their interface. In reality, however, no tensile stresses can be sustained between the two media, while the magnitude of developing shear tractions cannot violate Coulomb's friction law. Hence, separation and sliding are likely to occur between sidewalls and backfill, depending primarily on the mode of vibration and the nature and method of placement of the soil. Field evidence, documented by Stokoe and Richart,[113] seems to indicate that separation and sliding are more likely with clayey than with sandy soils, in accord with intuition. Furthermore, it is expected that separation will be more significant with the two antisymmetric modes of vibration (swaying and rocking), whereas sliding will be of greater importance in the two symmetric modes (vertical and torsional). Ideally 'welded' foundations are studied first.

'Welded' cylindrical foundations in a homogeneous stratum

The results to be presented are based on the work of Kausel[33] and are strictly applicable to foundations having infinitely rigid sidewalls and mat, which are all in perfect contact with the soil. Moreover, the backfill must be of very good quality and have the same properties with the soil beneath the mat. These are rather extreme conditions and, thus, yield an upper bound of the possible effect of embedment.

Table 8 displays five simple and sufficiently accurate formulae for the static stiffnesses of cylindrical foundations, perfectly embedded in a homogeneous soil layer overlying bedrock. It is evident that embedment increases the values of the static stiffnesses substantially. The increase in D/R is especially beneficial to the two rotational modes, rocking and torsion; the two translational modes, vertical and horizontal, are considerably less affected (factors of 1/2 and 2/3 for vertical and horizontal loading, as compared to 2 and 2.67 for rocking and torsion).

In contrast, the effect of D/H is more visible in the vertical and horizontal modes, appreciably less important in rocking, and negligible in torsion; this is consistent with the expected depths of the corresponding 'pressure bulbs', discussed in the preceding sections.

Note that with embedded foundations the cross-coupling stiffness, K_{hr}, can no longer be neglected, being approximately equal to $0.4K_h D$.

The effect of embedment on the frequency variation of the dynamic stiffness and damping coefficients is demonstrated in Fig. 19. We notice that k is not very sensitive to D/R. In fact, Elsabee *et al.*[114] recommended that the actual frequency variation of k of an embedded foundation be approximated by the variation of the corresponding surface foundation. This seems to be very reasonable for all vibration modes at low frequencies. For rocking and torsion, in particular, the approximation will for all practical purposes be good throughout the frequency range examined; in other words, the beneficial effect of increasing D/R on the static rotational stiffnesses is preserved even at higher values of a_0, at least for not very large D/R ratios. However, beyond the first resonant frequency, vertical and swaying vibrations exhibit undulations in k which cannot be well reproduced with the results of surface foundations.

All damping coefficients increase substantially with increasing embedment, although below the first resonance, a_{0r}, they remain small. It has been recommended[90,114] that for $a_0 > a_{0r}$, c be taken equal to a constant value, corresponding to the average value of c of a foundation embedded in a halfspace. To estimate this latter value of c, use may be made of the simple expressions derived by Dobry *et al.*[95] on the basis of simple but realistic physical approximations. For the two translational modes, the frequency-independent damping coefficients for cylindrical foundations embedded in a halfspace are approximated by:

$$c_h \simeq \frac{\pi(2-\nu)}{8} \cdot \frac{1+1.3(D/R)[1+(3.6/\pi(1-\nu))]}{1+\frac{2}{3}(D/R)} \tag{64}$$

and

$$c_v \simeq 0.85\, \frac{1+1.85(1-\nu)(D/R)}{1+\frac{1}{2}(D/R)} \tag{65}$$

The increase of the two damping coefficients with D/R is reflected in the much larger coefficients they are multi-

*Table 8. Static stiffnesses of rigid embedded cylindrical foundations 'welded' into a homogeneous soil stratum-over-bedrock**

Type of loading	Static stiffness	Profile
Vertical	$\frac{4GR}{1-\nu}\left(1+1.28\frac{R}{H}\right)\left(1+\frac{1}{2}\frac{D}{R}\right)\left(1+\ 0.85-0.28\frac{D}{R}\ \frac{D/H}{1-D/H}\right)$	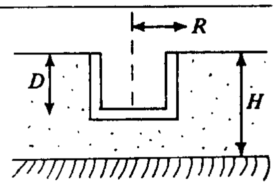
Horizontal	$\frac{8GR}{2-\nu}\left(1+\frac{1}{2}\frac{R}{H}\right)\left(1+\frac{2}{3}\frac{D}{R}\right)\left(1+\frac{5}{4}\frac{D}{H}\right)$	
Rocking	$\frac{8GR^3}{3(1-\nu)}\left(1+\frac{1}{6}\frac{R}{H}\right)\left(1+2\frac{D}{R}\right)\left(1+0.7\frac{D}{H}\right)$	Range of validity:
Coupled horizontal-rocking	$0.40K_hD$	$\frac{D}{R}<2$
Torsion	$\frac{16}{3}GR^3\left(1+2.67\frac{D}{R}\right)$	$\frac{D}{H}<0.5$†

* From Elsabee *et al.*[114] and Kausel *et al.*[95]
† For foundation with deeper embedment the formulae underpredict the 'actual' increase in the stiffnesses

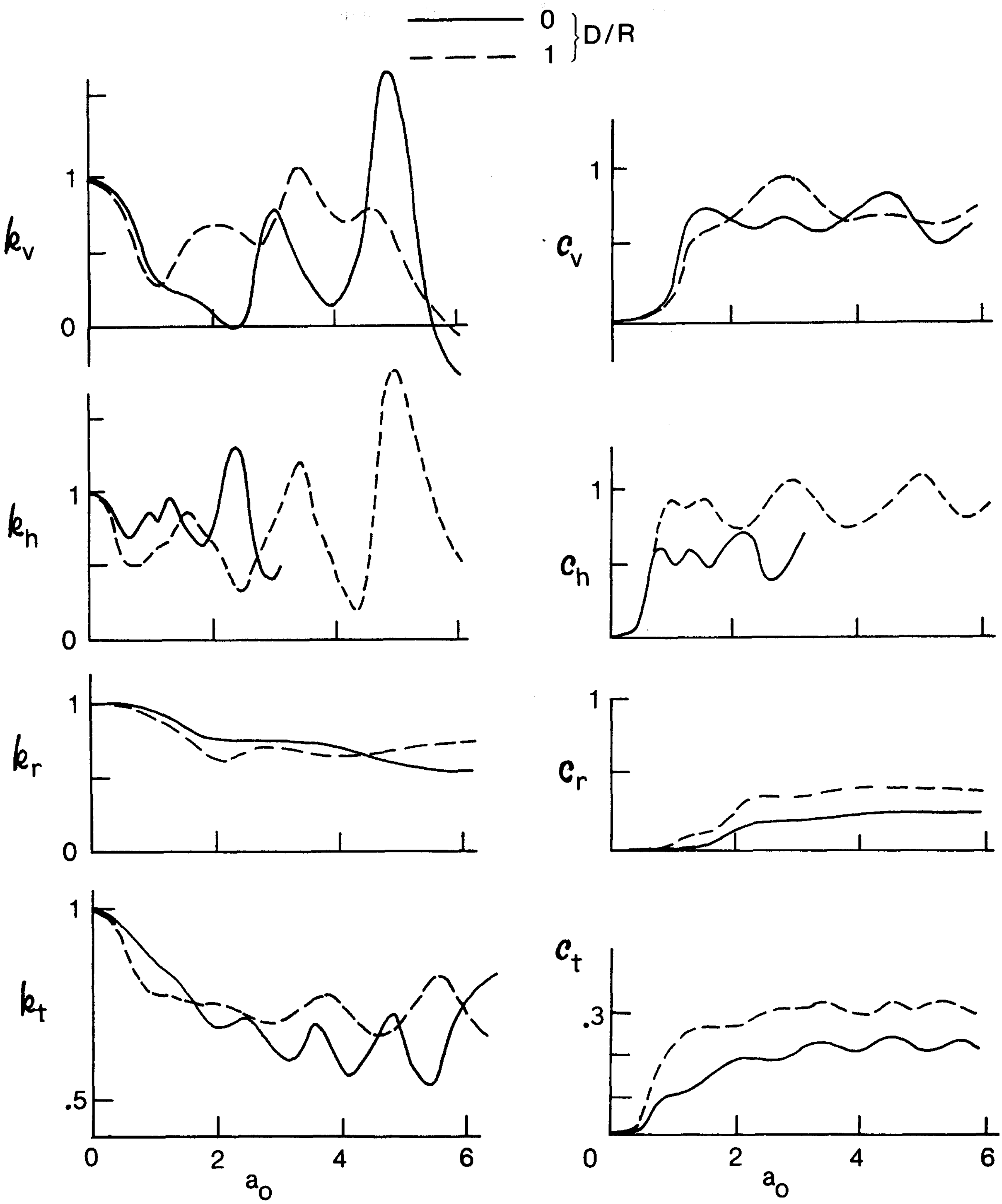

Figure 19. Effect of embedment on dynamic coefficients of a rigid cylindrical foundation on stratum-over-bedrock ($H/R = 3$, $\nu = 1/3$, $\xi = 0.05$)[33, 88, 90]

plied with in the numerator than in the denominator; e.g. for $\nu = 0.40$, c_h is proportional to $(1+3.8D/R)/(1+0.67\,D/R)$ and c_v is proportional to $(1+1.1D/R)/(1+0.5D/R)$. Expressions similar to those of equations (64)-(65) have not been developed for rocking and torsion.

It is finally noted that, with very good accuracy, one may set for the cross-coupling impedance:

$$k_{hr} = 1; \quad c_{hr} = 0 \tag{66}$$

Imperfect contact between sidewall and backfill

Two recent studies have addressed the question of the dynamic response of embedded foundations, the sidewalls of which are not perfectly bonded to the backfill.[88, 115] In both studies, the nonlinear contact phenomena associated with separation and sliding are modeled in an approximate way. Thus, Tassoulas assumes that no contact exists between sidewall and backfill near the ground surface but that a perfect contact is effective over a height equal to d above the basement. By allowing d to vary between 0 and D all cases between the extremes of 'no-contact' and 'welded-contact' could be studied. On the other hand, Novak *et al.* considers the sidewalls to be in contact not with the undisturbed soil but with a cylindrical zone consisting of softer material. By allowing the shear modulus of this zone to take values between the shear modulus of the backfill and zero, various qualities of contact could be considered. Note that a similar parametric study for statically loaded foundations, the sidewalls of which are surrounded by a soft cylindrical zone, has been presented by Johnson *et al.*[116] Only results from Tassoulas[88] are shown herein.

The sensitivity of the static stiffnesses to variation in the contact-height over embedment ratio, d/D, is graphically displayed in Fig. 20. The effect is essentially independent of H/R and D/R; hence only one curve is plotted for each mode. Consistent with the observations made in the previous subsection, the effects of d/D are very significant for rocking and torsional loading, substantial for horizontal loading and secondary for vertical loading. For instance, the 'welded-contact' stiffnesses ($d/D = 1$) are 2.74, 2.33, 1.60 and 1.30 times larger than the 'no-contact' stiffnesses ($d/D = 0$) for rocking, torsional, horizontal and vertical loading, respectively.

Figure 21 portrays the effect of d/D on the variation of k and c versus a_0. The stiffness coefficients are only slightly affected by d/D at low frequencies; at higher frequencies, however, the sharpness of the resonant valleys decreases as d/D increases. On the other hand, the damping coefficients show a substantial decline as the 'welded-contact' height, d, between sidewalls and backfill, decreases. Exception: c_v, which is less affected by d/D as well as by D/R (see equation (65) and Fig. 19). Notice also that the influence of d/D on c_r depends strongly on the particular frequency of oscillation.

Embedded strip foundations

Dynamic compliance functions of rigid strip foundations embedded in a homogeneous soil stratum overlying bedrock have been obtained by Chang-Liang.[87] Perfect contact is assumed between the two sidewalls and the backfill, and the results are cast in the form of equation (20) (i.e. dynamic compliances normalized with the static stiffnesses).

Jakub and Roesset,[56,65] by utilizing the results of an extensive parametric study, developed simple expressions for the static horizontal and rocking stiffnesses, which are displayed in Table 9. It is evident that the influence of embedment is much smaller for strip than it is for circular foundations. In fact, the two coefficients multiplying D/B in Table 9 (1/3 and 1) are exactly one-half of those multiplying D/H in Table 8 (2/3 and 2, respectively). Intuitively, these results appear to be very reasonable since a strip foundation has sidewalls along two sides only. Thus, per unit length, the ratio of sidewall area to basement area is equal to $2D/2B = D/B$. Whereas, for a circular foundation the ratio of the two areas is $2\pi RD/\pi R^2 = 2(D/R)$! This seems to imply that the influence of D/R or D/B is proportional to the sidewall-over-basemat area ratio.

The two normalized compliance functions, $f_{h1} + if_{h2}$ and $f_{r1} + f_{r2}$, show practically *no* sensitivity to the D/B ratio and hence are not reproduced herein. Reference is made to the original publication[87] for more detailed information.

Rectangular foundations embedded in halfspace

Dominguez and Roesset[47] developed a boundary element formulation on the basis of which they derived unique results for embedded rectangular foundations perfectly bonded into a homogeneous halfspace. Figure 22 presents a few of their results for a foundation with an aspect ratio $L/B = 2$ and three embedment ratios, $D/B = 0$, 2/3 and 4/3. Only the stiffness and damping coefficients are plotted in Fig. 22 versus a_0.

Results for the static stiffnesses are not shown here. It appears, however, that the sensitivity of most stiffnesses on D/B is not as strong as in the case of circular foundations, but is quite stronger than that of a strip footing. Note that the sidewall-basemat area ratio in this case becomes equal to $4(B+L)D/(2B \cdot 2L) = 1.5(D/B)$, which is in between the 1 and 2 times the embedment ratio of the previous two cases!

The dependence on D/B of the k and c versus a_0 curves, shown in Fig. 2, reveals the following trends.

1. In the frequency range examined the sensitivity of the stiffness coefficients to large variations in D/B is quite small. For all modes, the decline of k with a_0 at low frequencies becomes sharper as the level of embedment increases.

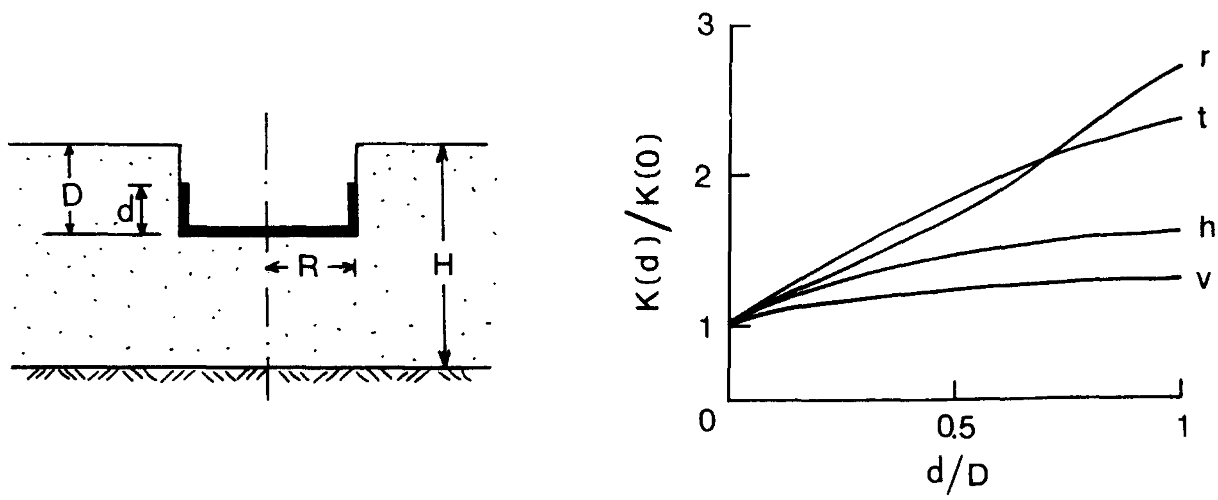

Figure 20. Static stiffnesses of cylindrical foundations with different d/D ratios (H/R = 3, D/R = 1, ν = 1/3)[88]

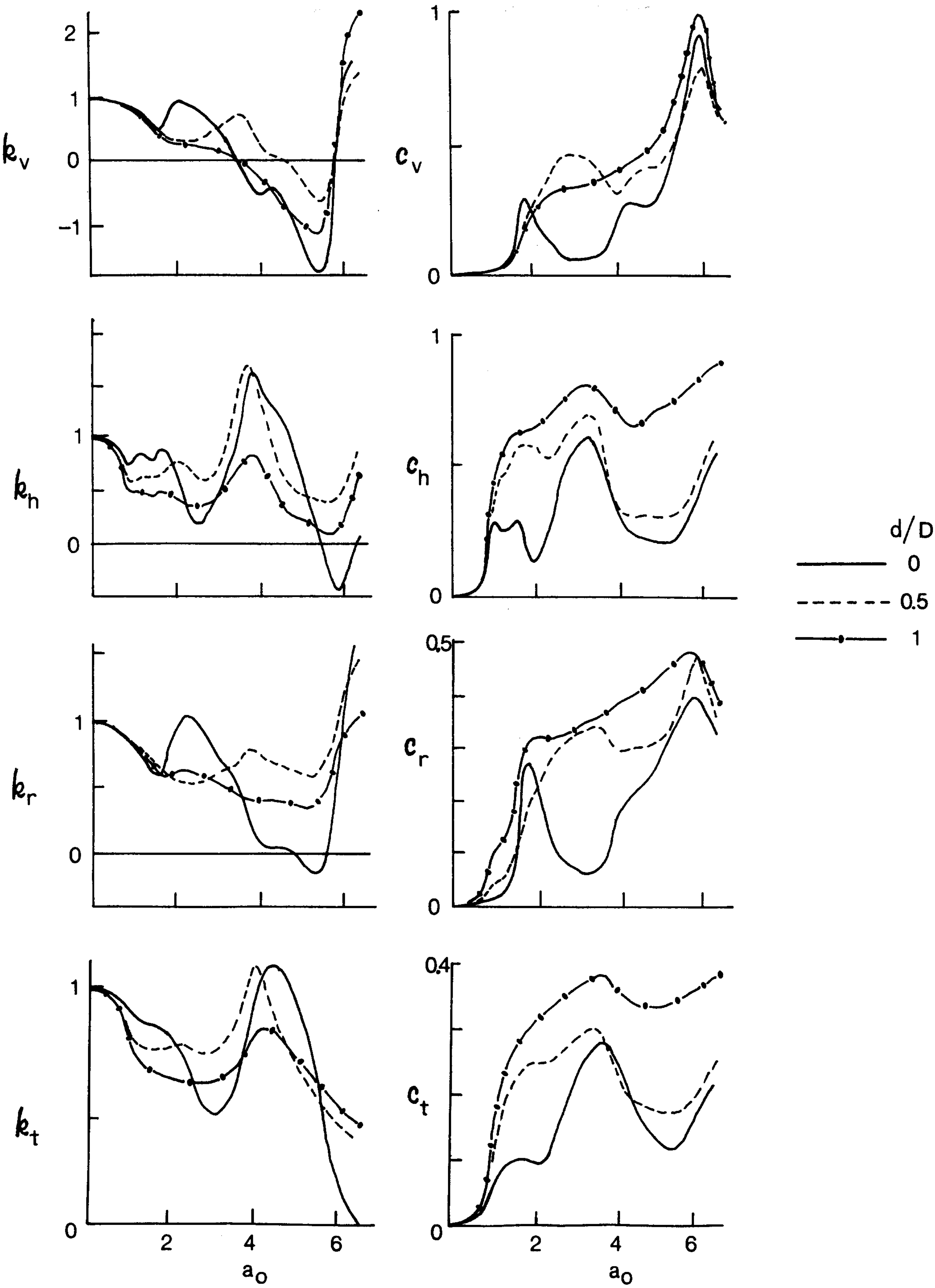

Figure 21. Dependence of dynamic coefficients of cylindrical foundations on height of sidewall-backfill contact ($H/R = 3$, $D/R = 1$, $\nu = 1/3$, $\xi = 0.05$)[88]

*Table 9. Static stiffnesses of rigid embedded strip foundations 'welded' into a homogeneous stratum-over-bedrock**

Type of loading	Static stiffness	Profile
Horizontal	$\frac{2.1G}{2-\nu}\left(1+2\frac{B}{H}\right)\left(1+\frac{1}{3}\frac{D}{B}\right)\left(1+\frac{4}{3}\frac{D}{H}\right)$	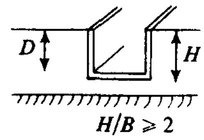
Rocking	$\frac{\pi G B^2}{2(1-\nu)}\left(1+\frac{1}{5}\frac{B}{H}\right)\left(1+\frac{D}{B}\right)\left(1+\frac{2}{3}\frac{D}{H}\right)$	$H/B \geqslant 2$ $D/B \leqslant 2/3$

* From Jakub and Roesset[56,65]

2. All the damping coefficients increase substantially with increasing D/B. The effect is particularly important for the rotational modes. Indeed, for rocking and torsion c does not tend to zero in the low frequency range when the foundation is embedded. The practical significance of this phenomenon is obvious, especially in cases involving small amounts of hysteretic damping in the soil.

SYNTHESIS: COMPARATIVE STUDY AND PRACTICAL RECOMMENDATIONS

The previous sections have studied the effects of crucial problem parameters, related to the soil profile and the foundation geometry, on the dynamic response of massless rigid foundation plates. It is interesting, however, to also investigate the influence of these parameters on the response of a *massive* foundation, and thus develop a better perspective of the role of some of these parameters. We note that, in such a study, equations (39)-(46) can be directly utilized to obtain amplitudes of steady-state motion, once the dynamic impedance functions have been evaluated.

The goal of the comparative study described here is to investigate the sensitivity of the response of massive foundations to the exact variation with frequency of the dynamic stiffness and damping coefficients, k and c. To this end, two different foundations, both circular in plan, are considered. Foundation A is a relatively heavy one, having a radius $R = 2$ m, a mass $m = 40\rho R^3$ and a central mass moment of inertia $I_{0x} = m(0.75R)^2$. Foundation B is a relatively light one, having $R = 1$ m, $m = 5\rho R^3$ and $I_{0x} = mR^2$. The center of gravity of the machine-foundation system is located in both cases at a distance $z_c = 1.10R$ above the base. Both foundations support a machine with an unbalanced mass m_0 rotating with an eccentricity d_0 at frequencies ω; the center of rotation is located at a distance $z_0 = R$ above the center of gravity of the system, in each case. Thus, the excitation forces, referred to the center of gravity, are:

$$Q_v = m_0 d_0 \omega^2 \exp[\mathrm{i}(\omega t + 90°)] \tag{67}$$

$$Q_h = m_0 d_0 \omega^2 \exp(\mathrm{i}\omega t) \tag{68}$$

$$M_r = Q_h \cdot z_0 \tag{69}$$

and the solution can be derived from equations (39), (41) and (42) by substituting: $Q_v = m_0 d_0 \omega^2$, $\phi_v = 90°$, $Q_h = m_0 d_0 \omega^2$, $\phi_h = 0$, $M_r = z_0 Q_h$ and $\phi_r = 0$.

Four different sets (1, 2, 3 and 4) of dynamic impedance functions, K expressed in the form of equation (17), are considered. Set 1 corresponds to a surface foundation on a halfspace (Fig. 5). Set 2 corresponds to a surface foundation on a stratum-over-bedrock with $H/R = 2$ (Fig. 8). Sets 3 and 4 correspond to a foundation embedded in a stratum with $H/R = 3$ and $D/R = 1$; 'welded' sidewall-backfill contact is assumed for set 3, no contact for set 4 (Fig. 21). Material (hysteretic) damping is invariably taken equal to 0.05.

In our desire to isolate the effects of the dynamic parts of the impedance, $k + \mathrm{i}a_0 c$, from the effects of the static stiffnesses, K, the latter are assumed to be the same in all four sets. Thus, the four cases differ only in the corresponding k and c values. In reality, of course, the static stiffnesses of each set differ substantially from the corresponding stiffnesses of the other sets. For instance, the horizontal stiffnesses corresponding to sets 1, 2, 3 and 4, are in the ratio of 1:1.25:2.76:1.725, respectively. The appreciable influence of these static stiffnesses on the foundation response is well known, however, and requires no further demonstration. After all, the profession can determine static displacements with sufficient confidence, and the numerous closed-form expressions offered in this paper make very simple the task of reliably estimating the static stiffnesses of essentially arbitrary foundations on/in a variety of soil profiles.

The question then which we try to answer in this section is the following: After having properly determined the static stiffnesses of a foundation, how important is it to also accurately determine the dynamic stiffness and damping coefficients at the frequency range of interest?

Figure 22 compares the four response spectra of foundations A and B, corresponding to the aforementioned cases 1, 2, 3 and 4. Plotted in this figure is the variation with a_0 of the normalized amplitude of the horizontal displacement, $|u_t|$, experienced by the highest point of each foundation, at a distance $z_t = 1.2R$ above the center of gravity. The following trends are worthy of note in Fig. 22.

1. For frequency factors $a_0 > 1$, no differences exist between the four response curves, of either the heavy or the light foundation. In fact, the four displacement curves attain a nearly constant value which is apparently controlled by the static stiffnesses of each foundation. (Remember that in our study these stiffnesses do not change from case to case.) Such a behavior is consistent with the high-frequency response of a 1-dof oscillator under a rotating-mass-type excitation.[7] The implication is clear: at relatively high frequency factors, the motion of a rigid massive foundation is controlled by its static stiffnesses and it is not influenced by the exact variation of k and c with a_0; therefore, one can safely use for k and c the values obtained for surface foundations on halfspace, regardless of the actual soil profile and depth of embedment!

2. In the low frequency range $a_0 < 1$, the response curves depend on the assumed dynamic coefficients as well as the inertia characteristics of the foundation.

The 'heavy' foundation experiences two resonant peaks. The first occurs at a frequency $a_0 \simeq 0.15$ regardless of the exact values of k and c. The only difference from case to case is in the maximum displacement amplitude, which is

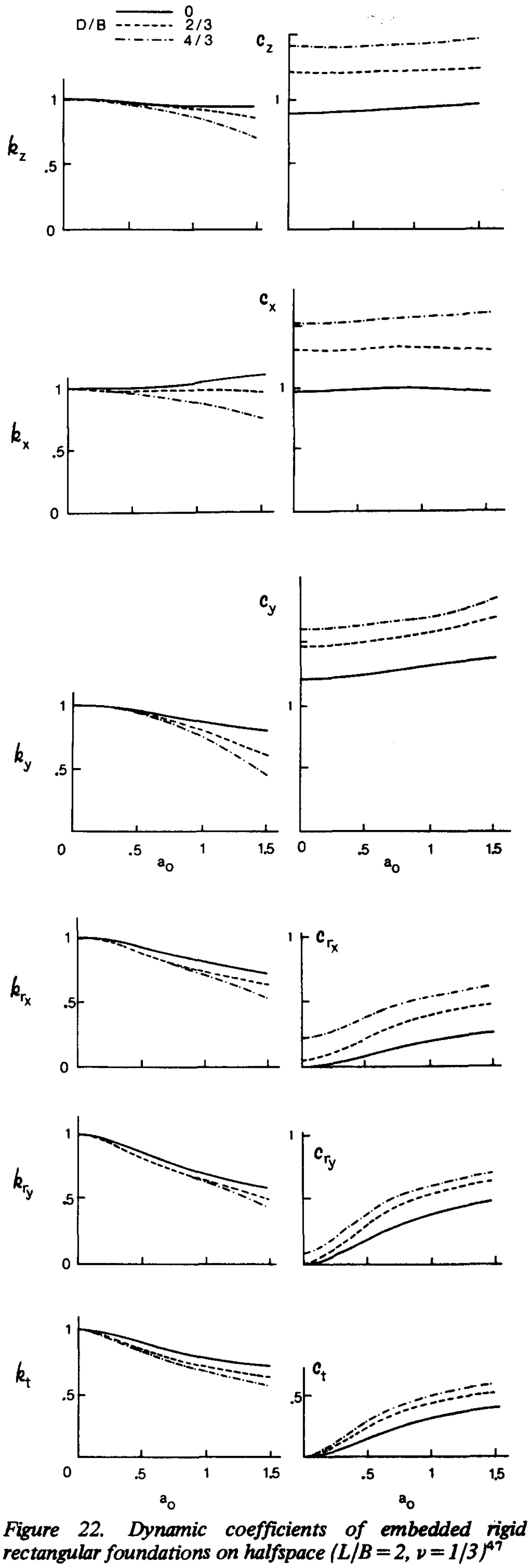

Figure 22. Dynamic coefficients of embedded rigid rectangular foundations on halfspace ($L/B=2$, $\nu=1/3$)[47]

apparently controlled by the inertia characteristics and the radiation damping of each system. (At such frequencies $k \simeq 1$, while the hysteretic damping is invariably equal to 0.05.) As a result, use of the available halfspace curves for c leads to an underprediction of the peak response.

The second resonant frequency and resonant peak are both sensitive to the assumed values of k and c. It appears that these peaks are the result of resonance phenomena due to standing waves in the soil stratum, and, hence, they are very little influenced by the foundation inertia. Notice that for the halfspace (case 1) the resonance is very flat since no standing waves can be generated in the soil. Thus, once more, the halfspace assumption proves unconservative.

The 'light' foundation, on the other hand, experiences only one resonance which reflects the characteristics of both the foundation inertia and the system dynamic coefficients. The main influence of k and c is seen on the peak amplitudes. Notice again that the halfspace values lead to the flattest peak, a consequence of the high radiation damping in a boundless medium.

On the basis of these observations and the results of some other case studies not presented herein, the following practical recommendation can be made: At relatively low frequency factors, the motion of a rigid massive foundation is controlled by its static stiffnesses, K, as well as its

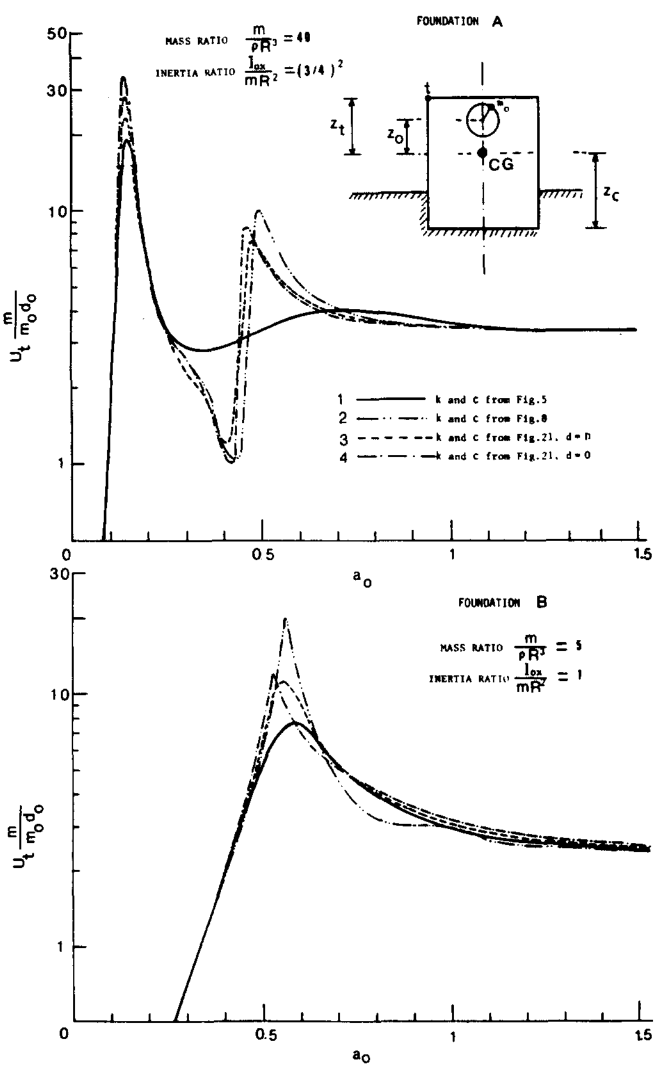

Figure 23. Sensitivity of the response of two massive foundations on the exact variation of k and c with a_0 ($\xi=0.05$)

dynamic stiffness and damping coefficients, k and c; c can be assumed to be equal to:

$$c = \begin{cases} 0 & \text{for } f \leqslant f_1 \\ c_{\text{halfspace}} & \text{for } f > f_1 \end{cases} \tag{70}$$

where $f_1 = V/4H$ is the first resonant frequency of the soil-foundation system for each particular mode; k can be approximated with the values obtained for surface foundations on a stratum-on-rigid-base; if, however, such solutions are not available, use can be made of the halfspace values of k provided that the latter are approximately corrected at and near the fundamental natural frequencies of the actual stratum, using as a guide the results of Fig. 8.

The above conclusions and recommendations are strictly applicable to rigid massive foundations carrying rotating-mass-type machines. For constant-force-type excitations the recommendations are still reasonably accurate. Frame-foundations, however, may be quite sensitive to the exact variation of k and c at frequencies around the fundamental frequency of the superstructure.

SOME OTHER TOPICS

The dynamic behavior of pile foundations, the effects of a finite flexular mat rigidity, and the dynamic interaction between adjacent foundations, are three topics that have received considerable attention in recent years. However, present knowledge and understanding of the phenomena related to these problems is more limited than for (single) rigid shallow foundations. Research is currently underway in several institutions, aimed at filling the existing gaps of knowledge in these three areas. This section is restricted to a brief general discussion of these topics and a listing of pertinent references for a more detailed study.

Dynamic impedances of piles

Results have been presented by numerous authors for end-bearing and floating single piles subjected to vertical, horizontal, rocking and torsional loading. One may broadly classify the developed formulations within three categories: (a) dynamic Winkler-foundation type formulations, which neglect the coupling between forces and displacements at various points along the pile-soil interface;[41–43, 57, 116, 118] (b) analytical continuum-type formulations, which neglect the secondary components of deformation and enforce the boundary conditions at the soil-pile interface by expanding the contact pressure distribution to an infinite series in terms of the natural modes of vibration of the soil layer;[73–76, 78] and (c) finite-element formulations.[119–121]

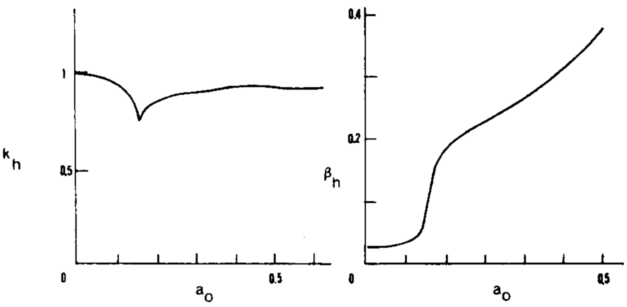

Figure 24. Lateral dynamic coefficients of single pile in an inhomogeneous stratum[122]

Figure 24 presents a typical variation of the horizontal impedance K_h versus a_0, for an end-bearing pile with length-over-diameter ratio, H/D, equal to 15. The soil-stratum consists of material with moduli increasing linearly with depth and a constant Poisson's ratio of 0.40, which is typical for normally consolidated clays. The pile is of circular cross-section and has a Young's modulus $E_p = 8000E_s$, where E_s is the soil modulus at a depth $z = H/4$. This figure has been adapted from a recent study by Velez *et al.*,[122] who utilized the finite-element formulation of Blaney *et al.*[119] The dynamic impedance is expressed in the form:

$$\mathcal{K}_h = K_h(k_h + 2i\beta_h) \tag{71}$$

where K_h = static horizontal stiffness, k_h = dynamic stiffness coefficient, and β_h = equivalent critical damping ratio.

It is evident from this figure, that the general characteristics of the pile behavior are similar to those of a shallow foundation on a soil stratum. The first resonance occurs almost precisely at the fundamental frequency of the inhomogeneous stratum in vertical shear waves, and no radiation damping occurs below this frequency. At higher frequencies, k_h attains an essentially constant value; the second resonance is barely noticeable, and hence of minor importance, despite the relatively small amount of assumed hysteretic damping (0.05).

Reference is made to the aforementioned publications for detailed studies of the influence of the main problem parameters on the response of single piles.

In the last few years, interest has switched to the dynamics of *groups* of piles, a substantially more complex problem than that of a single pile. The first results, based on a rigorous formulation,[123] indicate that the dynamic stiffness and damping coefficients of a large group of closely-spaced piles may be drastically different from the coefficients obtained by a simple superposition of the results for a single pile. More extensive parametric studies are, however, needed before definitive conclusions can be drawn and before simple formulae and dimensionless graphs of direct applicability are developed for practical use.

Effects of finite foundation rigidity

The in-plane (membrane) rigidity of mat foundations is practically infinitely large, when compared to the deformability of soils; hence, for horizontal and torsional loading most foundations clearly qualify as 'rigid', and the results of the preceding sections of this paper are thus pertinent. However, in many practical situations, the foundation response to vertical and rocking loading cannot be properly predicted without accounting for the finite out-of-plane (flexural) rigidity of the mat.

A few studies have appeared lately on the dynamic behavior of flexible circular and rectangular plates resting on a homogeneous halfspace.[49–51] The additional dimensionless parameter which in this case controls the foundation response is the relative flexural rigidity factor $RF = (E_f/E_s)\cdot(1-\nu_f^2)\cdot(t/B)^3$, where E_f, ν_f and t are, respectively, the Young's modulus, Poisson's ratio and thickness of the foundation raft. In addition, moreover, the exact distribution of the applied loading influences appreciably the behavior, especially of very flexible foundations.

The results of the aforementioned studies indicate a reduction in the vertical and rocking damping coefficients

C_v and C_r as the relative rigidity of the plate decreases. On the other hand, for small RF values, the stiffness coefficients k_v and k_r do not exhibit as steep a decay with a_0 as the one observed with rigid foundations (Fig. 5, for $\nu \geq 1/3$). Although additional parameter studies are needed to draw definitive conclusions, the author believes that the main influence of a decreasing RF on the response of a machine foundation materializes through the corresponding decrease of the static stiffnesses; in other words, the effect of the changes in k and c can be neglected, at least for realistic values of the RF factor. The results of the comparative study offered in the preceding section clearly support such a recommendation.

An idea of how sensitive the static stiffnesses, K_v and K_r, are to changes in the relative rigidity factor, RF, can be obtained from the results of Table 10. The vertical static stiffness of a circular mat supported by a homogeneous halfspace and loaded by either a uniformly or a parabolically distributed load, are expressed in the form of equation (55). The 'correction' factor J_v, which accounts for the mat flexural rigidity, is given as a function of RF. The J_v versus RF relationship was computed on the basis of some recent results by the author;[124] the average of the center and edge settlements were used in deriving the stiffness of the flexible mat.

Dynamic interaction between adjacent foundations

The vibration of a machine foundation may sometimes appreciably affect a nearby structure; conversely, the presence of such a structure may influence the response of the machine foundation itself. This 'coupling' in the motion of two adjacent structures through the soil is referred to as 'structure-soil-structure' interaction, and was first studied analytically by Warburton *et al.*,[175] in connection with cylindrical rigid foundations on a halfspace. More recently, comprehensive studies have been presented by Chang-Liang[87] who considered two rigid strip foundations on a stratum-over-bedrock and by Roesset *et al.*[126] for two rigid rectangular massive foundations or two structures idealized as simple 1-dof systems and also resting on the surface of a homogeneous stratum. The following conclusions may be drawn from the results of these studies.

1. The presence of a nearby ('passive') mass has a rather small overall influence on the motion of the foundation carrying the machine ('active'). Perhaps the most important effect from a design point of view is the appearance of rocking motions, even under vertical excitation; this is apparently the result of waves that are reflected by the 'passive' foundation. These effects increase when the masses of the two foundations increase, when the distance between them decreases, and when the thickness of the soil stratum increases. But even for distances as small as $5B$ (or $5R$) the presence of the second mass will in most cases be of secondary importance, in view of the many other uncertainties of the problem. It is noted, however, that the natural frequencies of the soil-foundation system may also change due to the interaction.

2. The motions induced in the 'passive' foundation are larger than the motion changes due to interaction effects on the 'active' foundation. This is a quite logical result since waves emanating from the 'active' foundation excite the 'passive' foundation before they are 'reflected' back to the 'active' one. Typically, one may expect the motions in the second foundation to be about 20% of those experienced by the excited mass, for distances of the order of $5R$ and hysteretic damping ratio in the soil of 5%. However, for strip foundations (plane-strain problem) on deep soil deposits, the above value may increase to about 50%.

To protect sensitive structures from the vibrations induced by a nearby machine foundation, 'active' and/or 'passive' isolation measures may frequently be necessary. Results of experimental and theoretical investigations on the effectiveness of several isolation schemes have been published by Barkan,[10] Richart *et al.*[7] and Haupt.[127]

Table 10. Static vertical stiffness of flexible circular mat on halfspace†

General expression	RF	$J_v(RF)$ Uniform load	$J_v(RF)$ Parabolic load*
$K_v = \dfrac{4GR}{1-\nu} J_v(RF)$	0.01	0.67	0.46
	0.1	0.72	0.54
	1	0.92	0.82
	10	0.99	0.97
	100	1.00	0.98

* $p = 2p_0(1 - r^2/R^2)$
† Based on results by Gazetas[124]

CONCLUSION

The state-of-the-art of analysing the forced oscillations of shallow and deep foundations has advanced remarkably in the last 15 years and has reached a mature stage of development. Several formulations and computer programs have been developed to determine in a rational way the response of foundations having various shapes and supported on/in any kind of soil deposit. Numerous studies have been published exploring the nature of associated phenomena and shedding light on the role of the key parameters influencing the response. This paper has reviewed these developments and presented results in the form of simple formulae and dimensionless graphs for the dynamic impedance functions of circular, strip, rectangular and arbitrary-plan-shape foundations. The various results have been synthesized in a case study referring to two massive foundations, and practical recommendations have been made on how to inexpensively predict the response of foundations in practice.

This progress in developing new methods of analysis for machine foundations has been paralleled by an equally impressive progress in our understanding of the dynamic behavior of soils and the development of excellent *in situ* and laboratory procedures to obtain representative values of dynamic soil parameters.

The author believes that, at present, there is a great need to calibrate our analytical procedures by means of actual case histories. Systematic post-construction observations of actual foundation performances are the key to this so important task. After all, confidence in advanced methods of analysis can only be gained if these are proved capable of predicting the field behavior of actual foundations.

Analytical work is also needed to improve the present knowledge and understanding of, among other topics, the dynamic behavior of groups of piles, including the influence of the pile-cap; the response of flexible mats founded on a soil stratum; the dynamic characteristics of foundations consisting of multiple isolated footings; and the effects of the non-uniform initial distribution of static stresses in the soil, arising from the weight of the structure.

ACKNOWLEDGEMENTS

I would like to acknowledge financial support by the US National Science Foundation (Grant CEE-82-00955) and by the Rensselaer Polytechnic Institute (BUILD program). I am also pleased to express my gratitude to my mentor Jose M. Roesset, who encouraged my interest in the subject of dynamic soil-foundation interaction. During the course of this work I had fruitful discussions with Ricardo Dobry who, also, read a draft of the paper and offered valuable comments. Professor Frank E. Richart, Jr., reviewed the paper and offered many useful suggestions. Finally, my thanks are extended to the Organizing Committee of the International Conference on Soil Dynamics and Earthquake Engineering for the invitation to prepare and present this state-of-the-art paper.

REFERENCES

1 Whitman, R. V. and Richart, F. E. Design procedures for dynamically loaded foundations, *J. Soil Mech. Fdn. Engrg., ASCE*, 1967, **93**, SM6, 169
2 McNeil, R. L. Machine Foundations: The State-of-the-Art. *Proc. Soil Dyn. Spec. Sess. 7th ICSMFE*, pp. 67–100, 1969
3 Woods, R. D. Measurement of Dynamic Soil Properties. *Proc. Earthq. Engrg. Soil Dyn., ASCE*, Pasadena, 1978, **1**, 91
4 Ozaydin, K., Richart, F. E., Dobry, R., Ishihara, K. and Marcuson, W. F. III. Dynamic Properties and Behavior of Soils. *Proc. 7th WCEE*, State-of-the-Art Volume, Istanbul, 1980
5 Woods, R. D. Parameters affecting elastic properties, *Dyn. Meth. Soil Rock Mech.*, 1977, **1**, 37
6 Richart, F. E. Field and laboratory measurements of dynamic soil properties, *Dyn. Meth. Soil Rock Mech.*, 1977, **1**, 3
7 Richart, F. E., Woods, R. D. and Hall, J. R. *Vibrations of Soils and Foundations*, Prentice-Hall, 1970
8 Tschebotarioff, G. P. and Ward, E. R. The Response of Machine Foundations and the Soil Coefficients Which Affect It, *Proc. 2nd ICSMFE*, 1948, **1**, 309
9 Selvadurai, A. P. S. *Elastic Analysis of Soil-Foundation Interaction*, Elsevier Scientific Publishing Co., 1979
10 Barkan, D. D. *Dynamics of Bases and Foundations*, McGraw-Hill (translated), 1962
11 Prakash, S. *Soil Dynamics*, McGraw-Hill, 1981, pp. 361–7
12 Barkan, D. D. and Ilyichev, V. A. Dynamics of Bases and Foundations, *Proc. 9th ICSMFE*, Tokyo, 1977, **2**, 630
13 Gibson, R. E. The analytical method in soil mechanics, *Geotechnique*, 1974, **24**, No. 2, 115
14 Reissner, E. Stationare, axialsymmetrische, durch eine schut-telnde Masse erregte Schwingungen eines homogenen elastischen Halbraumes, *Ing. Arch.*, 1936, **7**, 381
15 Sung, T. Y. Vibration in Semi-infinite Solids Due to Periodic Surface Loading, *Sc.D. thesis*, Harvard University, 1953
16 Quinlan, P. M. The Elastic Theory of Soil Dynamics, *Symp. on Dyn. Test. of Soils*, 1953, ASTM STP No. 156, 1953, 3–34
17 Arnold, R. N. Bycroft, G. N. and Warburton, G. B. Forced vibrations of a body on an infinite elastic solid, *J. Appl. Mech. ASME*, 1955, **22**, 391
18 Bycroft, G. N. Forced vibration of a rigid circular plate on a semi-infinite elastic space and an elastic stratum, *Phil. Trans. Royal Soc. Lond.*, 1956, **A248**, 327
19 Awojobi, A. D. and Grootenhuis, P. Vibration of Rigid Bodies on Elastic Media, *Proc. Royal Soc. Lond.*, 1965, A287, 27
20 Lysmer, J. Vertical Motions of Rigid Footings, *Ph.D. thesis*, University of Michigan, Ann Arbor, 1965
21 Elorduy, J., Nieto, J. A. and Szekely, E. M. Dynamic Response of Bases of Arbitrary Shape Subjected to Periodical Vertical Loading, *Proc. Int. Symp. Wave Prop. & Dyn. Rop. Earth Mat.*, University of New Mexico, Albuquerque, 1967, 105–21.
22 Hsieh, T. K. Foundation Vibrations, *Proc. Inst. Civil Engrs.*, 1962, **22**, 211
23 Richart, F. E. and Whitman, R. V. Comparison of footing vibration tests with theory, *J. Soil Mech. Fdn. Engrg. Div.*, 1967
24 Whitman, R. V. Soil-platform Interaction. *Proc. Conf. on Behav. of Offshore Struct.*, NGI, Oslo, 1976, **1**, 817
25 Luco, J. E. and Westmann, R. A. Dynamic response of a rigid footing bonded to an elastic halfspace, *J. Appl. Mech., ASME*, 1968, **35E**, 697
26 Karasudhi, P., Keer, L. M. and Lee, S. L. Vibratory motion of a body on an elastic half plane, *J. Appl. Mech. ASME*, 1968, **35E**, 697
27 Luco, J. E. and Westmann, R. A. Dynamic response of circular footings, *J. Engng. Mech. Div., ASCE*, 1971, **97**, EM5, 1381
28 Veletsos, A. S. and Wei, Y. T. Lateral and rocking vibrations of footings, *J. Soil Mech. Found. Div., ASCE*, 1971, **97**, SM9, 1227
29 Veletsos, A. S. and Verbic, B. Vibration of viscoelastic foundations, *Int. J. Earthq. Engrg. Struct. Dyn.*, 1973, **2**, 87
30 Kuhlemeyer, R. Vertical Vibrations of Footings Embedded in Layered Media, *Ph.D. thesis*, University of California, Berkeley, 1969
31 Waas, G. Analysis Method for Footing Vibrations Through Layered Media, *Ph.D. thesis*, University of California, Berkeley, 1972
32 Chang-Liang, V. Dynamic Response of Structure in Layered Soils, *Ph.D. thesis*, MIT, 1974
33 Kausel, E. Forced Vibrations of Circular Foundations on Layered Media, *Research Rep.* R74-11, MIT, 1974
34 Lysmer, J., Udaka, T., Seed, H. B. and Hwang, R. LUSH – A Computer Program for Complex Response Analysis of Soil-Structure Systems, Report No. EERC 74-4, University of California, Berkeley, 1974
35 Luco, J. E. Impedance functions for a rigid foundation on a layered medium, *Nucl. Engrg. Des.*, 1974, **31**, 204
36 Gazetas, G. Dynamic Stiffness Functions of Strip and Rectangular Footings on Layered Soil, *S.M. Thesis*, MIT, 1975
37 Hadjian, A. H. and Luco, J. E. On the Importance of Layering on Impedance Functions, *Proc. 6th WCEE*, New Delhi, 1977
38 Gazetas, G. and Roesset, J. M. Forced vibrations of strip footings on layered soils, *Meth. Struct. Anal., ASCE*, 1976, **1**, 115
39 Gazetas, G. and Roesset, J. M. Vertical vibration of machine foundations, *J. Geotech. Engng. Div., ASCE*, 1979, **105**, GT12, 1435
40 Novak, M. Vibrations of Embedded Footings and Structures, *ASCE Natl. Struct. Engrg. Meet.*, 1973, Reprint 2029
41 Novak, M. Dynamic stiffness and damping of piles, *Canad. Geotech. J.*, 1974, **11**, 574
42 Novak, M., Nogami, T. and Aboul-Ella, F. Dynamic Soil Reactions for Plane Strain Case, *Res. Rep. BLWT-1-77*, University of Western Ontario, 1977
43 Novak, M. and Aboul-Ella, F. Impedance functions for piles in layered media, *J. Engrg. Mech. Div. ASCE*, 1978
44 Wong, H. L. and Luco, J. E. Dynamic response of rigid foundations of arbitrary shape, *Earthq. Engrg. Struct. Dyn.*, 1976, **4**, 579
45 Awojobi, A. O. and Tabiowo, P. H. Vertical vibration of rigid bodies with rectangular bases on elastic media, *Earth. Engrg. Struct. Dyn.*, 1976, **4**, 439
46 Kitamura, Y. and Sakurai, S. Dynamic stiffness for rectangular rigid foundations on a semi-infinite elastic medium, *Int. J. Anal. Num. Meth. Geomech.*, 1979
47 Dominguez, J. and Roesset, J. M. Dynamic Stiffness of Rectangular Foundations, *Research Report R78-20*, MIT, 1978
48 Savidis, S. A. Analytical methods for the computation of wavefields, *Dyn. Meth. Soil Rock Mech.*, 1977, **1**, 225
49 Lin, Y. J. Dynamic response of circular plates on visco-elastic halfspace, *J. Appl. Mech., ASME*, 1978, **45E**, 379
50 Whittaker, W. L. and Christiano, P. Dynamic response of plate on elastic halfspace, *J. Engrg. Mech. Div., ASCE*, 1982, **108**, EM1, 133
51 Iguchi, M. and Luco, J. E. Dynamic response of flexible rectangular foundations on an elastic halfspace, *Earthq. Engrg. Struct. Dyn.*, 1981, **9**, 239
52 Awojobi, A. O. Vibration of a rigid circular foundation on Gibson soil, *Geotechnique*, 1972, **22**, No. 2, 333
53 Gazetas, G. Static and dynamic displacements of foundations on heterogeneous multilayered soils, *Geotechnique*, 1980, **30**, No. 2, 159
54 Gazetas, G. Strip foundations on cross-anisotropic soil layer subjected to static and dynamic loading, *Geotechnique*, 1981a, **31**, No. 2, 161

55 Gazetas, G. Machine foundations on deposits of soft clay overlain by a weathered crust, *Geotechnique*, 1981d, **31**, No. 3, 387
56 Jakub, M. and Roesset, J. M. Nonlinear Stiffness of Foundations, *Research Report* R77-35, MIT, 1977a
57 Dobry, R., Vicente, E., O'Rourke, M. and Roesset, J. M. Horizontal stiffness and damping of single piles, *J. Geotech. Engrg. Div., ASCE*, 1982a, **108**, GT3, 439
58 Kagawa, T. and Kraft, L. M. Lateral load-deflection relationships of piles subjected to dynamic loadings, *Soils & Foundations*, 1980, **20**, No. 4, 19
59 Novak, M. Vertical vibration of floating piles, *J. Engrg. Mech. Div., ASCE*, 1977, **103**, EM1, 153
60 Roesset, J. M. Stiffness and damping coefficients of foundations, *Dyn. Resp. Pile Fdns., ASCE*, 1980a, 1–30 (O'Neil and Dobry, eds.)
61 Bland, D. R. *The Theory of Linear Viscoelasticity*, Pergamon Press, 1960
62 Veletsos, A. S. and Verbic, B. Basic response functions for elastic foundations, *J. Engrg. Mech. Div., ASCE*, 1974, **100**, EM2, 189
63 Lysmer, J. Foundation vibrations with soil damping, *Civ. Engrg. & Nucl. Power, ASCE*, 1980, **II**, 10/4/1–18
64 Hadjian, A. H., Luco, J. E. and Tsai, N. C. Soil-structure interaction: continuum or finite-element?, *Nuclear Engrg. Des.*, 1974, **31**, 151
65 Jakub, M. and Roesset, J. M. Dynamic Stiffness of Foundations: 2-D vs 3-D Solutions, *Research Report R77-36*, 1977b, MIT
66 Luco, J. E. Vibrations of a rigid disc on a layered viscoelastic medium, *Nucl. Engrg. Des.*, 1976, **36**, 325
67 Kirkner, D. J. Steady-state Response of a Circular Foundation on a Transversely Isotropic Half-space, *PhD thesis*, Case Western Reserve University, 1979
68 Wong, H. L. Dynamic Soil-Structure Interaction, *Rep. No. EERL 75-01*, California Institute of Technology, 1975
69 Cruse, T. A. and Rizzo, F. J. A direct formulation and numerical solution of the general transient elastodynamic problem, *I. J. Math. Anal. & Appl.*, 1968, 22
70 Gazetas, G. and Roesset, J. M. Plane-strain Soil-Structure Interaction for Seismic Response, *Proc. 6th Symp. Earthq. Engng.*, Roorkee, India, 1978, **1**, 259
71 Kobori, T., Minai, R., Suzuki, T. and Kusakabe, K. Dynamical Ground Compliance of Rectangular Foundations, *Proc. 16th Natl. Cong. for Appl. Mech.*, 1966
72 Beredugo, Y. O. and Novak, M. Coupled horizontal and rocking vibration of embedded footings, *Canad. Geotech. J.*, 1972, **9**, 477
73 Tajimi, H. Dynamic Analysis of a Structure Embedded in an Elastic Stratum, *Proc. 4th WCEE*, Chile, 1969
74 Nogami, T. and Novak, M. Soil-pile interaction in vertical vibration, *Earthq. Engrg. Struct. Dyn.*, 1976, **4**, 277
75 Nogami, T. and Novak, M. Resistance of soil to a horizontally vibrating pile, *Earthq. Engrg. Struct. Dyn.*, 1977, **5**, 249
76 Harada, T., Kubo, K. and Katayama, T. Dynamic Soil-structure Interaction by Continuum Formulation Method, *Inst. Indus. Sc.*, University of Tokyo, 1981, **29**, No. 5
77 Takemiya, H. and Yamada, Y. Layered soil-pile-structure dynamic interaction, *Earthq. Engrg. Struct. Dyn.*, 1981, **9**, 437
78 Akiyoshi, T. Soil-pile interaction in vertical vibration induced through a frictional interface, *Earthq. Engrg. Struct. Dyn.*, 1982, **10**, 135
79 Ang, A. H-S. and Harper, G. N. Analysis of contained plastic flow in plane solids, *Engrg. Mech. Div., ASCE*, 1964, **90**, EM5, 397
80 Agabein, M. E., Parmelee, R. A. and Lee, S. L. A Model for the Study of Soil-structure Interaction, *Proc. 8th Conf. Int. Assoc. Bridge & Struct. Engrg.*, New York, 1968
81 Krizek, R. J., Gupta, D. C. and Parmelee, R. A. Coupled sliding and rocking of embedded foundations, *J. Soil Mech. Fdn. Engrg., ASCE*, 1972, 98, 1347
82 Tseng, N. M. and Robinson, A. R. A Transmitting Boundary for Finite Difference Analysis of Wave Propagation in Solids, *Civ. Eng. Report No. 240*, University of Illinois, Urbana-Champain, 1975
83 Lysmer, J. and Kuhlemeyer, R. L. Finite dynamic model for infinite media, *J. Engrg. Mech. Div., ASCE*, 1969, **95**, EM4, 895
84 Valliappan, S., White, W. and Lee, I. K. Energy absorbing boundary for anisotropic material, *Num. Mech. Geomech., ASCE*, 1975, **2**, 1013
85 Lysmer, J., Udaka, T., Tsai, C-F. and Seed, H. B. FLUSH – A Computer Program for Approximate 3-D Analysis of Soil-Structure Interaction Problems, *Report No. EERC 75-30*, University of California, Berkeley, 1975
86 Luco, J. E. and Hadjian, A. H. Two-dimensional approximations to the three-dimensional soil-structure interaction problem, *Nucl. Engrg. Des.*, 1974, 31, 195
87 Chang-Liang, V. Dynamic Response of Structure in Layered Soils, *Ph.D. thesis*, MIT, 1974
88 Tassoulas, J. L. Elements for the Numerical Analysis of Wave Motion in Layered Media, *Research Rep. R81-2*, MIT, 1981
89 Kausel, E. and Roesset, J. M. Dynamic stiffness of circular foundations, *J. Engrg. Mech. Div., ASCE*, 1975, **101**, EM12, 771
90 Kausel, E. and Ushijima, R. Vertical and Torsional Stiffness of Cylindrical Footings, *Research Rep. R76-6*, MIT, 1979
91 Roesset, J. M. The use of simple models in soil-structure interaction, *Civ. Engrg. & Nucl. Power, ASCE*, 1980b, **II**, 10/3/1-25
92 Gerrard, C. M. and Harrison, W. J. *Circular Loads Applied to a Cross-Anisotropic Halfspace*. Paper 8. Commonwealth Scientific and Industrial Research Organization: Div. Appl. Mech., Australia, 1970a
93 Gazetas, G. Torsional displacements and stresses in non-homogeneous soil, *Geotechnique*, 1981e, **31**, No. 4, 487
94 Borodachev, N. M. Determination of the settlement on rigid plates, *Soil Mech. Fdn. Engrg. (USSR)*, 1964, **1**, 210
95 Dobry, R. and Gazetas, G. Stiffness and Damping of Arbitrary-shaped Embedded Foundations, *Research Rep. CE-82-04*, RPI, 1982
96 Egorov, K. E. Calculation of Bed for Foundation with Ring Footing, *Proc. 6th ICSMFE*, 1965, **2**, 41
97 Dhawan, G. K. A transversely-isotropic halfspace indented by a flat annular rigid stamp, *Acta Mechanica*, 1979, **31**, 291
98 Dhawan, G. K. An asymmetric mixed boundary value problem of a transversely-isotropic halfspace subjected to moment by an annular rigid punch, *Acta Mechanica*, 1981a, **38**, 257
99 Dhawan, G. K. A mixed boundary value problem of a transversely-isotropic halfspace under torsion by a flat annular rigid stamp, *Acta Mechanica*, 1981b, **41**, 289
100 Brown, P. T. and Gibson, R. E. Surface settlement of a deep elastic stratum whose modulus increases linearly with depth, *Can. Geotech. J.*, 1972, **9**, 467
101 Gibson, R. E. and Kalsi, G. S. The surface settlement of a linearly inhomogeneous cross-anisotropic elastic halfspace, *Z. Angew. Math. Phys.*, 1974, **24**, 843
102 Rowe, R. K. and Booker, J. R. The behavior of footings resting on a non-homogeneous soil mass with a crust. I. Strip footings. II. Circular footings, *Cand. Geotech. J.*, 1981a,b, **18**, 250
103 Oda, M. Initial fabrics and their relations to the mechanical properties of granular material, *Soils & Foundations*, 1972, **12**, 17
104 Barden, L. Influence of structure on deformation and failure in clay soil, *Geotechnique*, 1972, **22**, No. 1, 159
105 Yamada, Y. and Ishihara, K. Anisotropic deformation characteristics of sand under three-dimensional stress conditions, *Soils & Foundations*, 1979, **19**, 79
106 Gazetas, G. Deformational Soil-Cross-Anisotropy: Experimental Evaluation and Mathematical Modelling, *Research Rep. CE-8102*, Case Western Reserve University, 1981b
107 Gerrard, C. M. and Harrison, W. J. *Stresses and Displacements in a Loaded Orthorhombic Halfspace*. Paper 9. Commonwealth Scientific and Industrial Research Organization: Div. Appl. Mech., Australia, 1970b
108 Gazetas, G. Importance of soil anisotropy on foundation displacement functions, *Advances in Geotech. Earthq. Engrg. Soil Dyn.*, 1981c, **3**, 1039
109 Gazetas, G. Dynamic compliance matrix of rigid strip footing bonded to a viscoelastic cross-anisotropic halfspace, *Int. J. Mech. Sc.*, 1981f, **23**, No. 9, 547
110 Kausel, E., Roesset, J. M. and Christian, J. T. Nonlinear behavior in soil-structure interaction, *J. Geotech. Engrg. Div., ASCE*, 1976, **102**, GT12, 1159
111 Novak, M. and Beredugo, Y. O. Vertical vibration of embedded footings. *J. Soil Mech. Fnd. Engrg. Div., ASCE*, 1972, **00**, SM12, 000

112 Johnson, G. R., Christiano, P. and Epstein, H. I. Stiffness coefficients for embedded footings. *J. Geotech. Engrg. Div., ASCE*, 1975, **101**, GT8, 789
113 Stokoe, K. H. and Richart, F. E. Dynamic response of embedded machine foundations, *J. Geotech. Engrg. Div., ASCE*, 1974, **100**, GT4, 427
114 Elsabee, F. and Morray, J. P. Dynamic Behavior of Embedded Foundations, *Research Rep. R77-33*, MIT, 1977
115 Novak, M. and Sheta, M. Approximate approach to contact effects of piles, *Dyn. Resp. Pile Fdns., ASCE*, 1980 (O'Neil and Dobry, eds.)
116 Johnson, G. R. and Epstein, H. I. Backfill effects on circular foundation stiffnesses, *J. Geotech. Engrg. Div., ASCE*, 1977, **103**, GT8, 899
117 Kagawa, T. and Kraft, L. M. Lateral pile response during earthquakes, *J. Geotech. Engrg. Div., ASCE*, 1981, **107**, GT12, 1713
118 Liou, D. D. and Penzien, J. Seismic Analysis of an Offshore Structure Supported on Pile Foundations, *Report No. EERC77-25*, University of California, Berkeley, 1977
119 Blaney, G. W., Kausel, E. and Roesset, J. M. Dynamic Stiffness of Piles, *Proc. 2nd Int. Conf. Num. Meth. Geomech.*, Blacksburg, Virginia, 1976
120 Kuhlemeyer, R. Static and Dynamic Laterally Loaded Piles, *Research Rep. CE76-9*, University of Calgary, 1976
121 Angelides, D. C. and Roesset, J. M. Nonlinear lateral dynamic stiffness of piles, *J. Geotech. Engrg. Div., ASCE*, 1981, **107**, GT11, 1443
122 Velez, A., Gazetas, G. and Krishnan, R. Lateral Stiffness and Damping of Piles in Non-homogeneous Soil, *Research Rep. CE-82-04*, RPI, 1982
123 Wolf, J. P. and von Arx, G. A. Impedance function of a group of vertical piles, *Earthq. Engrg. & Soil Dyn., ASCE*, 1978, **II**, 1024
124 Gazetas, G. Variational estimations of raft settlement on cross-anisotropic soil, *Soils and Foundations*, 1981g, **21**, No. 4, 109
125 Warburton, G. B., Richardson, J. D. and Webster, J. J. Forced vibrations of two masses on an elastic half space, *J. Appl. Mech., ASME*, 1971, **38**, E
126 Roesset, J. M. and Gonzalez, J. J. Dynamic interaction between adjacent structures, *Dyn. Meth. Soil Rock Mech.*, 1977, **1**, 127
127 Haupt, W. A. Surface waves in non-homogeneous halfspace, *Dyn. Meth. Soil Rock Mech.*, 1977, **1**, 335
128 Richart, F. E., Jr., personal communication, 1982

NOTATION

The following symbols are frequently used in the paper:

Related to geometry

B = half-width of a strip footing or the shortest half-width of a rectangular footing
D = depth of embedment
d = height of perfect sidewall-backfill contact above the foundation base
H = thickness of soil stratum
L = one-half of the longest side of a rectangular foundation
R = radius of a cylindrical foundation
R_0 = radius of 'equivalent' circular foundation (equations (47)-(50))
z_c = distance of center of gravity of a machine-foundation system above the base.

Related to material properties

G = shear modulus of soil
$\tilde{m}$ = increase of shear modulus from the surface to a depth equal to R or B (applicable to inhomogeneous soil deposits)
n = E_H/E_V, where E_H and E_V are the horizontal and vertical Young's moduli of a cross-anisotropic soil
ν = Poisson's ratio of soil
ξ = hysteretic critical damping ratio of soil

Related to foundation impedances

K = static stiffness referred to the base of the foundation (Fig. 1)
$\mathbf{K}$ = dynamic impedance function of frequency; it may be expressed in one of the following alternative forms:

$$= K_1(\omega) + \mathrm{i}K_2(\omega)$$
$$= K(\mathbf{k} + \mathrm{i}a_0\mathbf{c})(1 + 2\mathrm{i}\xi)$$
$$= K(k + \mathrm{i}a_0 c)$$

Calligraphic characters are used on the figures in place of the bold $\mathbf{K}$, $\mathbf{k}$ and $\mathbf{c}$.

k and $\mathbf{k}$ = (dynamic) stiffness coefficients, functions of ω
c and $\mathbf{c}$ = (dynamic) damping coefficients, functions of ω
a_0 = $\omega B/V_s$ or $\omega R/V_s$ (dimensionless frequency factor)
F = dynamic compliance function of ω; it may be expressed in one of the following alternative forms:

$$= F_1(\omega) + \mathrm{i}F_2(\omega)$$
$$= \frac{1}{K}\,[f_1(\omega) + \mathrm{i}f_2(\omega)]$$

Subscripts

v = vertical (also designated by z)
h = horizontal (also x, y)
r = rocking (also r_x, r_y)
t = torsion (also r_z)
hr = coupled horizontal-rocking (also xr_y, yr_x)